Medicine in Evolution

Printed at: WALDPRESS, Timisoara,
64 Divizia 9 Cavalerie Street,
Phone/Fax: 0040256422247

Edited at: EUROSTAMPA, Timisoara
26, Revolutiei 1989 Street,
Phone: 0040256204816

TRANSLATIONAL AND EXPERIMENTAL CLINICAL RESEARCH CENTER IN ORAL HEALTH (TEXC-OH)
CENTER FOR CONTINUOUS MEDICAL EDUCATION

ISSN 2065-376X medinevolution.umft.ro

REDUCE ŞI AJUTĂ LA PREVENIREA PROBLEMELOR GINGIVALE ÎN 4 SĂPTĂMÂNI PENTRU A ÎNTRERUPE CICLUL GINGIVITEI

IULIE 2010 | IANUARIE 2011 | IULIE 2011

IANUARIE 2012 | IULIE 2012 | IANUARIE 2013

blend-a-med | Oral-B | CLINIC LINE GUM PROTECTION SYSTEM

Recomandați Sistemul blend-a-med Oral-B Clinic Line Gum Protection
Este dovedit clinic că reduce si ajută la prevenirea problemelor gingivale în 4 săptămâni pentru a ajuta pacienții să întrerupă ciclul gingivitei. Sistemul combină acțiunea chimică puternică a fluorurii de staniu stabilizate, suplimentată de apă de gură, cu acțiunea mecanică a periuței de dinți Pro-Flex, suplimentată de ață dentară, facând din acesta completarea perfectă a tratamentului din cabinetul dumneavoastră.

P12125.01

Continuă îngrijirea ce începe în cabinetul dumneavoastră

blend-a-med RESEARCH CENTERS Oral-B

Volume XXVIII, Nr. 1, 2022, Timişoara, Romania
ISSN 2065-376X

MEDICINE IN EVOLUTION

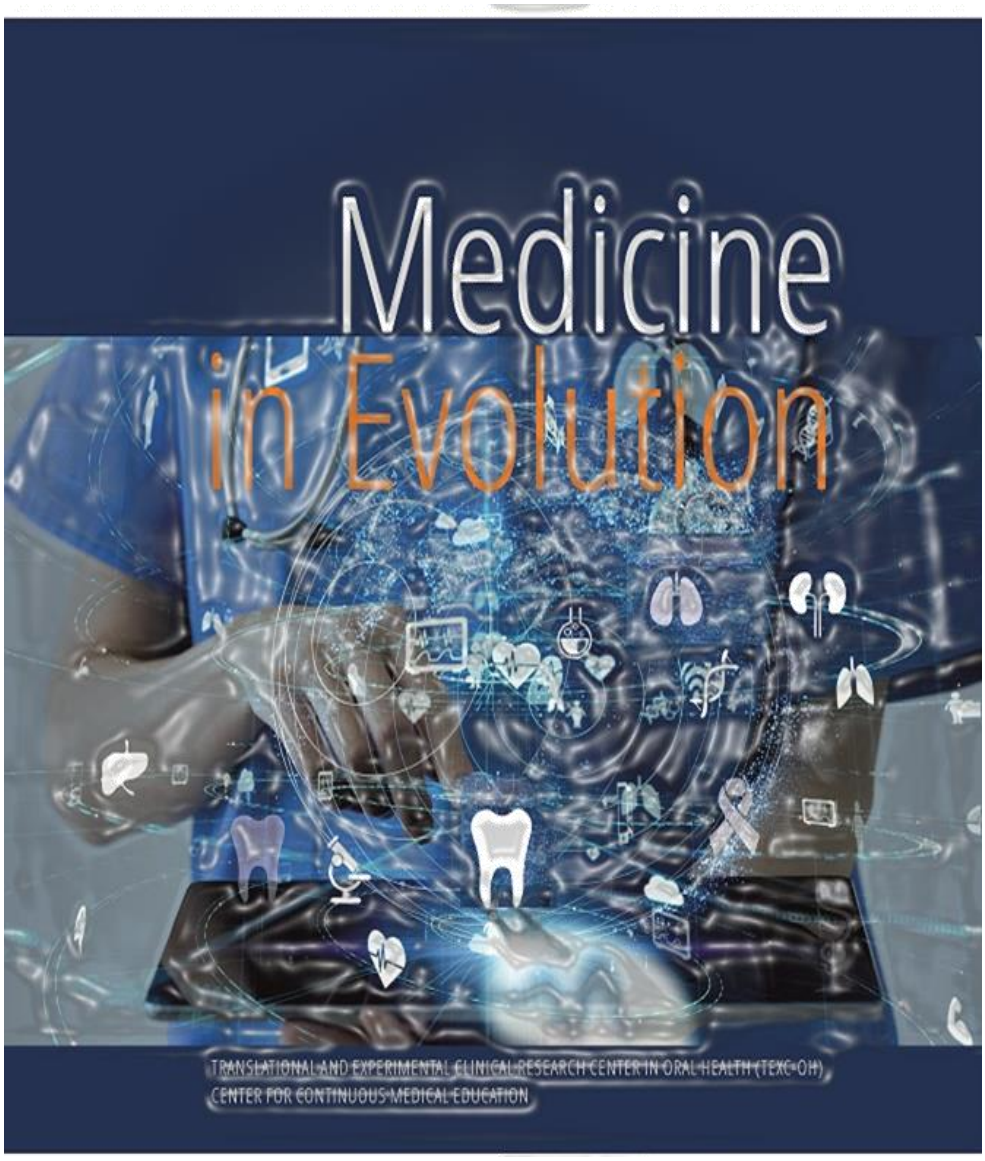

TRANSLATIONAL AND EXPERIMENTAL CLINICAL RESEARCH CENTRE IN ORAL HEALTH
CENTER FOR CONTINUOUS MEDICAL EDUCATION

medinevolution.umft.ro

Journal edited with the support of

Printed at: WALDPRESS, Timisoara,
64 Divizia 9 Cavalerie Street,
Phone/Fax: 0040256422247

Edited at: EUROSTAMPA, Timisoara
26, Revolutiei 1989 Street,
Phone: 0040256204816

EDITORIAL BOARD

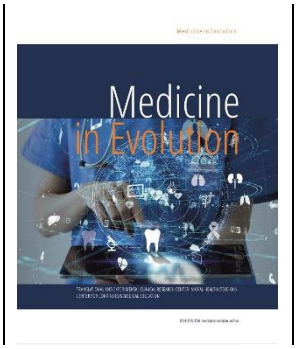

Noul elmex®SENSITIVE PROFESSIONAL cu tehnologia PRO-ARGIN

Calmarea **imediată* și de durată** a durerii din sensibilitatea dentară[1,2]

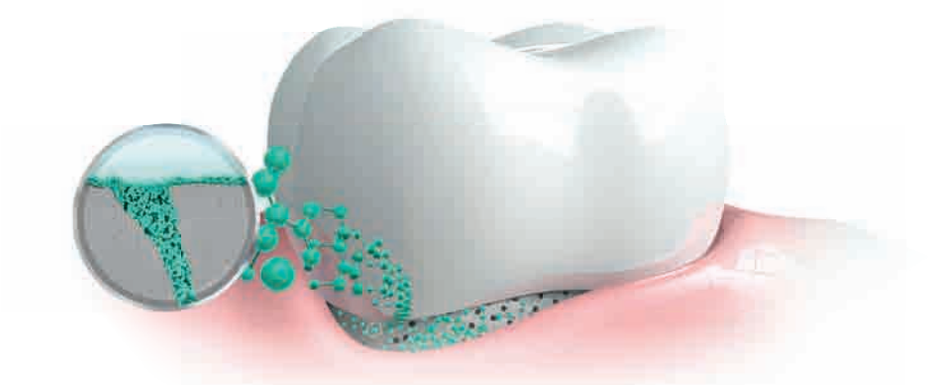

- În contact cu saliva, se formează un strat bogat în calciu, care obturează instant[1,*] tubulii dentinari deschiși
- Stratul rămâne intact în timp, chiar după expunerea la acizi, asigurând calmarea de durată a durerii din sensibilitatea dentară[2,3]

93% dintre pacienți confirmă calmarea durerii din sensibilitatea dentară[4]

93% dintre pacienți — confirmă reducerea hipersensibilității dentinare[4]

91% dintre pacienți — apreciază recomandarea medicului stomatolog[4]

Calmarea imediată* a durerii din sensibilitatea dentară[1]

Calmarea imediată* și de durată începe cu recomandarea dumneavoastră**

*Pentru calmare imediată, aplicați direct cu degetul pe dintele sensibil și masați ușor pentru 1 minut;
**Doar în legătură cu pasta de dinți

Referințe: 1. Nathoo S, et al. J Clin Dent. 2009;20(Spec Iss):123 –130; 2. Docimo R, et al. J Clin Dent. 2009;20(Spec Iss): 17– 22.; 3. Report Deon Hines-0003, 2016; 4. Studiu Ipsos cu privire la utilizarea produsului elmex® SENSITIVE PROFESSIONAL Repair & Prevent, efectuat în Polonia, rezultate după 2 săptămâni de utilizare, cu 325 de participanți (2017).

elmex® SENSITIVE PROFESSIONAL realizează obturarea superioară a tubulilor dentinari în comparație cu tehnologiile concurente[1,2,*]

Studiul 1[1,*]

Tehnologia cu fluorură de staniu/ fluorură de sodiu

Tehnologia PRO-ARGIN

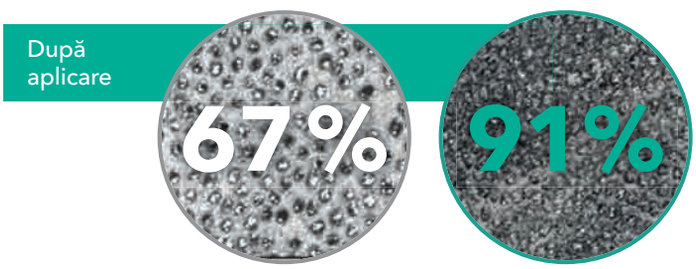

Studiul 2[2,*]

Tehnologia Novamin/ fluorură de sodiu

Tehnologia PRO-ARGIN

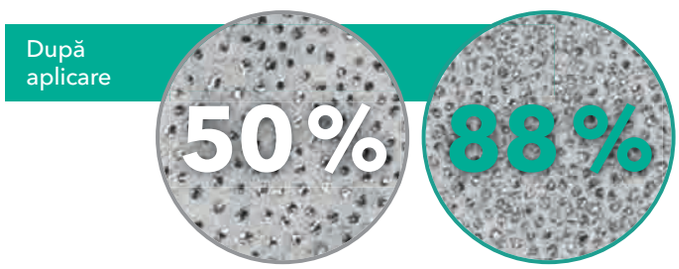

elmex® SENSITIVE PROFESSIONAL oferă calmare semnificativă imediată** și de durată a durerii din sensibilitatea dentară[3,4]

Calmarea semnificativă a durerii din sensibilitatea dentară instant[3,‡,**]

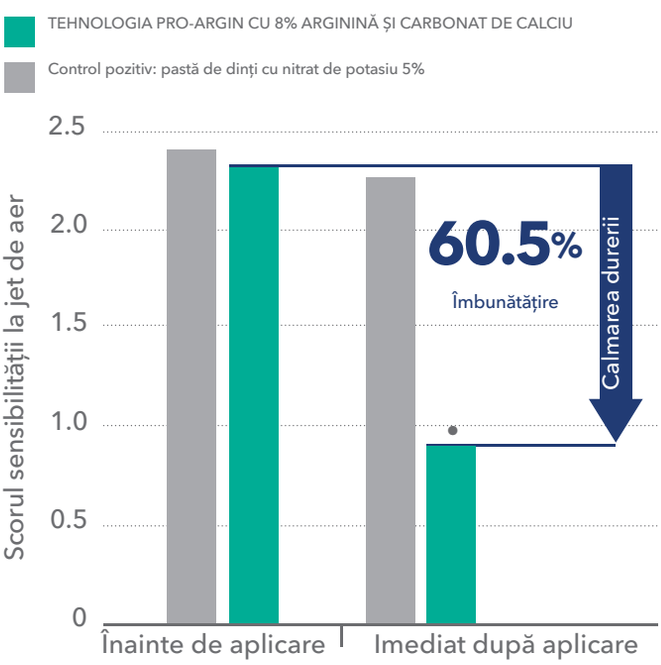

‡ În comparație cu starea inițială (sunt prezentate doar datele relevante)
• Semnificativ statistic (p<0,001)

Calmarea semnificativă de lungă durată a durerii din sensibilitatea dentară după 2, 4, și 8 săptămâni de utilizare[4,§,&]

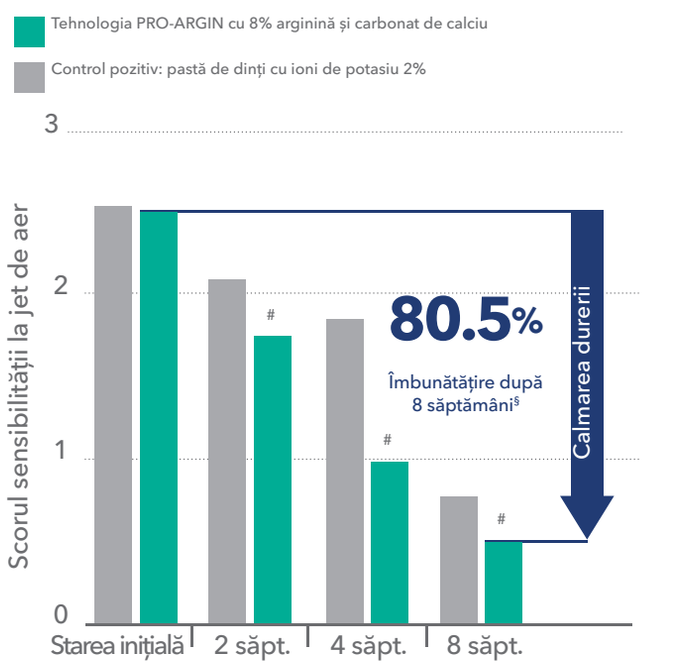

§ În comparație cu starea inițială
& În comparație cu o pastă de dinți comercială desensibilizantă, ce conține 2% ioni de potasiu și 1450 ppm de fluor (NaF)
# Semnificativ statistic (p<0,05)

*Studiu in vitro, imagini reale de microscopie confocală după 5 aplicări (p<0,05%);
**Pentru calmarea imediată aplicați direct pe suprafața sensibilă și masați ușor cu vârful degetului timp de 1 minut.

Referințe: 1. Hines D, et al. Poster acceptat, July 2018 IADR. Colgate- Palmolive Company 2018.; 2. Hines D, et al. Poster #0742, March 2018 AADR. Colgate-Palmolive Company 2018.; 3. Nathoo S, et al. J Clin Dent. 2009;20(Spec Iss):123 –130; 4. Docimo R, et al. J Clin Dent. 2009; 20(Spec Iss): 17– 22.

elmex®
SENSITIVE PROFESSIONAL

CONTENTS

ARTICLES

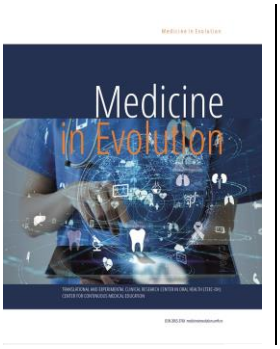

Laparoscopic incidence in acute appendicitis associated with demographic factors

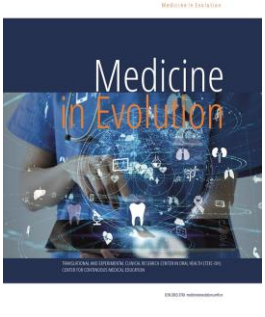

Gavrilă (Brata) R.D.[1], Maghiar T.T.[2], Maghiar O.[2], Domocoş D.[3], Bonta D.F.[3], Popovici-Muţ A.M.[3], Pogan M.D.[3]

[1]*Pelican Clinical Hospital Oradea, Oradea, Romania*
[2]*Faculty of Medicine and Pharmacy, University of Oradea, Romania*
[3]*Department of Dental Medicine, Faculty of Medicine and Pharmacy, University of Oradea, Romania*

Correspondence to:
Name: Domocoş Daniela
Address: Department of Dental Medicine, Faculty of Medicine and Pharmacy, University of Oradea, Romania, December 1st Square no.10, 410068 Oradea, Bihor County, Romania
Phone: +40747386260
E-mail address: danadd769@gmail.com

Abstract

Acute appendicitis is a surgical condition characterized by the inflammation of the vermiform appendix, being one of the most common causes of acute abdominal pathology. Appendectomy can be performed by open or laparoscopic methods, the latter being the preferred way. Once the diagnosis of acute appendicitis has been established, the appendicectomy should be performed urgently within the first hours of hospitalization.

Our findings on the impact of demographic factors on the incidence of acute appendicitis have led to a result showing that the laparoscopic incidence of acute appendicitis is higher among female patients, 52.04%, compared to male patients in the study group. The prevalence of acute appendicitis according to age was recorded in patients under 40 years, the highest incidence in this age group, after the analysis was recorded in patients under 20 years.

To date, the indications for laparoscopic appendicectomy are controversial and the benefits do not appear to be as convincing as those of cholecystectomy or hiatal hernia surgery. Laparoscopy has a dual role, being used for diagnosis and treatment. It allows complete and consecutive diagnosis, solving in the same operating session other possible surgical causes that are at the origin of the abdominal pain syndrome.

Keywords: acute appendicitis, demographic factors, laparoscopic surgery

INTRODUCTION

Acute appendicitis is one of the most common causes of acute abdominal pain in adults and children, with a higher lifetime risk in men compared to women [1].

The peak incidence of appendicitis usually occurs in the second and third decades of life. The condition can occur at any time in life, but is relatively rare at extreme ages. Men and women are equally affected, except for the period between puberty and 25 years when men predominate [2]. The peak incidence is between 10-14 years in female patients and between 15-19 in male patients [3]. Perforation is relatively more common in young children and the elderly, periods in which mortality is also higher [2].

In the observational study "The Significant Impact of Age on the Clinical Outcomes of Laparoscopic Appendectomy", authors shows that acute appendicitis (AA) is the most common surgical emergency and can occur at any age, with a cut-off point at 65 years, the peak incidence being recorded mainly in the younger population [4]. The risk of developing complications in the young population 48 hours after the onset of pain was lower compared to the population older than 40 years. Although the incidence of AA varies with age, being higher in younger patients, it still occurs in the last decades of life, the ratio of complicated appendicitis growing with age [5]. In terms of hospitalization rate, it was higher in the older population [4].

In the comparative study on the benefits of laparoscopic intervention compared with classic intervention in acute appendicitis, [6] reached the conclusion that the laparoscopic approach in elderly patients should be applied whenever possible as it is associated with reduced mortality and reduced rate of immobilized patients in bed.

Aim and objectives

The aim of this study is to assess the incidence of laparoscopic surgery in acute appendicitis related to demographic factors. The study identifies the demographic factors with high impact on the incidence of acute appendicitis treated laparoscopically with reduction of pre and postoperative complications among patients in the study group.

Objectives: Assessment of the incidence of acute appendicitis by age groups, Assessment of the incidence of acute appendicitis by gender, Laparoscopic incidence and its benefits in acute appendicitis.

MATERIAL AND METHODS

A prospective and retrospective study was used to achieve the proposed objectives. In this regard, a group of 171 patients diagnosed with acute appendicitis (AA) was created. All patients were hospitalized during 2019-2021 in the surgical units of the County Emergency Clinical Hospital from Oradea and of the Pelican Hospital from Oradea. Patients were selected on the basis of their medical records from the archives of the two hospital units.

The data obtained were interpreted based on the determination and calculation of several series of indices relevant for this study.

RESULTS

The incidence of age-related acute appendicitis (AA) shows a predominance of patients under the age of 40 years. The study group consisted of 171 patients of which 110 patients were under the age of 40 years (Table 1).

Table 1. Distribution of AA cases by age

Age group	Total AA / 2020-2021	
	No.	%
<20 years	40	23.39
21-30 years	37	21.63
31-40 years	33	19.29
41-50 years	27	15.78
51-60 years	19	11.11
61-70 years	11	6.43
>70 years	4	2.34
Total	**171**	**100.00**

Patients aged 10-40 years represented 64.32%, patients aged 60-70 years represented 6.43% and patients aged over 70 years represented 2.34% of the incidence of acute appendicitis in the study group (Figure 1).

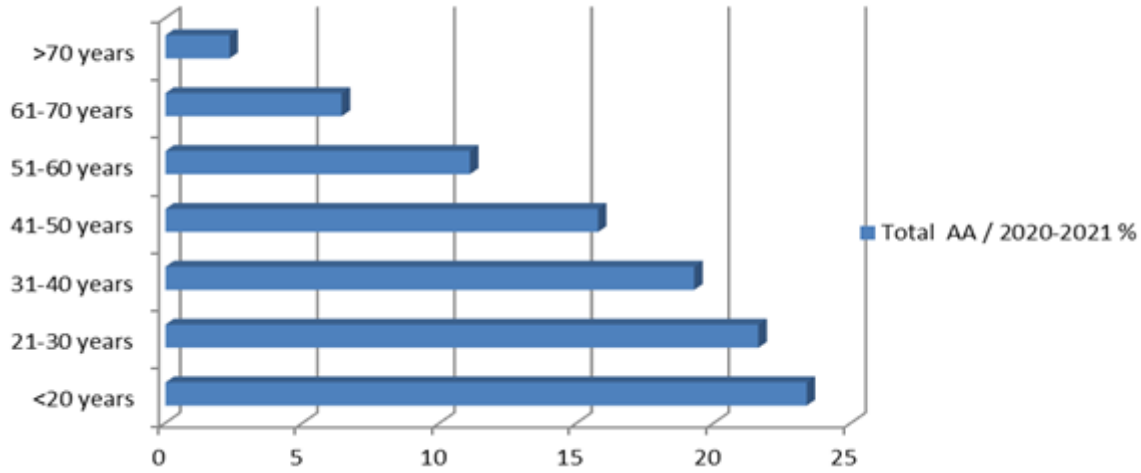

Figure 1. Distribution of cases of acute appendicitis by age

The distribution by gender (Table 2) shows a predominance of female patients, without significant difference, the female to male ratio being 1.08:1.

Table 2. Distribution of AA cases by gender

Gender	Total of AA /2020-2021	
	No.	%
Women	89	52.04
Men	82	47.95
Total	**171**	**100.00**

The distribution of AA cases (Table 3) by age and gender indicates a female to male ratio of 2:1 only in the case of the patients aged 21-30 years, the ratio being reversed in the group aged 31- 40 years where the incidence of acute appendicitis is higher in male patients. Of the four people over the age of 70 years, three were women.

Table 3. Distribution of AA cases by age and gender

Age group	Female		Male	
	No.	%	No.	%
<20 years	20	22.47	20	24.39
21-30 years	25	28.08	12	14.63

31-40 years	15	16.85	18	21.95
41-50 years	11	12.36	16	19.51
51-60 years	9	10.11	10	12.19
61-70 years	6	6.74	5	6.09
>70 years	3	3.37	1	1.22
Total	**89**	**100.00**	**82**	**100.00**

The incidence of acute appendicitis (AA) was 5% higher in male patients in the age group 40-50 years and 7% higher in male patients in the age group 50-60 years. The incidence of acute appendicitis was similar in patients aged 60-70 years.

DISCUSSIONS

The data observed in our study show similar evolution to the data presented in the literature, as concluded in the retrospective study of the clinical-epidemiological profile of acute appendicitis conducted by Pereira Lima et al., 2016. In this study, the authors observed a higher incidence of this surgical pathology in young adults (19-44 years) and male patients (65.20%).

According to the study on hospitalization trends for acute appendicitis [7], the incidence of acute appendicitis in people aged over 50 years was estimated at 1 in 35 men and at 1 in 50 women. In those older than 70 years, the chances were less than 1 in 100, similar data being observed in our study. Hospitalizations by age groups were of 25.3% in children aged 0–14 years; of 41.1% in patients aged 15–34 years; of 12.2% in patients aged 35–44 years; of 13.8% in patients aged 45-64 years and of 7.6% in patients aged over 65 years, the average age being 29.8 years [8, 9].

Many studies have concluded that in adolescents and young adults, acute appendicitis is more frequent in men, with a female to male ratio of 1.3:1 cases [10].

The risk of acute appendicitis during life is considered to be higher in men than in women. The lifetime risk in the United States has been estimated at 8.6% in men and at 6.7% in women [11]. but with an insignificant difference similar to the results observed in our study.

The study on the prevalence of acute appendicitis among hospitalized patients with suspected acute abdomen in Ethiopia showed that the overall prevalence of acute appendicitis was 44.27%. This study, compared and completed with recent data presented in the literature, reports a higher incidence in female patients (62.98%) from India. This difference suggests that the study depends on the region subjects come from [12].

The observational study "Hospitalization Trends for Acute Appendicitis in Spain, 1998 – 2017" [7], which analysed the hospital admission rates for acute appendicitis by age, gender and age group, showed that 58.9% of the subjects included in the study group were male patients and 41.1% were female patients. The trend in hospital admissions for acute appendicitis related to age showed that the incidence of this disease decreased in 2009 in people younger than 35 years. Acute appendicitis mainly affects adolescents and young adults, those aged 20 to 30 years presenting the highest risk and those under 5 years presenting the lowest risk [8, 9].

CONCLUSIONS

Exploratory laparoscopy is a procedure that allows to differentiate the pathomorphological aspects of acute appendicitis and the degree of the extent of peritonitis.

Acute appendicitis presents a higher prevalence in women and young people.

The highest laparoscopic incidence of acute appendicitis in the study group occurred in the age group of 21-40 years (40.92%).

The impact of laparoscopically treated acute appendicitis was higher in male patients aged 31-50 years.

There is an upward trend in female patients from the age group 21-30 years, the female to male ratio being 2:1.

The analysis of the evolution of the age to gender ratio in the study group shows that it was higher in the case of female patients as opposed to male patients, but the difference is not significant.

Laparoscopy is a method to establish the diagnosis and eventually treat the suspected acute appendicitis. It is also a method to distinguish AA from another acute intra-abdominal pathology.

REFERENCES

1. Snyder MJ, Guthrie M, Cagle S. Acute Appendicitis: Efficient Diagnosis and Management. Am Fam Physician. 2018 Jul 1;98(1):25-33.
2. Romano N, Prosperi V, Gabellieri C, Biondi G, Andreini R, Basili G, Carnesecchi P, Goletti O. Laparoscopic approach in acute appendicitis: experience with 501 consecutive cases. Chir Ital. 2009, 61(3):327-35.
3. Amanda Pereira Lima, Felipe José Vieira, Gabriela Procópio De Moraes Oliveira, Plínio Dos Santos Ramos, Marielle Elisa Avelino, Felipe Garcia Prado, Gilson Salomão Júnior, Francisco Campos Silva, João Vicente Linhares Rodrigues. Clinical-epidemiological profile of acute appendicitis: retrospective analysis of 638 Cases. Rev. Col. Bras. Cir. 2016; 43(4): 248-253.
4. Lasek A, Pędziwiatr M, Kenig J, et al. The significant impact of age on the clinical outcomes of laparoscopic appendectomy: Results from the Polish Laparoscopic Appendectomy multicenter large cohort study. Medicine (Baltimore). 2018 Dec;97(50):e13621.
5. Sartelli M, Baiocchi GL, Di Saverio S, et al. Prospective Observational Study on acute Appendicitis Worldwide (POSAW). World J Emerg Surg 2018;13:19.
6. Southgate E, Vousden N, Karthikesalingam A, et al. Laparoscopic vs open appendectomy in older patients. Arch Surg 2012;147:557–62.
7. Carratalá-Munuera C, Pilco JDR, Orozco-Beltrán D, Compañ A, Quesada JA, Nouni-García R, Gil-Guillén VF, García-Ortíz L, López-Pineda A. Hospitalization Trends for Acute Appendicitis in Spain, 1998 to 2017. Int J Environ Res Public Health. 2021 Dec 2;18(23):12718.
8. Wickramasinghe DP, Xavier C, Samarasekera DN. The Worldwide Epidemiology of Acute Appendicitis: An Analysis of the Global Health Data Exchange Dataset. World J Surg. 2021 Jul;45(7):1999-2008.
9. Ferris M, Quan S, Kaplan BS, Molodecky N, Ball CG, Chernoff GW, Bhala N, Ghosh S, Dixon E, Ng S, Kaplan GG. The Global Incidence of Appendicitis: A Systematic Review of Population-based Studies. Ann Surg. 2017 Aug;266(2):237-241.
10. Pogorelić Z, Domjanović J, Jukić M, Poklepović Peričić T. Acute Appendicitis in Children Younger than Five Years of Age: Diagnostic Challenge for Pediatric Surgeons. Surg Infect (Larchmt). 2020 Apr;21(3):239-245.
11. Bessoff KE, Forrester JD. Appendicitis in Low-Resource Settings. Surg Infect (Larchmt). 2020 Aug;21(6):523-532.
12. Mohammed Suleiman Obsa, Bulcha Guye Adema, Getahun Mola Shanka, Eyasu Alem Lake, Gedion Asnake Azeze, Robera Olana Fite. Prevalence of acute appendicitis among patient admitted for acute abdomen in Ethiopia: Systematic review and meta-analysis. International Journal of Surgery Open. 2020; 26:154-160.

The impact of the presence of risk factors for fragility fractures in people with osteoporosis

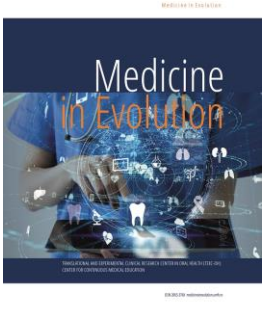

Nae A.[1], Simionescu A.A.[2], Beiu C.[3], Popescu M.N.[4], Stanescu A.M.A.[5]

[1]"Carol Davila" University of Medicine and Pharmacy, 050474, Bucharest, Romania
[2]"Carol Davila" University of Medicine and Pharmacy, Department of Obstetrics and Gynecology Filantropia Clinical Hospital, 011132, Bucharest, Romania
[3]"Carol Davila" University of Medicine and Pharmacy, Department of Oncologic Dermatology, "Elias" Emergency University Hospital, 011461, Bucharest, Romania
[4]"Carol Davila" University of Medicine and Pharmacy, Department of Physical and Rehabilitation Medicine-"Elias" Emergency University Hospital, 011461, Bucharest, Romania
[5]Department of Family Medicine, "Carol Davila" University of Medicine and Pharmacy, Bucharest, 050474, Romania

Correspondence to:
Name: Anca Angela Simionescu
Address: Department of Obstetrics and Gynecology, Filantropia Clinical Hospital 11-13 Ion Mihalache 11-13, district 1, Bucharest, Romania
Phone: +40 3188930/262
E-mail address: anca.simionescu@umfcd.ro and asimion2002@yahoo.com

Abstract

Osteoporosis is an important clinical problem due to the increased bone fragility that predisposes to fractures. The objective of this study was to analyse the implication of risks factors for fragility fractures in people with osteoporosis and the differences between people with osteoporosis without fragility fractures and those with fragility fractures. MATERIAL AND METHODS: We conducted a retrospective study of people diagnosed with osteoporosis. Two groups were formed: one that included people diagnosed with osteoporosis who had fragility fractures that required surgery and one that included people diagnosed with osteoporosis who did not have fractures at the time of inclusion. We compare the two groups in order to differentiate the significance of risk factors for fractures associated osteoporosis. RESULTS: The gender distribution of the two groups highlights the predominance of females, and the average age was 79.8 years with a tendency to distribute osteoporosis to old age; all women in both groups were menopausal; the sedentary lifestyle and reduced physical activity were seen in both groups; 77% of those included in the study showed functional impotence; frequent falls, which predispose to fragility fractures, is noted in the case group at 41 of the 59 included in the study compared to 8 in the control group; the presence of hypertension was noted in 43 people in the case group and 40 in the control group, respectively, while the presence of diabetes and stroke have no statistical significance in this study. CONCLUSIONS: Women and old age are prone to osteoporosis. The presence of menopause and a sedentary lifestyle predispose to functional impotence. In terms of risk factors, falls prevention, screening for hypertension requires careful management of medication that influences bone mineral density.

Keywords: osteoporosis, age, obesity, previous fracture

INTRODUCTION

Osteoporosis, for older men and women, is a major clinical problem. Almost any bone can fracture due to the increased bone fragility of osteoporosis. These are associated with much higher health care costs, physical and mental disability, impaired quality of life, and increased mortality [1,2]. Owing to the incidence of osteoporotic fracture is increase with age, measures to diagnose and prevent osteoporosis and its complications are a significant public health concern [3]. Many other modifiable and non-modifiable risk factors for osteoporosis have also been identified [4]. The treatment of potentially modifiable risk factors and exercise and supplementation with calcium and vitamin D form an essential adjunct to the pharmacological management of osteoporosis. Improved household safety can reduce the risk of falling [5]. Hip protectors are effective in the nursing home population [6,7]. Bone mineral density (BMD) measurement is used to diagnose osteoporosis before an incident fracture and predict fracture risk [8]. Recommendations for treating and preventing osteoporosis are presented based on the bone mineral density score published by the World Health Organization and the National Osteoporosis Foundation [9].

The incidence of hip fractures accelerates at about ten years after menopause in women and after 70 in men. About one million Americans suffer from fragility fractures each year at the cost of more than $ 14 billion [10]. Disability, mortality, and the cost of hip and vertebral fractures are substantial in the rapid population growth, so the prevention of osteoporosis is a significant public health problem [11].

All women aged 65 years or older should be screened for osteoporosis by measuring BMD in the hip and lumbar spine using dual X-ray absorption (DXA) [12].

This recommendation is universally endorsed by the US Preventive Services Task Force (USPSTF) and other professional societies. Although the prevalence of osteoporosis in this patient population is almost 25%, recent data suggest that 1 in 4 women aged 65 to 85 have never had BMD tests. The risk assessment strategy for selecting postmenopausal young women for osteoporosis screening is uncertain [13,14].

Despite the rapid rate of bone loss in the lumbar spine during the menopausal transition, the absolute risk of fracture for a particular BMD is much lower in young postmenopausal women than in older women. In particular, the absolute probability of 5 years of hip fracture is less than 1% until the age of 70-79, when it begins to increase exponentially. Data on the benefits and harms of drug treatment starting at the age of 50-64 and continuing for the next three decades of life are not available [15]. The use of drug treatment in younger women leaves them with fewer pharmacotherapy options at age 70, when the risk of hip fracture begins to increase. However, there is no consensus on all the specific risk factors that should be considered in this decision [2].

Aim and objectives

The objective of this study was to analyze the implication of risks factors for fragility fractures in people with osteoporosis and the differences between people with osteoporosis without fragility fractures and those with fragility fractures.

MATERIAL AND METHODS

We conducted a retrospective observational study between 2020 to 2021 of people diagnosed with osteoporosis. All patients signed written consent at hospital admission for participation in studies research. These data are used for an MD thesis, and local ethical approval was obtained.

This study aimed to determine unmodifiable and modifiable risk factors for fracture in people with osteoporosis. Two groups were formed: one that included people diagnosed with osteoporosis who had fragility fractures that required surgery and one that included people diagnosed with osteoporosis who did not have fragility fractures at the time of inclusion. We want to study if there were differences between the two groups regarding risk factors for fractures as age, weight, physical activity, heredocolateral osteoporosis.

The inclusion criteria were represented by a definite diagnosis of osteoporosis and age over 18 years. The exclusion criteria were age under 18, the uncertainty of the diagnosis of osteoporosis, the presence of other osteoarticular diseases that could cause fractures or functional impotence.

The descriptive data and outcomes for this study were collected from the electronic database, and the observation sheets within the Bucharest University Emergency Hospital and the electronic database and the patient files from the family medicine office. The data were statistically processed using Excel programs. The statistical processing did not allow the identification of any person included in the study, respecting the confidentiality of personal data.

RESULTS

We analyzed 118 persons, men and women. we found more than 80 % of fragility fractures in the hip in women, in the right femoral col, followed by fractures in the left distal radius.

The gender distribution of the two groups reveals the predominant presence of females in both groups, namely 76% (case group) and 71% (control group), compared to males with a presence of only 24% (case group) and 29% (lot witness).

In terms of age, it was between 61 and 97 years in the case group, and the average age was 79.8 years +/- 9.14 standard deviation (ds). the control group was between 57 years and 91 years, with an average age of 79.1 years +/- 8.95 ds. comparing the two groups from the perspective of age groups, older ages in the case group are highlighted (Figure 1).

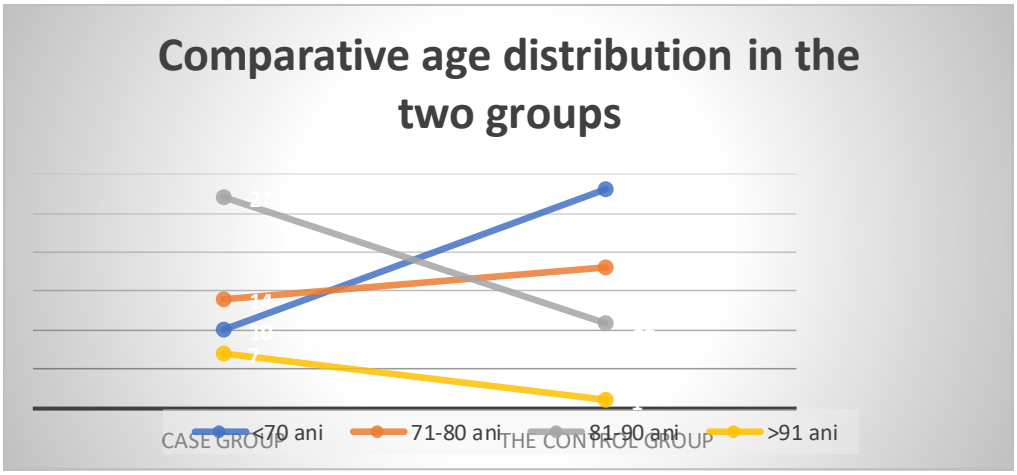

Figure 1. Comparative age distribution in the two groups

Heredocolateral history of osteoporosis reveals the presence of osteoporosis in 21 people in the control group and 25 people in the case group (Figure 2).

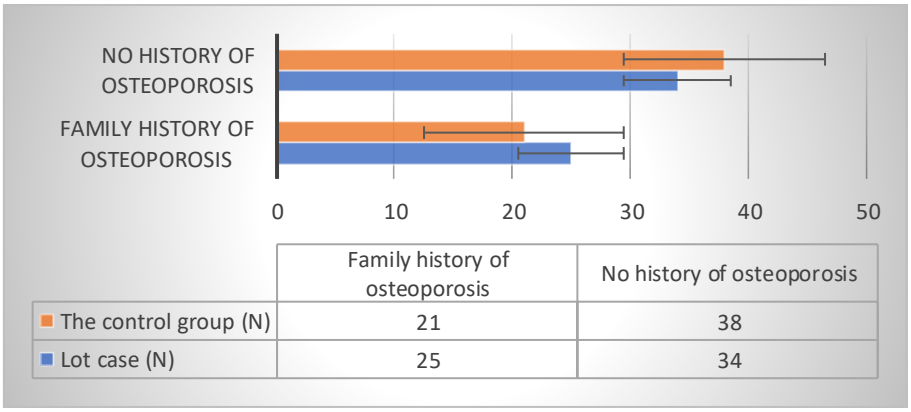

	Family history of osteoporosis	No history of osteoporosis
The control group (N)	21	38
Lot case (N)	25	34

Figure 2. Hereditary collateral history of osteoporosis in both groups

Among the risk factors, smoking was present in only 8% of the people included in the case group; instead, 61% of smokers were in the control group. Alcohol consumption, another risk factor, is present in only 4 of the 59 included in the case group and 8 of the 59 included in the control group. The weight distribution by groups is shown in Figures 3 A and B.

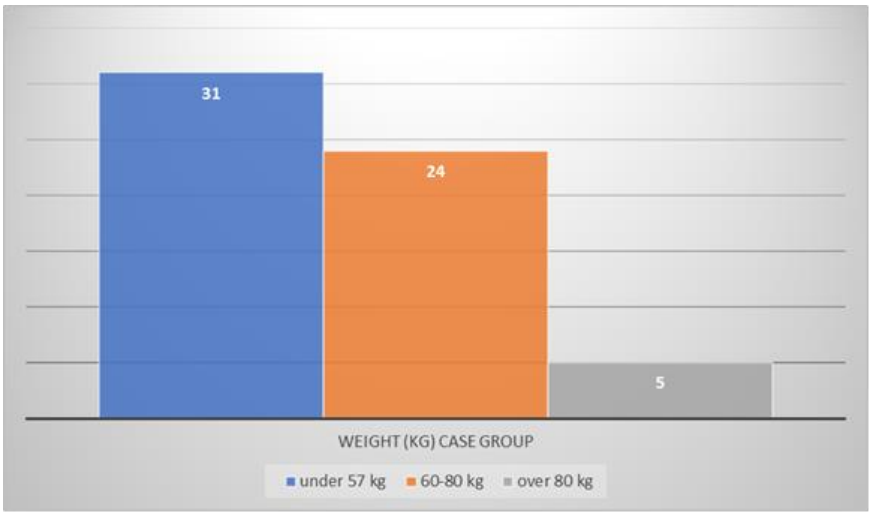

Figure 3A. Distribution by groups according to weight - case group

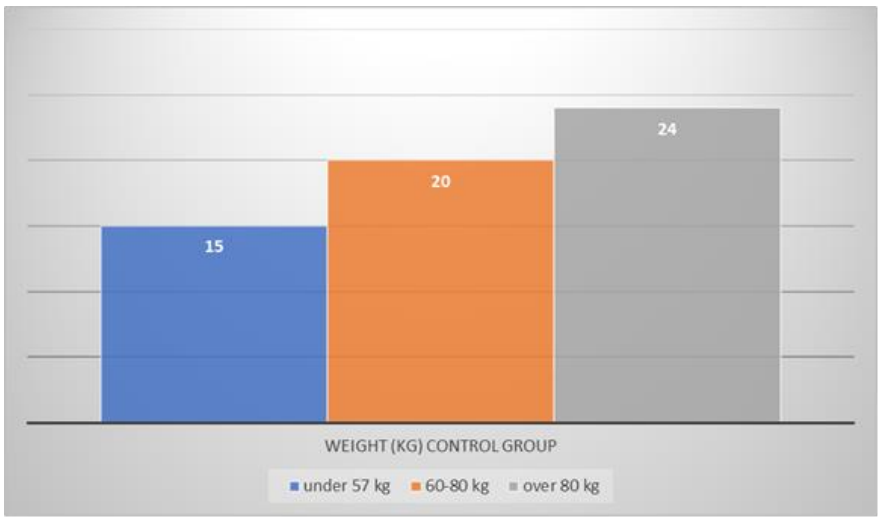

Figure 3B. Distribution by age groups by weight - control group

The lowest body mass index in the case group was 17.6, and the highest of 32.14.

Physical activity in the case group reveals the predominance of a sedentary lifestyle and reduced physical activity. No study participants showed intense physical activity. Physical activity in the control group reveals the presence of reduced physical activity in most patients, 42 out of a total of 59. Intense physical activity is missing. Osteoporosis can be observed in the case group in the heredocolateral antecedents in 70% of people (n=25), and 19 of the 25 people were female. Osteoporosis in the control group is relevant in 66% of study participants.

The presence of menopause in all women included in the study in both groups is noticeable.

Of the total number of people included in the study, all in the case group had functional impotence and only 18 in the control group. A total of 77% showed functional impotence, compared to 23% without functional impotence.

Analysing each comorbidity of patients with osteoporosis, we note the presence of hypertension in 43 people in the case group and 40 in the control group. Diabetes was highlighted as a comorbidity in 8 people in the case group and 12 in the control group. The stroke was highlighted as a personal pathological antecedent in 4 people in the case group and six people in the control group. Regarding obesity as a risk factor, it was found in only 3% of the case group, respectively, in 7% of those who make up the control group.

There is an increased frequency of frequent falls in the case group compared to the control group, where only 9% had frequent falls in the background.

The presence of previous fractures is higher in the case group than in the control group, where only two people had a history of fractures (Figure 4).

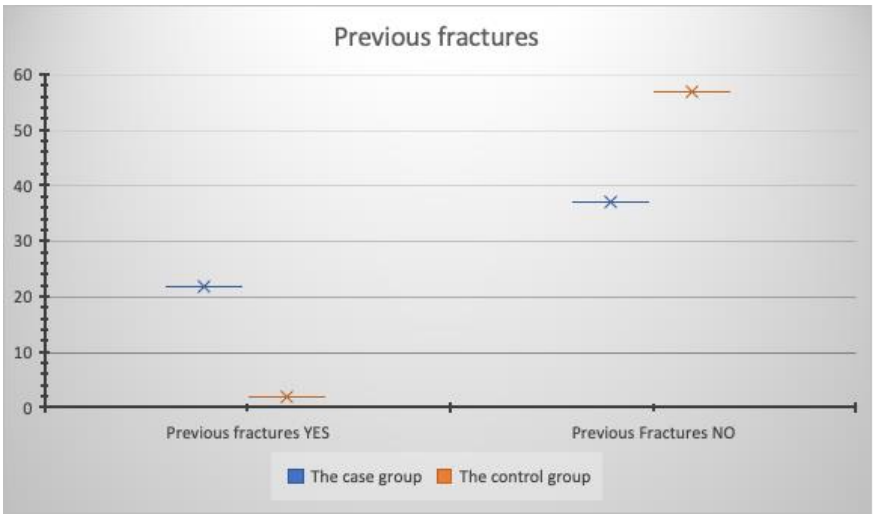

Figure 4. Previous fractures for case group and control group

Medication that may influence bone mineral density or the risk of falling used in the case group and the control group are shown in Figures 5 A and B.

Figure 5. A. Medication - case group (A)

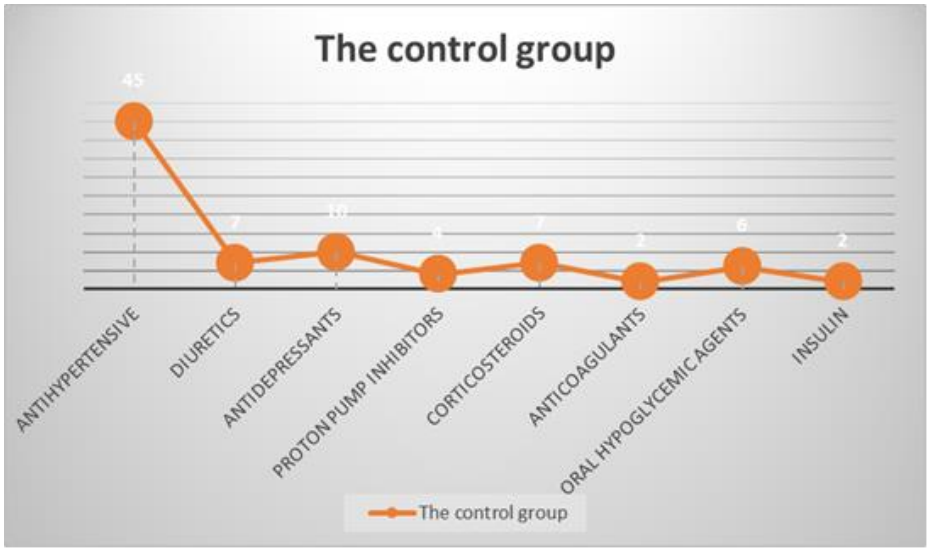

Figure 5. B. Case-control group (B)

From our data it can be seen that femoral neck and PTH fractures predominate, especially among women.

DISCUSSIONS

Our study demonstrates differences between risk factors for fragility predisposing. Osteoporosis remains a common disease among the elderly and is a significant public health problem worldwide. After the age of 30, the reduction of bone mass is an inevitable process, and, consequently, changes in the bone remodelling cycle will lead to bone fragility and an increased risk of bone fractures [16]. A fracture is considered osteoporotic (fragility fracture) if it is caused by relatively low trauma, such as a fall from orthostatism, caused by a force that would not be expected to cause a fracture in a healthy adult. Frequent falls predisposed to fragility fractures are noted in the case group in 41 of the 59 included in the study, while only 9% of the control group had frequent falls. Another factor that predisposes to fragility fractures is previous fractures. These being present in 22 of those included in the case group compared to only 2 in the control group.

Numerous factors that can be classified into the group of risk factors that cannot be influenced (unchangeable factors) and risk factors that can be modified (variable or preventable factors) are involved in osteoporosis [17,18].

As the population ages increases, the incidence of osteoporosis and resulting fragile osteoporotic fractures is increasing. Our study confirms the presence of older ages in the case group. Over 57% of patients with fragility fractures were over 80 years old.

The presence of a family history of osteoporosis does not reveal statistically significant differences between the two groups. Both groups have a high percentage of osteoporosis in the family, clearly a predisposing factor for the development of osteoporosis.

While osteoporosis is diagnosed more frequently in women than men, its incidence in men is also increasing [19]. The present study also reveals the predominance of females in both groups (over 70%). Osteoporosis is rarely diagnosed in premenopausal women. However, the prevalence increases with age due to progressive bone loss. In the United States, it has been estimated that up to 54% (16.8 million) postmenopausal women have low bone mass (t-score of -2.0), and another 20% to 30% (6.9 million) have osteoporosis [20]. In the United States, osteoporosis increases from 15% at age 50 to 70% at age 59 in women aged 80 years. Epidemiological studies in other countries have reported similar findings [21,22]. In the present study, all women in both groups were menopausal.

CONCLUSIONS

The clinical and economic consequences of osteoporosis indicate the need for intervention in high-risk elderly people. A multitude of risk factors can have a significant impact on bone mineral density in the elderly. These factors should be considered in the risk management of fracture to determine if the patient needs further evaluation and/or treatment. Women and old age are prone to osteoporosis. The presence of menopause and a sedentary lifestyle predispose to functional impotence. In terms of risk factors, proper management is required, frequent preventive falls, screening for hypertension also requires careful management of medication that influences bone mineral density.

REFERENCES

1. Eurostat database available at https://ec.europa.eu/eurostat/statistics-explained/index.php?title=Population_structure_and_ageing/ro. Accessed on 01 March 2021
2. Chan MY, Center JR, Eisman JA, Nguyen TV. Bone mineral density and association of osteoarthritis with fracture risk. Osteoarthritis and Cartilage 2014, 22:9 :1251-1258,
3. Hemmatian, H., Bakker, A.D., Klein-Nulend, J, van Lenthe GH. Aging, Osteocytes, and Mechanotransduction. Curr Osteoporos Rep. 2017 ,15:401–411.
4. Chen YW, Ramsook AH, Coxson HO, Bon J, Reid WD. Prevalence and Risk Factors for Osteoporosis in Individuals With COPD: A Systematic Review and Meta-analysis. Chest. 2019, 156(6):1092-1110.
5. Baccaro LF, Machado Vde S, Costa-Paiva L, Sousa MH, Osis MJ, Pinto-Neto AM. Factors associated with osteoporosis in Brazilian women: a population-based household survey. Arch Osteoporos. 2013, 8, 138.
6. Makan AM, van Hout H, Onder G, van der Roest H, Finne-Soveri H, Topinková E, et al. Pharmacological management of osteoporosis in nursing home residents: the Shelter study. Maturitas. 2021, 143, 184-189.
7. Turk AC, Sahın F, Kucukler FK, Devecı H. Analysis of kyphosis, vertebral fracture and bone mineral density measurement in women living in nursing homes. Saudi Med J. 2018;39(7):711-718.

8. Link TM, Kazakia G. Update on Imaging-Based Measurement of Bone Mineral Density and Quality. Curr Rheumatol Rep. 2020, 22(5):13.
9. Vytrisalova M, Touskova T, Fuksa L, Karascak R, Palicka V, Byma S, Stepan J. How General Practitioners and Their Patients Adhere to Osteoporosis Management: A Follow-Up Survey among Czech General Practitioners. Front Pharmacol. 2017 May 11; 8:258
10. GBD 2017 DALYs and HALE Collaborators. Global, regional, and national disability-adjusted life-years (DALYs) for 359 diseases and injuries and healthy life expectancy (HALE) for 195 countries and territories, 1990-2017: a systematic analysis for the Global Burden of Disease Study 2017. Lancet 2018 Nov 10;392(10159):1859-1922.
11. Kucukler FK, Simsek Y, Turk AÇ, Arduc A, Guler S. Osteoporosis and Silent Vertebral Fractures in Nursing Home Resident Elderly Men in Turkey. J Clin Densitom. 2017 Apr-Jun;20(2):188-195.
12. Compston JE, McClung MR, Leslie WD. Osteoporosis. Lancet. 2019 Jan 26;393(10169):364-376.
13. Kanis JA, Cooper C, Rizzoli R, et al. Scientific Advisory Board of the European Society for Clinical and Economic Aspects of Osteoporosis (ESCEO) and the Committees of Scientific Advisors and National Societies of the International Osteoporosis Foundation (IOF). Correction to: European guidance for the diagnosis and management of osteoporosis in postmenopausal women. Osteoporos Int. 2020 Jan;31(1):209. doi: 10.1007/s00198-019-05184-3. Erratum for: Osteoporos Int. 2019 Jan;30(1):3-44.
14. Yusuf AA, Cummings SR, Watts NB, Feudjo MT, Sprafka JM, Zhou J, Guo H, Balasubramanian A, Cooper C. Real-world effectiveness of osteoporosis therapies for fracture reduction in post-menopausal women. Arch Osteoporos. 2018 Mar 21;13(1):33.
15. Albert SG, Reddy S. Clinical evaluation of cost efficacy of drugs for treatment of osteoporosis: a meta-analysis. Endocr Pract. 2017 Jul;23(7):841-856.
16. Musumeci G, Castrogiovanni P, Trovato FM, Weinberg AM, Al-Wasiyah MK, Alqahtani MH, Mobasheri A. Biomarkers of Chondrocyte Apoptosis and Autophagy in Osteoarthritis. International Journal of Molecular Sciences.2015, 16(9):20560-20575.
17. Wimalawansa SJ, Razzaque MS, Al-Daghri NM. Calcium and vitamin D in human health: Hype or real? J Steroid Biochem Mol Biol. 2018 Jun; 180:4-14.
18. Armas LA, Recker RR. Pathophysiology of osteoporosis: new mechanistic insights. Endocrinol Metab Clin North Am. 2012, Sep;41(3):475-486.
19. Bowden Davies KA, Pickles S, Sprung VS, Kemp GJ, Alam U, Moore DR, Tahrani AA, Cuthbertson DJ. Reduced physical activity in young and older adults: metabolic and musculoskeletal implications. Ther Adv Endocrinol Metab. 2019 Nov 19; 10:2042018819888824.
20. Evenepoel P, Cunningham J, Ferrari S, Haarhaus M, Javaid MK, Lafage-Proust MH, et al. European Renal Osteodystrophy (EUROD) workgroup, an initiative of the CKD-MBD working group of the ERA-EDTA, and the committee of Scientific Advisors and National Societies of the IOF. European Consensus Statement on the diagnosis and management of osteoporosis in chronic kidney disease stages G4-G5D. Nephrol Dial Transplant. 2021 Jan 1;36(1):42-59.
21. Dardonville Q, Salguiero E, Rousseau V, Chebane L, Faillie JL, Gautier S, et al. Drug-induced osteoporosis/osteomalacia: analysis in the French and Spanish pharmacovigilance databases. Eur J Clin Pharmacol. 2019 Dec;75(12):1705-1711.
22. Nguyen KD, Bagheri B, Bagheri H. Drug-induced bone loss: a major safety concern in Europe. Expert Opin Drug Saf. 2018 Oct;17(10):1005-1014.

Image analysis of tumor infiltrating lymphocytes components of EGIST microenvironment

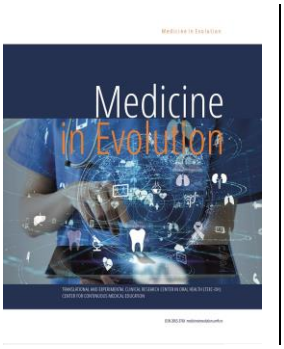

Moldovan V.T.[1,2], Sajin M.[1,3], Ginghina O.[4], Eftimie L.[5], Ali Leila[1,6]

1Department Pathology, University of Medicine and Pharmacy „Carol Davila ", Bucharest, Romania
2PhD student, Doctoral School University of Medicine and Pharmacy „Carol Davila ", Bucharest, Romania
3Department of Pathology, University Emergency Hospital, Bucharest, Romania
4Department of General Surgery University of Medicine and Pharmacy „Carol Davila ", Bucharest, Romania
5Department of Pathology, Central Military Emergency University Hospital "Dr. Carol Davila", Bucharest, Romania
6Department of Pathology of National Institute of Pathology „Victor Babeş ", Bucharest, Romania

Correspondence to:
Name: Leila ALI
Address: Department of Pathology, National Institute of Pathology "Victor Babeş", 99-101 Splaiul Independenţei, sector 5, Bucharest, Romania
Phone: +40720 369 555
E-mail address: dr.leila.ali@gmail.com

Abstract

Extra gastrointestinal stromal tumor (EGIST) are sarcomas originating from Cajal like cells. They are prone to events triggering inflammation.

Aimes and Objectives: To describe into a retrospective study, the intratumoral lymphocytes in a series of EGIST and correlate their density with the proliferation index and morphology.

Methods: Using antibodies against CD5, CD20, CD45, we demonstrated lymphoid cells and structures by using immunohistochemical methods. Slides were analyzed using QuPath for tumor-infiltrating lymphocyte (TIL) density. Tertiary lymphoid structures (TLS) were reported per sample. Statistical analysis was done using the Kruskal-Wallis corrected test and the Pearson coefficient.

Results: We selected 22 cases with an average age of 51 years. Histologically, the batch was composed of fusiform, epithelioid, and mixed EGIST (63%; 14% and 23%). Numerical analysis of immunohistochemical stains showed an average Ki67 of 19%. The average TIL density of T and B cells was 1.6*103 cells/mm2 and 263 cells/mm2. The TLS have an average of 2.41 households/sample. The correlation between T and B cell density and between TIL with Ki67 shows $p > 0.05$ in our EGIST series. The correlation between EGIST histological variants with TIL type density resumed a $p>0.05$.

Conclusion: TIL cell densities are independent histological parameters for EGIST. The TIL arrangement is inhomogeneous in EGISTs; T cells predominate.

Keywords: Extra gastrointestinal stromal tumor, tumor-infiltrating lymphocyte; digital image analysis

INTRODUCTION

Extra gastrointestinal stromal tumor (EGIST) are sarcomas located outside the digestive tube and originating from cells that show differentiation toward Cajal like cells [1]. Down regulation of immune system has been associated with development and progression of various malignancies. Intra-tumoral lymphocytes as part of the microenvironment is a histoprognostic factor as well as a therapeutic target in a large range of neoplasia. Sarcoma's microenvironment represents a frequent subject in numerous studies focusing on diverse components. The microenvironment represents a part of a general response of host organism to invading tumors. It is expected that even if the response is a generally a common one regardless of tumor type, it is modulated by tumoral intrinsic factors. This can lead to various amount of intra-tumoral lymphocytes as the host response must be triggered by different stimulating factors. Thus, the benefits of appreciating TIL into a specific type of neoplasia can be exploited only if a specific type of neoplasia is investigated descriptively from point of view of active actors in this process. Intra-tumoral leucocytes are represented by myeloid series, lymphocytes and histiocytes. Their proportion is expected to vary among neoplasm types as well as their subtypes. From the classical immunological point of view, main actors in tumors progression and suppression are theT cell. Accumulating evidence is supporting that the B cell lineage as well that histiocytes [2], [3]. Immune checkpoint regulating drugs acting on CTLA-4 and anti-PD1 / PD-L1 have been introduced in clinical practice, treating many cancers, including lung, breast, colon, and bladder cancers. The response to these drugs is only partial, estimated to around 30%. Few studies have investigated these actors in EGIST, both as presence and as possible correlation between their morphology, proliferative index, and TIL density. EGIST and their digestive tube counterpart are well known tumors that are susceptible to events that can't trigger host inflammatory responses.

Aim and objectives

We aim to describe in a prospective study, the intra-tumoral leucocytes in a small series of EGIST and corelate their density with the proliferation index and morphology. The text included in the sections or subsections must begin one line after the section or subsection title.

MATERIAL AND METHODS

Archives and databases of "Victor Babes" National Institute of Pathology (INCDVB) and Bucharest University Emergency Hospital (SUUB) were retrospective researched for EGIST cases. The included cases must have a confirmed diagnosis of EGIST and sufficient material for an elementary immunohistochemistry (IHC) testing and digital analysis. The research was based on paraffin embedded tissue and corresponding slides benefiting from Ethics and Scientific Research Committee of INCDVB Bucharest approval no. 83/2020.

Immunohistochemistry was performed to highlight the lymphoid cells and structures using monoclonal antibodies. We used antibodies against cluster of differentiation 5, 20 and 45 (CD5, CD20 and CD45 or leucocyte common antigen). For the proliferative index we estimate the fraction of active tumoral cells marked with Ki67 (clone Mib1). We have preferred monoclonal antibodies from current laboratory stock utilizing clones 4C7, L26 and X16/99 to detect T, B and Common Leukocyte Antigen from Leica Novocastra. Test were performed on a Leica Bond II automated immunostainer. Epitope retrieval was performed fallowing producer recommendations, utilizing Bond epitope retrieval solution 1 and 2. For detection a polymer kit (Bond Polymer-Refine-Detection) was used, and the stain was

performed using 3,3-diaminobezen (DAB) as chromogen. Counterstain was performed as a regular hematoxylin. Positive control slides with tonsillar tissue were performed in parallel with each batch.

Resulting slides were scanned using Leica Aperio LV1 IVD. Resulting files were imported into QuPath[4] software projects. A total of 10 areas of interests totalizing at least 2mm were chosen for each tumor. Small samples were process in totality. A cell detection step followed by positive count cell corresponding to each type of investigated cell lineage was performed. Review of the positive cell detection was made by two pathologists adjusting their morphometric parameters and excluding false positive cell detections. To evaluate tumor-infiltrating lymphocytes (TIL) for the series we used a modified version of the recommendations TILs Working Group 2014. All leucocytes were taken into account, reporting distinctively: lymphocytes B, T and other leukocytes (mainly histiocytes). Neutrophils and plasma cells were not accounted, as they were considered secondary actors and not markedby our immune pannel. The necrotic areas and surrounding leucocytes were avoided. Borders of the invasive tumors were included in the evaluation. Lymphoid tertiary structures (TLS) were reported as numbers per sample. The individual cell population of TLS was not quantified when reporting the density of TIL.

For statistical analysis software we opted for Excel Office 365 with extend statistical package ad-in. A corrected Kruskal-Wallis Test was performed to determine if median and rank of lymphocytes density per sample (T, B and a total number of including histocytes) is different for the three different morphological variants (epithelioid, mixt and spindle cell). Correlation between proliferative index and TIL specific lineage (B cells and T types) were calculated using the Pearson correlation coefficient. The chi squared values were calculated to retrieve the corresponding p value.

RESULTS

We selected 22 cases from a series of cases of EGIST resulted from prior investigations of our institutional database research (work in prepress). The average age of the EGIST lot was 51 years (interval 27-78 years old, with a median of 52 years). The gender was equally distributed with M/F ratio of 1 to 1. Histologically, most of the lot was composed of spindle cell morphology EGISTs (14 cases, 63%) while the remaining cases were composed of epithelioid (3 cases 14%) and mixed type cells morphology (5 cases, 23%). Histological examination showed in most of the cases areas of multiple foci of interstitial hemorrhages of recent type, see figure 1. Tumor front was of bulky type, some cases comporting to a pseudo-encapsulation made by compressing the nearby connective tissues. TILs were barely perceptible in HE, stains more obvious in the periphery of the tumor, but difficult to estimate as a density parameter.

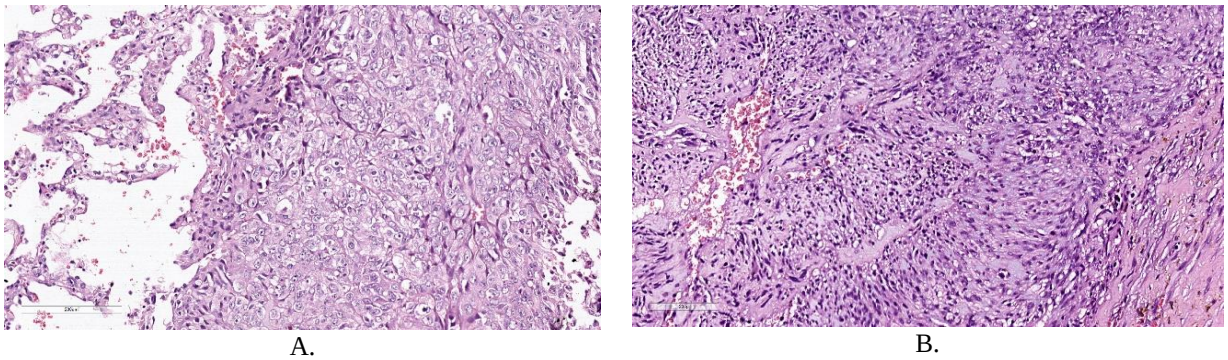

A. B.

Figure 1. Histologic types of EGIST. A. Photography of an epithelioid lung EGIST. Some examples of TIL are pointed by light blue arow heads. They are barely visible in HE stains and reduced in numbers in the epithelioid types of our series. Periphery of a bulky tumoral expansion. On left part of the panel, lung alveolar walls remnants are readily identifiable. Scale bar 200µm, lower left corner B. Spindle cell variant of EGIST. TILs are more abundant, sometimes forming lose aggregates around small vessels pointed by orange arrow (left upper quadrant). HE stains, scale bar 500µm, 100X.

IHC stains showed a proliferation index with Ki67 marking tumoral cells between 1% and 65% with an average 19%. The epithelioid cell type EGISTs comported an average Ki67 of 28%. The mixed types comported a slightly lower value of 26% activated tumor cells. The spindle cell variant comported the lowest ki67, with an average value of 14%.

IHC staining with CD5 CD20 and CD45 clearly delimited the TLS from lose or compact aggregates of lymphoid cells. Their numbers per sample was recorded with an average of 2,41 foci / sample (varying from 0 to 8 with a median value of 2 TLS), see figure 2 and 3.

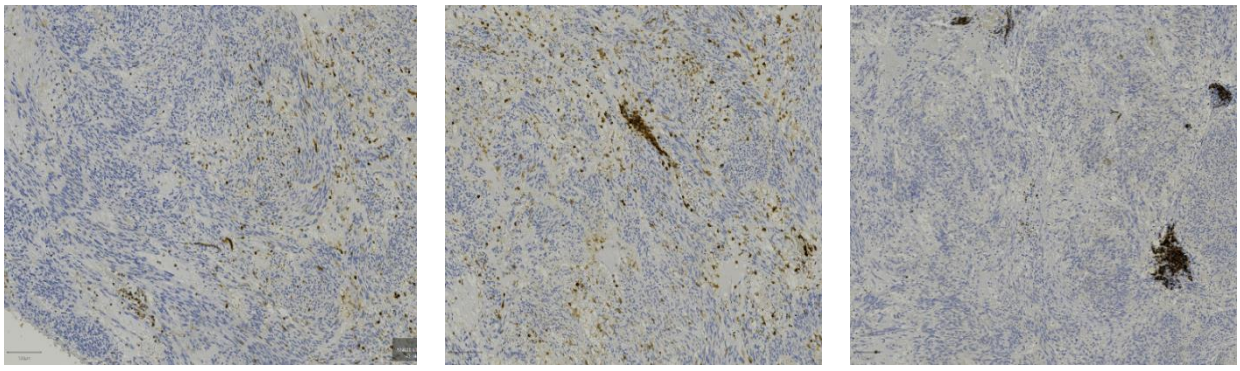

A. B. C.

Figure 2. Immunohistochemical detection of TIL. A. Spindle cells type EGIST exhibiting variable distribution of intra-tumoral leucocytes detected with CD45 (T and B lineage TIL as well as TAM (green arrow). Intravascular lymphocytes were avoided be selecting an appropriate region of interests (dark blue arrowhead left bottom corner). B. Picture is highlighting a compact aggregate of forming a true TLS (orange arrow). Distribution of isolated intra- tumoral leucocytes is relative diffuse and homogenous. Detection with anti CD45 antibody. C. Immunohistochemical detection of B lineage TIL using CD20antibody lights a few isolated cells as well as two compact TLS (green arrow heads) difficult to consider due to numerous overlaps. All stains were made with DAB, counterstain Hematoxylin. All photographs correspond to screen snapshoots exported from QuPath and contains a scale bar of 100µm located at bottom-left corner.

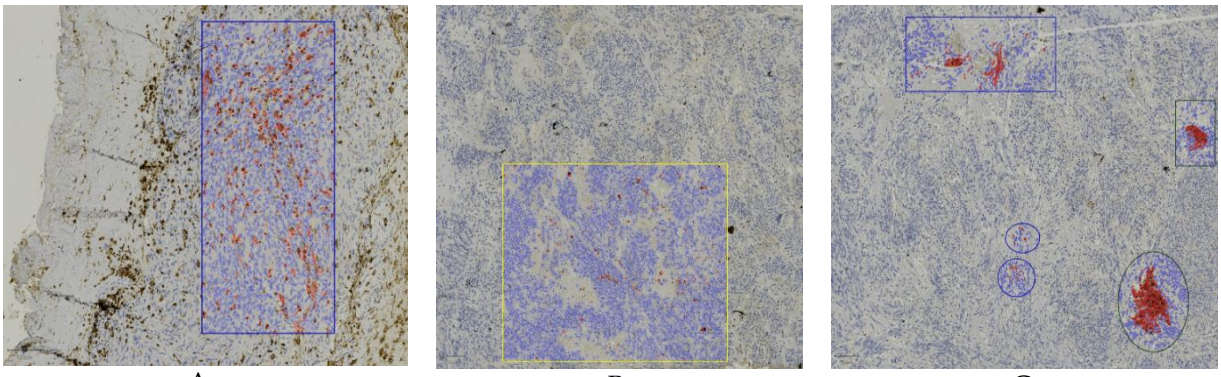

A. B. C.

Figure 3. Digital image analysis of TIL. A. Periphery of a cystically degenerated EGIST. Immunohistochemical detection of T lineage TIL using CD05 antibody. Region of interest marked by blue border rectangle. In translucent red are colored positive cell detection (with brown background as control). Tumoral cell marked as light blue cell shapes. Periphery of the sample contains lose clusters of T-cell TIL , overlapping each other making difficult to estimate. B. Central region of spindle cell type EGIST. Region of interest marked by yellow border rectangle. In translucent red are colored positive cell detected with CD05 antibody. Notably in this case it was a homogenous distribution and low density of T-cells TIL compared to case presented in figure 3A. C. Immunohistochemical detection of B-cell lineage TIL in the same EGIST case as in figure 2C. Positive B cell detected by QuPath software are marked in red. Regions of interest ellipse and rectangle marked with blue borders while the discarded All stains were made with DAB, counterstain Hematoxylin. All photographs correspond to screen snapshoots exported from Qu-Path and contains a scale bar of 100µm located at bottom-left corner

Image data analysis showed a predominance of T cell lineage TIL versus the B cell lineage. In average, the positive CD5 was 1,6*103 cells/mm (range 0,148-6,5*103/mm2; a trimmed average exclusion of 5% extreme values was 1,4*103/mm2). TIL positive for CD20 showed an average density of 263 B cells / mm2 (range 0,04-2,6*103/mm2; a trimmed average with exclusion of 5% extreme values was 153 B cells/mm2). TAM counting using nuclear size restriction parameters and CD45 detection did not yielded confident results.

Statistical analysis of correlation between the tumor type and number of T cell lineage and the other TIL revealed a p higher than the proposed α. Pearson correlation between number of T and B cell TIL with r=-0,156; t=0,674 and a p =0,5077. Same correlation coefficient was calculated to test the association between type of TIL and the ki67 values showing a r =0,096 with t=0,41; and a p =0,68 for T cell TIL density. The B cell density associated with the proliferative index has r=-0,268; t=1,14; and a p value of 0,2675 in our EGIST series.

The Kruskal–Wallis test to compare difference between histological variants of EGIST with T cell type TIL density resulted in H=0,00485 with a p=0,99 (two tailed test, df=2). Same test to compare the rank differences in B cell type TIL density and the three histological variants of EGIST, presented a H= 1.099 with p=0,577; see figure 4.

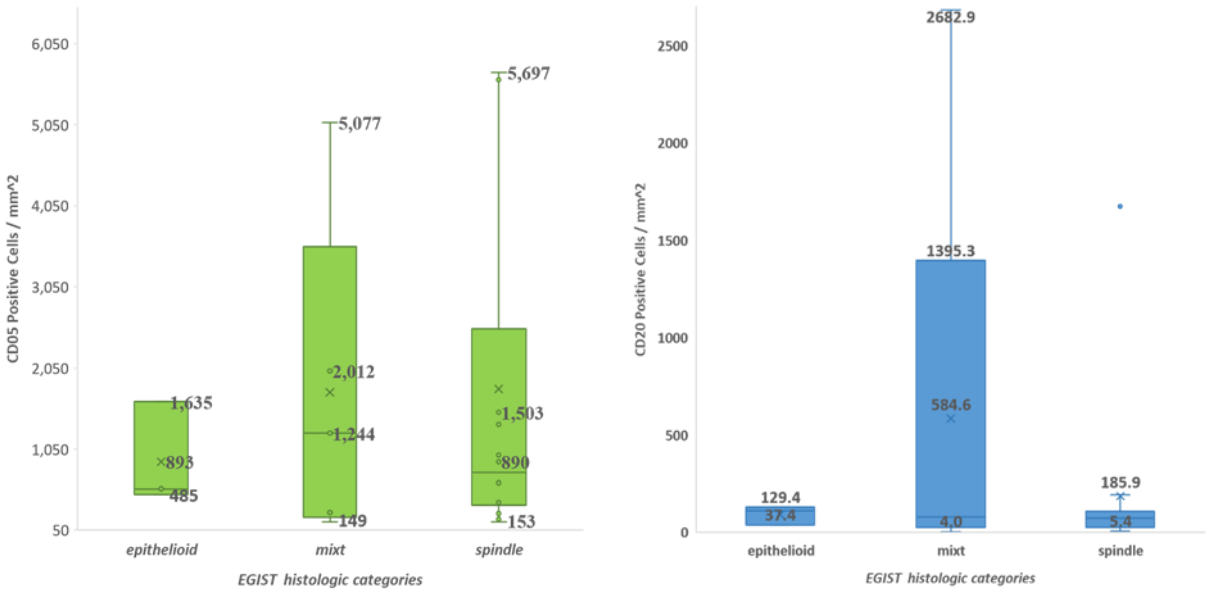

Figure 4. Graphical representation of the number of tumor T and B lymphocytes in the EGIST case series. Left panel: T lymphocyte (positive for CD05) count per square millimeter by histological categories. Values with an order of magnitude ranges from hundreds to a maximum 5,7 thousand. Further testing did not corelate the parameter with the histological category (see details in text). Right panel: Number of B lymphocytes (CD20 positive) per square mm, by EGIST histological categories. Inhomogeneous distribution with values spanning between tens and maximum 2.7 thousand, much lower than T lineage lymphocytes

DISCUSSIONS

The term GIST was first attributed by Mazur et Clark [5] in 1983 for tumors arising in the gastrointestinal tract that on electron microscopy showed both aspects of smooth muscle and nerve cell-like organelles. EGIST was documented as the localization of this type of neoplastic cells outside the digestive tract. It has been proven on small series that they do behave more aggressively that their counterpart in the digestive tract but share a common immunophenotype as well the same molecular defects.

Like other neoplasms, these sarcomas have a microenvironment with a varied composition. The tumor microenvironment contains three major structural components: microvessel (lymphatic and blood neoformation) tumor stroma, and host immune cells. To these, are added histological structures of the body that are incorporated by the neoplastic process as well as various precursor cells that take part in the process of tissue repair and construction (fibroblasts, myofibroblasts, etc.). Various cytokines and inflammatory factors along with various substances with a hormonal role in promoting and developing the neoplastic process are considered part of the tumor microenvironment. In recent years, the therapeutic advancement of immunotherapy has led to extensive morphological, proteomic, and genomic investigation of the entire tumor environment. From this point of view, sarcomas are difficult to investigate due to the low number of annual cases and the high number of histological types. While GIST is the most common sarcoma of digestive tract, the EGSIT remains an elusive target. The tumor infiltrating leucocytes contain both B and T cell lineages lymphocytes, as well as several macrophages recruited from circulating monocytes. Other inflammatory events that take part in the tumor development (cystic degeneration, necrosis, etc.) contribute to the tumoral environment, in addition to neutrophils and other myeloid derived leukocytes.

The mini-series of 22 EGIST cases that we selected in our study, showed a high density of T cell TIL compared to the B lineage by a factor of 6. Our initial hypothesis that T cell lineage TIL number and subsequent their density, could be correlated to the rate of

multiplication of the tumor and/or its histological variant showed a p>0,005 that could not reject the null hypothesis.

T cell lymphocytes are ubiquitous in all neoplasia. They play a central role in adaptive immune response and are the newest of the CART cell therapies. As a rule, their apparent role is to limit the tumor development as their presence results in better outcomes and prognosis correlating with increased amounts of T cells. This was shown in numerous studies for melanoma, breast cancer colorectal carcinoma, as well as for sarcomas. The immune-mediated cell death response in GIST was associated with presence of CD8 positive cells T cell, so called cytotoxic types. Their relationship with tumoral associated macrophages (TAM) is incompletely understood as their activity is normally enhanced by activated macrophages. In the context of GIST, some studies suggested that administrations of anti- CD40 or PDL 1 ligands activates TAM to an M1 form. The activated TAM increase secretion of diverse lymphokines that stimulates the cytotoxic activity of TIL. Furthermore the benefits of imatinib therapy is partially explained by it's indirect effect on decreasing tumoral expression of the indoleamine 2,3-dioxygenase in vitro models [6]– [8].

Using digital image analysis our investigations confirmed the general trend of a low B cell lineage TIL in EGIST. Their presence was scarce, leading to an apparent homogenous distribution. In our study we noticed they were more abundant intratumoral in the form of small aggregates around capillaries. Occasionally, intravascular spots were prominent, possibly as a result of a vascular marginalization and adhesion due surgical maneuvers. Their leukodiapedesis ability trending to form local TLS, has to be revealed by further studies. It is well accepted that B cell lymphocytes are the principal actors in humoral immune response. CD20 marks a plethora of B-cell types, excepting the very immature forms and highly differentiated plasma cells. In neoplasia development, their role remains elusive, an in general they are reduced in number compared to T cell lineage and located predominantly inside TLS. In neoplasia, it seems to fulfil the role of ambivalent agents, acting as regulators and as promoters of antitumoral activity. Their function as direct cytotoxic actor as well as stimulating T cell to secrete diverse cytokines was investigated in several studies [2], [9]. On the other hand, suppressive effects were noted when acting as B cell regulators, interfering with the functions of TAM and T cell TIL [3]:

In our study we tried to assess the presence on TAM. We have applied following technical setups to identify their presence. First, we setup the cell detector procedure to identify cells with a surface area bigger than 250 μm2, a nucleus dimeter bigger than 10μ, and membranous staining for CD45. These lead to some positive results, but the number of cells selected in these setups showed to be higher than the number of cells obtained after subtracting total TIL from the sum of fully positive cells with a cell diameter bigger or equal to 8 μm. This inadvertence can be partially explained by the difference between the section plans. Their presence in the context of neoplasia has been associated with poor prognosis [10]. In the case of the neoplasia, they will transform from attracted monocytes into TAM. Theoretically they can serve as a backbone for presenting tumoral antigens and triggering the immune response. Due to local secreted factors (mainly cytokines like IL6 IL8 IL10 as well as PDL1) in solid tumors their active role is suppressed [11], [12]. Acting like inhibitor cells that suppress the potential response of T cell has been shown in various studies [13], [14]. In GIST, the macrophages were investigated as potential targets for therapies, and they are characterized as the second most prominent immune cell population after the T cells [15], [16]. Till now, there are no studies that investigated their prevalence in EGIST.

In our pursuit to quantify the tertiary lymphoid structures (TLS) using digital analysis of slide images we faced the first impediment to distinguish them from lymphoid aggregates. Lack of cellular morphology and zonal distribution of antigen-specific B and T lymphocytes, facilitated their classification. TLS are found in solid tumors a microenvironment reaches in

inflammatory factors and cells. Their presence is associated with better prognosis and a better response to immune therapies in melanoma, breast carcinoma and sarcomas including GIST [17]– [19].

From our perspective, the study of TIL using the digital slides and corresponding software is the best approach in reporting immune components, as well as for gathering information about the immunophenotype status in the immune check points. The study is however limited in these aspects due to lack of multiplex IHC and subclassification of the TIL. Another drawback and time-consuming event were the identification of small foci of interstitial hemorrhages as they were prone to DAB precipitations leading to false positive identifications of TIL by the software. Very small amounts of individual red blood cells found in the interstitial spaces where more easily identifiable in visceral localization than in (pseudo)cystic degenerated structural parts of EGISTs. This was address by increasing the amount of saturation in the blue channel hist, searching for the presence of a central nucleus (blue), as well as revisiting manually each portion or region of interest on the physical slide by pathologists. Despite this, similarities with other studies and past experience of the authors recommends these method over the use of less accurate expression like "brisk" and "non-brisk TIL" [20]– [22].

CONCLUSIONS

In our study we were able to highlight the variable morphological immunophenotype spectrum of TIL EGISTs. The main cellular actor in the immune response to EGIST presence are T-cell TIL. The TIL and TLS disposition is inhomogeneous in EGIST. We underlined the potential of TIL density as a histological parameter independent from morphological variant as well as from proliferative rate in our EGIST.

The benefits of digital image analysis of TIL is enormous facilitating regions of samples to be inspected and supervised. Regardless of that, multiplexing methods are further necessary as they can precisely identified and localize the main immune cell actors in this act, leaving to proteomics tests the role to describe scenery.

REFERENCES

1. Angelo Paolo Dei Tos, Jason L. Hornick, Markku Miettinen, Ian R. Wanless, and Eva Wardelmann, "Gastrointestinal stromal tumour," in Soft tissue and bone tumours, 5th ed., vol. 3, Organisation mondiale de la santé, Ed. Geneva: OMS, 2020.
2. F. Petitprez et al., "B cells are associated with survival and immunotherapy response in sarcoma," Nature, vol. 577, no. 7791, pp. 556–560, Jan. 2020, doi: 10.1038/s41586-019-1906-8.
3. Y. Zhang, R. Morgan, E. R. Podack, and J. Rosenblatt, "B cell regulation of anti-tumor immune response," Immunol Res, vol. 57, no. 1–3, pp. 115–124, Dec. 2013, doi: 10.1007/s12026-013-8472-1.
4. P. Bankhead et al., "QuPath: Open source software for digital pathology image analysis," Sci Rep, vol. 7, no. 1, p. 16878, Dec. 2017, doi: 10.1038/s41598-017-17204-5.
5. M. T. Mazur and H. B. Clark, "Gastric stromal tumors. Reappraisal of histogenesis," Am J Surg Pathol, vol. 7, no. 6, pp. 507–519, Sep. 1983, doi: 10.1097/00000478-198309000-00001.
6. J. Q. Zhang et al., "Macrophages and CD8+ T Cells Mediate the Antitumor Efficacy of Combined CD40 Ligation and Imatinib Therapy in Gastrointestinal Stromal Tumors," Cancer Immunol Res, vol. 6, no. 4, pp. 434–447, Apr. 2018, doi: 10.1158/2326-6066.CIR-17-0345.
7. M. J. Cavnar et al., "KIT oncogene inhibition drives intratumoral macrophage M2 polarization," Journal of Experimental Medicine, vol. 210, no. 13, pp. 2873–2886, décembre 2013, doi: 10.1084/jem.20130875.

8. V. P. Balachandran et al., "Imatinib potentiates antitumor T cell responses in gastrointestinal stromal tumor through the inhibition of Ido," Nat Med, vol. 17, no. 9, pp. 1094–1100, Aug. 2011, doi: 10.1038/nm.2438.
9. M. Shen, Q. Sun, J. Wang, W. Pan, and X. Ren, "Positive and negative functions of B lymphocytes in tumors," Oncotarget, vol. 7, no. 34, pp. 55828–55839, Jun. 2016, doi: 10.18632/oncotarget.10094.
10. M. Ryder, R. A. Ghossein, J. C. M. Ricarte-Filho, J. A. Knauf, and J. A. Fagin, "Increased density of tumor-associated macrophages is associated with decreased survival in advanced thyroid cancer," Endocr Relat Cancer, vol. 15, no. 4, pp. 1069–1074, Dec. 2008, doi: 10.1677/ERC-08-0036.
11. A. L. Doedens et al., "Macrophage expression of hypoxia-inducible factor-1 alpha suppresses T-cell function and promotes tumor progression," Cancer Res, vol. 70, no. 19, pp. 7465–7475, Oct. 2010, doi: 10.1158/0008-5472.CAN-10-1439.
12. M. Casanova-Acebes et al., "Tissue-resident macrophages provide a pro-tumorigenic niche to early NSCLC cells," Nature, vol. 595, no. 7868, pp. 578–584, Jul. 2021, doi: 10.1038/s41586-021-03651-8.
13. A. A. Barkal et al., "CD24 signalling through macrophage Siglec-10 is a target for cancer immunotherapy," Nature, vol. 572, no. 7769, pp. 392–396, Aug. 2019, doi: 10.1038/s41586-019-1456-0.
14. A. Yadav, B. Kumar, J. Datta, T. N. Teknos, and P. Kumar, "IL-6 promotes head and neck tumor metastasis by inducing epithelial-mesenchymal transition via the JAK-STAT3-SNAIL signaling pathway," Mol Cancer Res, vol. 9, no. 12, pp. 1658–1667, Dec. 2011, doi: 10.1158/1541-7786.MCR-11-0271.
15. X. Mao et al., "Single-cell transcriptome analysis revealed the heterogeneity and microenvironment of gastrointestinal stromal tumors," Cancer Sci, vol. 112, no. 3, pp. 1262–1274, Mar. 2021, doi: 10.1111/cas.14795.
16. J. Chantharasamee et al., "Translating Knowledge About the Immune Microenvironment of Gastrointestinal Stromal Tumors into Effective Clinical Strategies," Curr Treat Options Oncol, vol. 22, no. 1, p. 9, Jan. 2021, doi: 10.1007/s11864-020-00806-z.
17. R. Cabrita et al., "Tertiary lymphoid structures improve immunotherapy and survival in melanoma," Nature, vol. 577, no. 7791, pp. 561–565, Jan. 2020, doi: 10.1038/s41586-019-1914-8.
18. N.-N. Zhang et al., "Prognostic impact of tertiary lymphoid structures in breast cancer prognosis: a systematic review and meta-analysis," Cancer Cell Int, vol. 21, no. 1, p. 536, Oct. 2021, doi: 10.1186/s12935-021-02242-x.
19. Q. Lin et al., "Tumor-associated tertiary lymphoid structure predicts postoperative outcomes in patients with primary gastrointestinal stromal tumors," Oncoimmunology, vol. 9, no. 1, p. 1747339, 2020, doi: 10.1080/2162402X.2020.1747339.
20. V. T. Moldovan, L. Ali, M. Costache, M. Sajin, and A. Lazaroiu, "Comparison of Digital and Conventional Measurements of the Morphometric Prognostic Parameters in Cutaneous Melanoma," Diagnostic Pathology, vol. 1, no. 8, 2016, doi: http://dx.doi.org/10.17629/www.diagnosticpathology.eu-2016-8:221.
21. L. Ali et al., "Digital assessment of depth of invasion in melanoma using different immunohistochemical stains," Arch Balk Med Union, vol. 55, no. (2), pp. 290–297, 2020, doi: https://doi.org/10.31688/ABMU.2020.55.2.12.
22. R. Hristu, L. G. Eftimie, S. G. Stanciu, R. R. Glogojeanu, P. Gheorghita, and G. A. Stanciu, "Assessment of Extramammary Paget Disease by Two-Photon Microscopy," Frontiers in Medicine, vol. 9, 2022, doi: https://doi.org/10.3389/fmed.2022.839786

Tear ferning test and ph of the tears at cell phone users

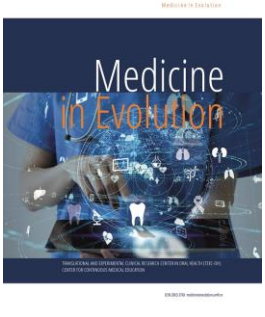

Jurca A. M.[1], Stanila A.[2], Gajta A.[3], Stanila D.[4]

[1,2,4]University "Lucian Blaga" of Sibiu, Sibiu, Romania.
[3]West University of Timisoara, Dept. of Physics, Bd. V. Parvan, no.4, Timisoara Romania General Hospital Dept. of Ophthalmology Vršac, Abraseviceva bb., Vršac, Serbia

Correspondence to:
Name: Alexandra Maria Jurca
Address: Splaiul Nistrului, nr. 6, etaj. 4, ap. 20, Timisoara, Timis
Phone: +40726657839
E-mail address: dr.alexandra.jurca@gmail.com

Abstract

Electromagnetic radiation emitted by mobile phones and other modern devices has potentially harmful effects on ocular surface. The aim of this paper was to investigate the effects of electromagnetic radiation emitted by the phone mobile on the tear film and to make an analysis of the changes that occur on the ocular surface after using the mobile phone. For this study, we selected a total of 55 subjects, young, healthy, without chronic treatment, who are not contact lens wearers and who have no history of ophthalmic surgery.

Tear pH and tear ferning test (TFT) were performed on all subjects before and after being exposed to electromagnetic radiation emitted by the mobile phone for 5 minutes. Following the analysis of the obtained results, electromagnetic fields generated from high frequency microwave radiation modifies pH of the tear film and quality of tears, leads to damaging effect on the tear film and ocular surface.

Keywords: tear ferning test, tear PH, cell phone user

INTRODUCTION

High frequency microwave electromagnetic radiation from mobile phones and other modern devices has the potential to damage eye tissues, but its effect on the tear film and ocular surface is insufficiently unknown at present. The tear film is a nourishing, lubricating and protecting layer that bathes the ocular surface.

A healthy and stable preocular tear film plays a vital role in maintaining both the optical quality of the eye and the health of the ocular surface. Modification of its components results in symptoms of discomfort, visual disturbance, tear film instability with potential damage to the ocular surface, accompanied by increased osmolarity of the tear film and inflammation of the ocular surface [1, 2]. With the increasing use of smartphones, recent studies have reported an association between ocular health and smartphone use. Because increased time of use of smartphones is related to Dry Eye Disease (DED), excessive use of smartphones may affect the tear film and the ocular surface [3].

A recent study indicated that blue light emitted from the smartphone screen had adverse effect on the corneal epithelial cells in humans. Overexposure to blue light caused deterioration of the tear film and increased levels of inflammatory markers and reactive oxygen species (ROS) production at the ocular surface of mice [4].

Aim and objectives

The aim of this study was to investigate the effects of high frequency microwave electromagnetic radiation (1.1GHz, 2.22 mW) on the tear film and PH of the tears in mobile phone users.

MATERIAL AND METHODS

The study included 55 subjects, aged between 18 and 25 years, healthy people without associated diseases, without allergies and without local and general chronic treatment. Schirmer I test was done to all subjects before cell phone use. Tear Ferning Test (TFT) and tear pH was done prior and after 5 minutes of cell phone use.

For Schirmer test we use standard paper strips. One free end is placed in the bottom of the conjunctival sac for 5 minutes. After 5 minutes, the amount of weething of the paper strips is measured and noted in milimeters. Normal values of Schirmer I measurements are > 15 mm/5 minutes.

For TFT a small sample of tears was collected along the lower tear meniscus using a glass capillary tube, the sample was expelled from the tube onto a glass slide and allowed to air dry. This was then evaluated under a microscope. The volume of the drop deposited on the slide should be sufficient to result in a stain at least 2-3 mm in diameter after drying, to provide sufficient field for crystallization and examination.

The results were evaluated using Rolando Classification [**5**], where type I has a lot of ferns with multiple trees, well represented and present on the entire surface of the drop. Type II, abundance of ferns with free spaces between them, type III has a rare or even unique fern, with large free spaces and type IV demonstrates the absence of ferns, being visible only some mucus threads.

Depending on the tear film composition, a variety of ferning patterns can be observed; healthy tear samples produce full dense ferning patterns [Figure 1], while the ferning pattern is fragmented or absent in a dry eye sample.

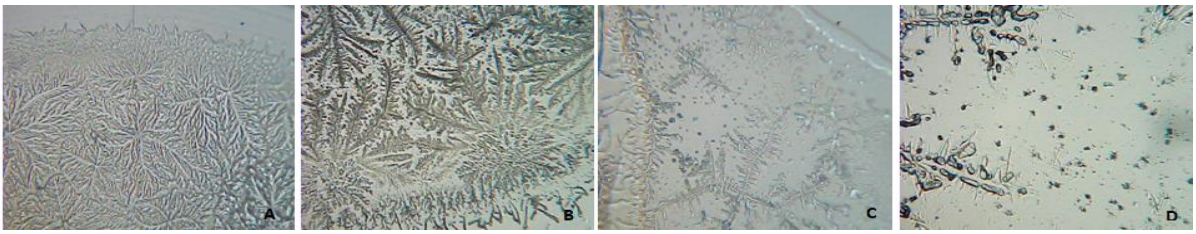

Figure 1. Tear Ferning Test type I (A), II (B), III (C), IV (D)

For the tear pH, we used pH strips of paper inserted into the conjunctival sac and left to soak with tears, then the color obtained was compared with the color of the test scale. Normal values are considered between 6.5 - 7.6.

RESULTS

Of the 55 subjects, 30 were female and 25 male [Figure 2], 33 smokers and 22 non-smokers.

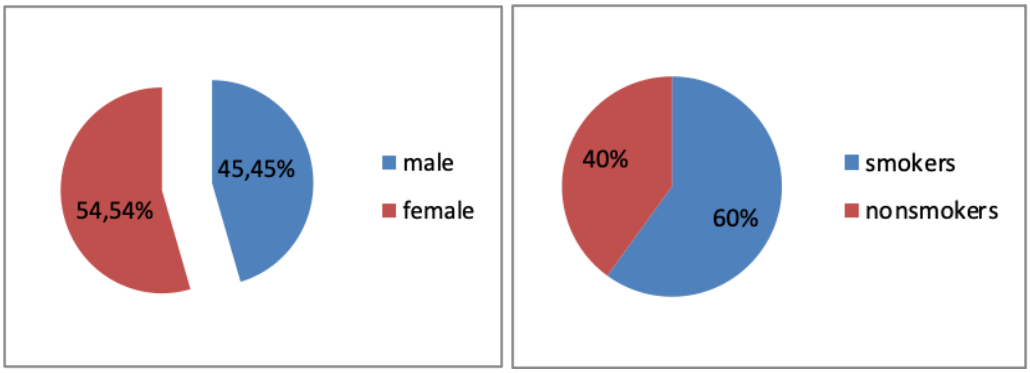

Figure 2. Distribution of patients by gender and by smokers / non-smokers

All the patients had normal values on the Schirmer test. The Schirmer test was performed prior to exposure to the mobile phone. The Schirmer I test after exposure to mobile phone was not performed due to long examination time, which would lead to false results.

Both, Tear PH and TFT were measurea before and after using mobile phone for 5 minutes. All investigations were done on one eye, the eye on which the mobile phone was kept for 5 minutes.

Tear pH values were divided into 3 groups: PH between 7-8, PH between 8 – 9, PH > 9. Tear PH measurements before using the mobile phone did not detect pH values above 9 in any patient. 89.09% of patients had a pH between 7 -8, and 10.90% had a pH value between 8-9.

After using the mobile phone for 5 minutes, the pH values were much changed. 10.90% of patients had a pH between 7 -8, 72.72% had a pH value between 8-9, and a pH above 9 was found in 9 (16.36%) of the patients. There is a tendency to alkalize the pH after using the mobile phone for 5 minutes [Figure 3] the trend that also occurs in Dry Eye Syndrome.

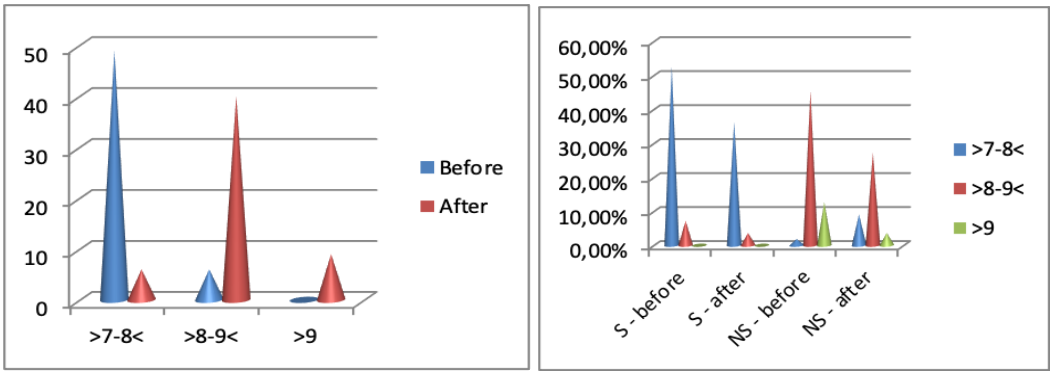

Figure 3. Tear PH values before and after using mobile phone.
*S – smokers; N-S – non-smokers

Regarding Tear Ferning Test (TFT), prior to exposure to mobile phones most of the patients had TFT type I and II, type III was found just in 4 of the patients. The results show that after 5 minutes of using the mobile phone, type I was found in 3 patients, type II in 8 of the patients and type III and IV was present in almost 80% of the subjects [Figure 4]. This is clear evidence that microwave radiation affects the quality of tears.

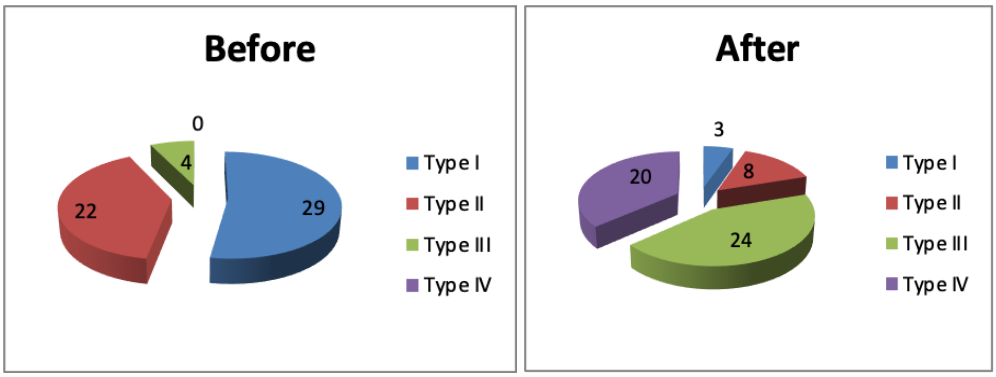

Figure 4. Distribution of patients according to the TFT result before and after exposure to the mobile phone

The image below [Figure 5] shows the results of TFT in patients before and after cell phone exposure.

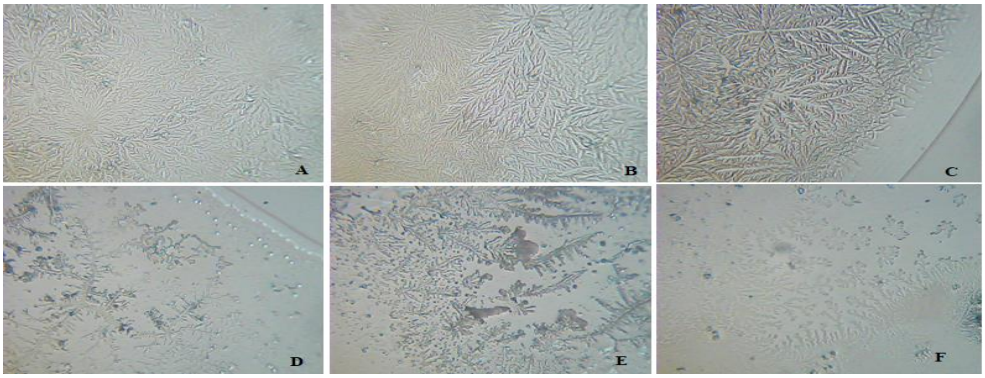

Figure 5. Tear ferning test before (A,B,C) and after(D,E,F) the exposure to mobile phone

DISCUSSIONS

Electromagnetic radiation emitted by mobile phones and other modern devices has potentially harmful effects on ocular surface. Their effects on the eye surface and tear film are little known so far. Most mobile phones have a small antenna attached to or built into the

phone. Because this antenna is very close to the user's head, there is a much higher radio frequency exposure than other types of radio frequency systems [6]. Changes in the human body occur as a result of exposure to high levels of radio frequency energy. This energy leads to the production of large amounts of heat that the body is not able to eliminate [7].

The pH values measured before using the mobile phone are lower compared to similar data corresponding to the pH test after using the phone, the differences having a statistical significance.

The group of smokers has higher PH values compared to non-smokers. The differences are statistically significant, both when the measurements were taken before and after the use of the mobile phone.

Fisher [8] reported an alkaline change of 2.5 ± 0.6 units pH / min associated with prolonged opening of the eyes, with a maximum value of 9.3, however, the tear film reaches equilibrium after 30-60 seconds.

A study by Willcox[9] shows that in the case of all the physical measures of the tear film, the place of collection can influence the result obtained. Tears collected for pH assessment are usually those in the lower meniscus and may not reflect the pH on the surface of the eye. Slight acidification of the tear film by approximately 0.2 pH units can be observed after closing the eyes overnight or for one hour [10].

The results of the tear ferning test show that microwave radiation emitted by the mobile phone signigicantly changes the physical appearance of the tear, affecting the quality of the tear film. In the past, some authors considered that the appearance of fern leaf, the crystallized tear, is due to the amount of mucus present in the tear film [11]. The crystallization of the tear in the form of "fern leaf", according to some authors, depends on the amount of protein in tears [12]. The low amount of protein in tears, in people with dry eye syndrome, forms different patterns of fern leaf. The test correlates with clinical signs and is an objective guide in tracking the effects of dry eye therapy. The combination of several risk factors presents more pronounced changes in the tear film and an increased risk for dry eye syndrome [13].

Regardless whether the measurements were made before or after exposure tothe mobile phone, there are no differences between the fe-male and male groups in terms of pH or TFT values.

CONCLUSIONS

In conclusion, electromagnetic fields generated from high frequency microwave radiation modifies pH of the tear film and quality of tears, leads to damaging effect on the tear film and ocular surface. It has also been recognized that a particularly vulnerable group might be children and young people, as they are likely to have the highest cumulative exposure to radiowaves from mobile devices.

It is recommended to use cell phones from a distance to minimize exposure, thus reducing any potential harmful effects of cell phone use on the tear film and ocular surface.

REFERENCES

1. McCollumCJ, Foulks GN, Bodner B, et al. Rapid assay of lactoferin in keratoconjunctivitis sicca. Corneea.1994; 13:505-508
2. Pflugfelder SC, Jones D, Ji Z, Alfonso A, Monroy D. Altered cytokine in the tear fluid and conjunctiva of patients with Sjogren`s syndrome keratoconjunctivitis sicca. Curr Eye Res. 1999; 19: 201-211

3. Choi JH, Li Y, Kim SH, et al. The influences of smartphone use on the status of the tear film and ocular surface. PLoS One. 2018;13(10):e0206541. Published 2018 Oct 31. doi:10.1371/journal.pone.0206541
4. Lee HS, Cui L, Li Y, Choi JS, Choi JH, Li Z, et al. Influence of light emitting diode-derived blue light overexposure on mouse ocular surface. PLoS One. 2016;11(8):e0161041 10.1371/journal.pone.0161041
5. Rolando M. Tear mucus ferning test in normal and keratoconjunctivitis sicca eyes. Chibret Int J Ophthalmol,1984 2;33-41
6. Zhonghua Lao Dong Wei Zhi Ye Bing Za Zhi. Pub med.2003 Oct;21(5):346-9
7. Elder JA. Ocular effects of radiofrequency energy. Bioelectromagnetics.2003;(Suppl 6):S148–161.[PubMed]
8. Fischer FH, Wiederholt M. Human precorneal tear film pH measured by microelectrodes. Graefes Arch Clin Exp Ophthalmol. 1982;218:168–70
9. Willcox MDP, Argüeso P, Georgiev GA, Holopainen JM, Laurie GW, Millar TJ, Papas EB, Rolland JP, Schmidt TA, Stahl U, Suarez T, Subbaraman LN, Uçakhan OÖ, Jones L. TFOS DEWS II Tear Film Report. Ocul Surf. 2017 Jul;15(3):366-403
10. Carney LG, Hill RM. Human tear pH. Diurnal variations. Arch phthalmol. 1976;94:821–4
11. Am M, Ra F, El-Naggar AH, Tm A; Akhtar S. Structure and microanalysis of tear film ferning of camel tears, human tears, and Refresh Plus. Mol Vis. 2018 Apr 16; 24:305-14
12. Sharanjeet-Kaur, Ho CY, Mutalib HA, Ghazali AR. The Relationship Between Tear Ferning Patterns and Non-invasive Tear Break-up Time in Normal Asian Population. J Optom. 2016;9(3):175-81. DOI: 10.1016/j.optom.2015.10.004
13. Bârjovanu F, Mocanu C, Mercuț G. Testul de cristalizare a lacrimilor in sindromul sicca [The tear crystallization test in sicca syndrome]. Oftalmologia. 2006;50(4):54-9.

Usefulness of digital light processing based three-dimensional printing in the digital production of provisional restorations

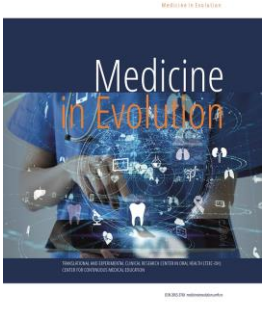

Burde A.V.[1], Vigu A.L.[2], Sava S.[2]

[1]*Department of Propaedeutics and Aesthetic Dentistry, Faculty of Dental Medicine, "Iuliu Haţieganu" University of Medicine and Pharmacy Cluj-Napoca, Romania*
[2]*Department of Dental Materials, Ergonomics, Faculty of Dental Medicine, "Iuliu Haţieganu" University of Medicine and Pharmacy Cluj-Napoca, Romania*

Correspondence to:
Name: Vigu Alexandra Lucia
Address: Avram Iancu St, No. 31, Cluj-Napoca, Romania
Phone: +40 745 571 377
E-mail address: alexandravigu@yahoo.com

Abstract

Digital light processing (DLP) based 3D printing is an additive digital technique that allows manufacturing of a complex three-dimensional structure by projecting light on a light cured resin. After each exposure, the platform of the printer descends, with a distance equal to the thickness of a layer, and the process repeats until the final product is obtained. Our study aims to present the laboratory steps necessary for the manufacturing of temporary restorations consisting of provisional crowns by DLP based 3D printing. The temporary restorations obtained fulfilled the targeted aesthetic and functional characteristics and restored the morphological and functional integrity of the maxillary arch, until the application of the final fixed dental prostheses. In addition to ease and accuracy, significant time saving can be achieved for both the dental office and the laboratory, as well as for the patient, eliminating a number of steps by the advantages of 3D printing technology over conventional techniques.

Keywords: 3D printing, provisional restorations, additive manufacturing

INTRODUCTION

There are multiple advantages to using three-dimensional (3D) printing in the digital workflow of the dental laboratory in general and for provisional restorations in particular. This type of restorations is an essential part of the therapeutic process. Technological developments are directly proportional to the quality of treatment, which has reached high levels over time. The patient's comfort is linked to the preservation of his social life, implicitly of the functions of the dento-maxillary apparatus, by avoiding the unwanted impact of the appearance of an edentation or of a prepared tooth for a future prosthetic restoration, on the patient's psyche. Along with the emotional aspect, the provisional restoration assures the protection of the remaining dental tissues and, to the same extent, the verification of the correctness of the future final restoration. Thus, the dental protocols recommend the application of temporary restorations in case of dental procedures that will disturb the integrity and function of the dental organ [1]. If we draw a parallel with the conventional workflow, we will be able to identify a series of benefits, which will position the digital manufacturing processes ahead of the conventional procedures. Starting with the financial advantage, provided by the lower cost of materials used in three-dimensional printing, and continuing with the accuracy of the restorations created through this process. The fact that several prosthetic restorations can be produced simultaneously through 3D printing is also a significant advantage. These are some of the reasons why more and more conventional steps are eliminated and replaced by digital protocols [2].

By comparison to the substractive manufacturing technology- CAD-CAM (Computer Assisted Design - Computer Assisted Manufacturing) which is based on computer numerical control (CNC) milling, 3D printing offers the advantage of unlimited design flexibility, a single stage process necessary for prosthetic restorations of great structural complexity and ease of use, thanks to the processing of files accessed in STL (Standard Triangle Language) format. Thus, it is easy to perceive 3D printing as a preferred solution for provisional restorations, followed by CAD-CAM milling, and conventional manufacturing [3]. Recent data ranks the top additive manufacturing processes preferred by dental practitioners: Vat Photopolymerization, Fused Filament Fabrication (FFF), Photopolymer Jetting (Poly jet), Binder Jetting and Powder Bed Fusion (PBF) [4].

There are 2 technological variants of the Vat Photopolymerization process: Stereolithography (SLA) and Digital Light Processing (DLP). Derived from SLA, DLP has the same principle of use and identical components. The difference lies in the light radiation source, which in this case will be a projector or a mono or multi-chrome screen. Therefore, the light curing will be done by projecting a black and white image of each layer on the surface of the resin placed in the printer's tank. Gradually, after each brief exposure to the projected light beam, the workbench will descend with a distance equal to the thickness of a layer and the process is resumed until the final product is obtained. The improved working speed of DLP printers, as well as the tendency to have a lower price than those based on stereolithography, determine their predominant acquisition by laboratories [5].

In 3D printing, the material of choice is light-cured resins, along with different types of plastics, metallic alloys or ceramics [6, 7]. Polymethyl methacrylate (PMMA) is characterized by increased hardness, rigidity and strength, reduced water absorption and is a scratch-resistant material. For these reasons, temporary 3D printed restorations made of PMMA are often used [8].

Aim and objectives

Our study aims to present the laboratory steps necessary for the manufacturing of temporary restorations, consisting of provisional crowns, through the use of DLP based 3D printing technology in combination with a light-cured acrylic resin, with a wavelength spectrum between 390-405 nm.

MATERIAL AND METHODS

The case described in this study concerns a patient with multiple wear lesions, mainly in the frontal area, palatal abrasions and an unsatisfactory aesthetic appearance as a whole, both in terms of colour and shape of the maxillary arch.

After the removal of periodontal irritation factors such as supra and subgingival calculus deposits and the dental treatment for restoring and filling the multiple maxillary cervical lesions was done, the treatment continued with the preparation of teeth 1.6 to 2.6. The proposed treatment for the prepared teeth was a series of full coverage crowns fixed partial manufactured out of lithium disilicate, treatment protocol which was explained to and accepted by the patient.

The moment of transition to the final fixed restorations is the subject of this study and it involves the manufacturing of the temporary restorations by DLP based 3D printing. The technique of indirect manufacturing of the provisional crowns will require the design of a digital mock-up in a CAD software, based on the scanned maxillary dental cast with removable dies, which reproduces the preparations made by the dentist.

Impressions and dental casts

The conventional impressions of the 2 arches arrived in the dental laboratory and went through the disinfection phase (Figure 1-A). Next, the models were cast using type IV gypsum. The working cast was sectioned in order to obtain the removable dies, by using the Willi Geller method. The obtained removable dies were repositioned in the maxillary impression (Figure 1-B).

In order to maintain the precise position of the abutments, a wax rod of 5 mm was applied to the end of each abutment, then the root portion of the mobile abutments was insulated and at the end the individual rods were secured by a wax rod that followed the curvature of the maxillary arch (Figure 1-C, D).

The maxillary impression was coated with a silicone impression material to obtain the base of the final cast and the model containing the dies was cast using type IV extra hard gypsum,(Figure 1-E).

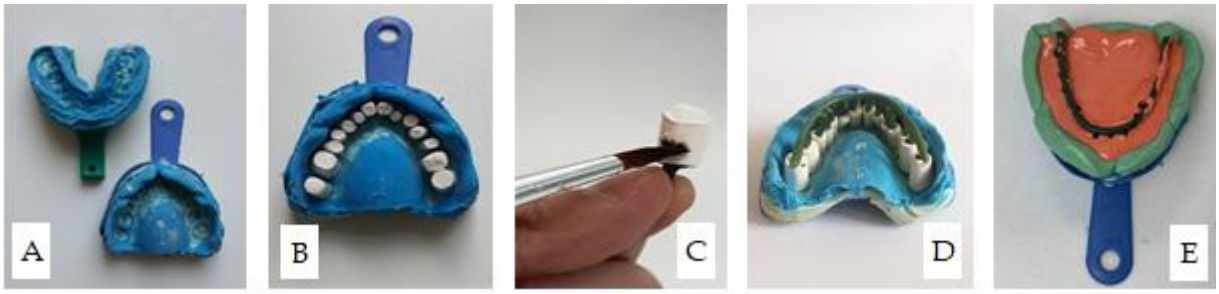

Figure 1. A– The impressions of the 2 arches; B- Removable dies positioned in the maxillary impression; C- Insulation of the root portion of the removable dies; D- Individual wax sprues secured together; E– The casting of the model with removable dies

After casting the mandibular model, the maxillary and mandibular models were finished in order to have uniform edges and bases (Figure 2-A). The articulator used was an

articulator with average values, programmed with the slope of the articular tubercle of 33 degrees, the Bennett angle between 15 and 18 degrees, and the fixed intercondylar distance of 105 mm (Figure 2-B). The bite registration, made of wax foil with aluminium, was used to mount the mandibular cast.

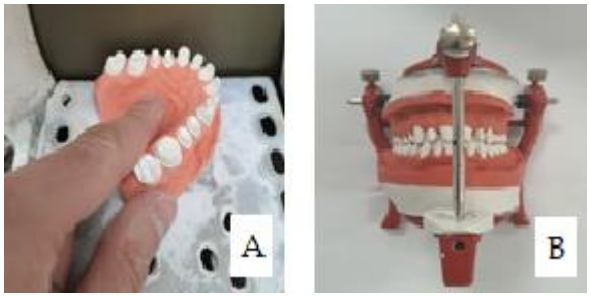

Figure 2. A- The maxillary final cast; B- Casts and articulator with average values

Scanning and design

The inEos X5 (Sirona Dental Systems Gmbh, Bensheim, Germany) scanner was used to scan the working cast, the removable dies and, the antagonist cast and the occlusion (Figure 3-A, B, C, D).

Figure 3. A- SIRONA inEos X5 Scanner; B- Working cast scanning; C- Mobile abutments scanning; D- Occlusion scanning

The Computer Assisted Design (CAD) stage followed, in which the structure of the future restorations was made, according to the requirements of the case. The inLab CAD software version 4.2 (Sirona Dental Systems Gmbh, Bensheim, Germany) was used and after loading the case, the first stage of – *Administration* - began (Figure 4-A). In this stage the restorations were defined, and the printer and the material were selected. For the design mode, - *Biogeneric individual* - was chosen and for the type of restoration – *Dental crown* – was selected. The – *Scan* - stage followed, in which the scans of the 2 arches, maxillary and mandibular, and bite registration were uploaded in the system (Figure 4-B).

Figure 4. A- Administration stage; B- Scan stage - maxillary scan

The next stage was the – *Model* - stage. Tracing the margins of the provisional restorations, for each tooth is the first step, followed by the adjustment of the insertion axis for each provisional crown (Figure 5-A, B).

Figure 5. A- Tracing the margins of the restorations; B- Setting the insertion axis for the provisional crown for 2.6.

In the -*Tools*- section, there is also the - *Buccal Bite Registration* - option, which displays the existing contact points between the maxillary and mandibular casts (Figure 6-A). These contacts can be noticed at the level of the second molars of both arches, having variable intensity. From the same section of tools, there is also the possibility to set the cast axis according to the antagonist arch position, through the - *Set Model Axis* - function (Figure 6-B).

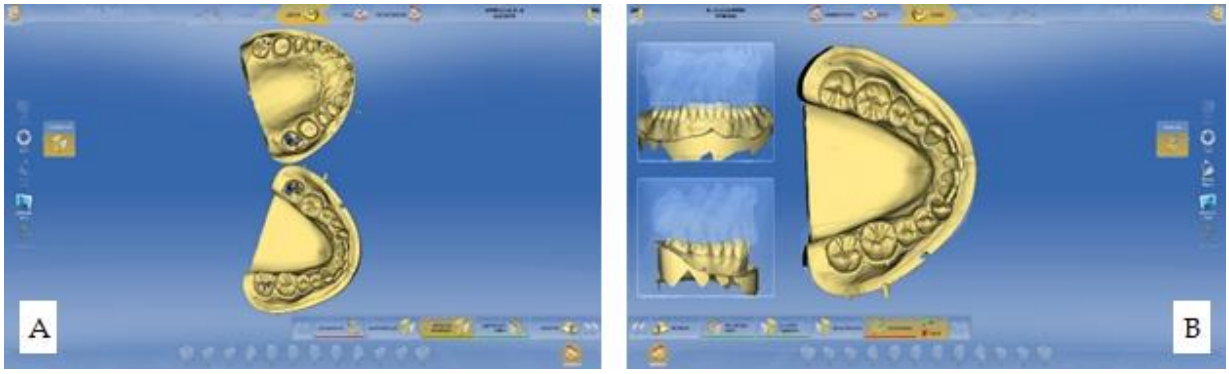

Figure 6. A- Model stage - intermaxillary contact points; B- Cast axis selection

The actual design stage followed. At the beginning, the parameters of the restoration can be set for all the provisional restorations: the space allowed for the luting cement can be adjusted, how tight the proximal and occlusal contacts are or the minimum thickness of the

restoration (Figure 7A). These parameters were adjusted as needed by the - Restoration Parameters - function.

In the next stage, the design of each provisional restoration was performed, checking both the morphology and the contacts with the neighbouring and antagonists teeth (Figure 7 B, C). For a better view of the tooth on which changes were made, the - Colour Model – option was checked. The tools that helped to create the shape of the restoration (- Shape -) were selected from the - Tools - section. These actions were performed under the - Edit Restoration - option. Immediately after this stage, each restoration was saved as a STL (Standard Triangle Language) file.

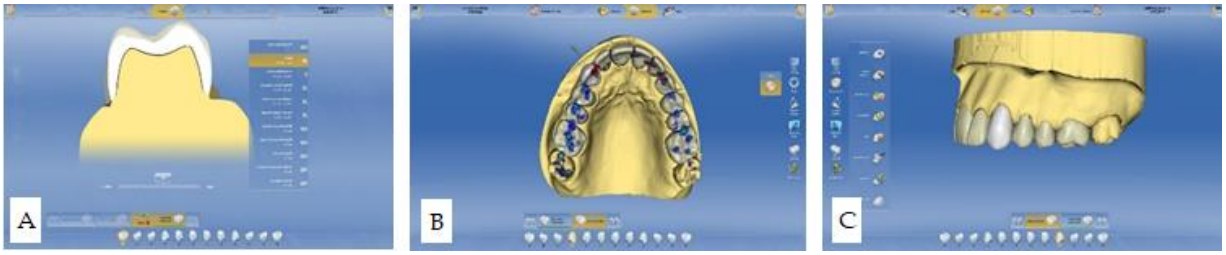

Figure 7. A– Adjustable parameters of the restoration; B- Restoration design for 1.3 - occlusal view; C- Restoration design for 1.3 - right side view

CAM file preparation

After the design stage has been completed, the CAM (Computer Aided Manufacturing) stage started and the STL files were imported into the CAM software, in order to prepare them for printing. From the CAM software interface, the Asiga Max UV 385 (Asiga, Alexandria, Australia) was selected and the chosen material was polymethyl methacrylate (PMMA) - Asiga DentaTOOTH (Asiga, Alexandria, Australia). The thickness of the layers can also be set, which in this case was 0.05 mm.

In the context of this 3D printing technology, supports must be generated for each restoration through the - *Generate Support* - function and then the parameters for the supports can be adjusted. The role of the supports is to hold up the future provisional crowns on the printer's workbench and to distribute the internal tensions resulting from the printing process.

After the settings were saved by pressing the - *Save Settings* - button, the software generated the supports, which were displayed in a purple colour and were distributed below the incisal edges and occlusal surfaces of the provisional crowns about to be printed (Figure 8 B). The shape of the supports is conical, with the base placed in contact with the platform. The initial position and number of the supports can be changed manually by adding or removing supports, as needed.

If support overlays occur, the – *Remove* - function can be used to select and delete unnecessary supports. Thus, out of 2 superimposed supports, only one will be printed. In the same way, in the areas where there are no supports, the – *Add* - function can be used, adding supports in the desired number and areas. The following stage was the generation of the printing strategy using the - *Build Wizard* - function, which will specify the printer for the process - *Destination Printer* - and will specify the estimated time, which in our case was one hour, 13 minutes and 10 seconds (Figure 8 C).

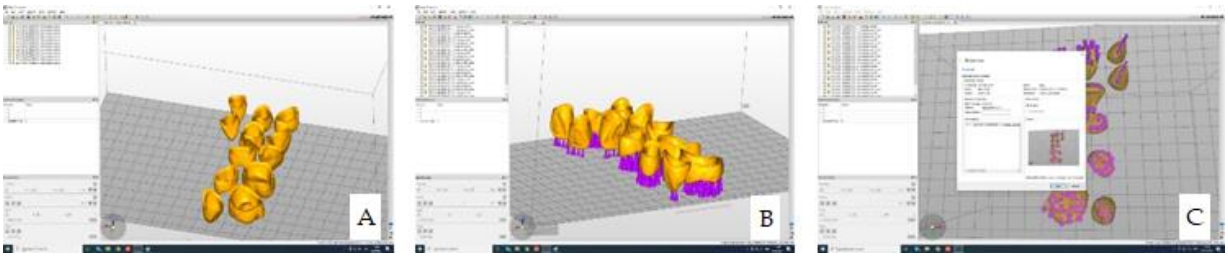

Figure 8. A- The designed provisional crowns on the digital workbench; B -Initial design of supports; C- Printing strategy selection

Also, within the printing strategy, there is the possibility to adjust some parameters, as well as to check the - *Fast Print Mode* - which registers the delamination of the layer at the end of the printing process and results in a shorter printing time. The - *Separation Detect mode* – can also be checked, in order to know when the resin can be detached from the printer's workbench.

At this stage, the design of the provisional crowns was converted to a series of black and white images, each corresponding with one layer (Figure 9 A). The portions represented in white are the target areas for light curing, and the black portions will not cure. After pressing the - *Next* – button, the summary of the printing process was displayed and the information package was sent to the 3D printer.

Printer preparation, printing and post-processing

The 3D printing was performed in this case with the Asiga Max UV 385 printer and a type of acrylic resin for provisional crowns Asiga DentaTOOTH (color A2) was used (Figure 9- B, C).

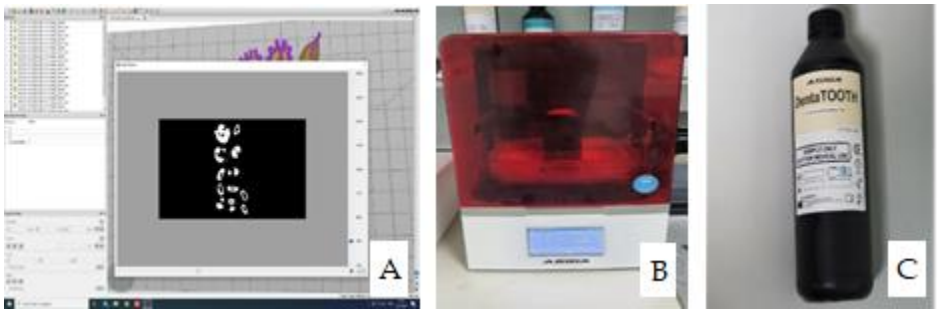

Figure 9. A- 2D image of the designed provisional crowns in black and white format; B- Asiga Max UV 385 printer; C- Acrylic resin for provisional crowns Asiga DentaTOOTH

It is recommended to wipe down the workbench of the printer with a roll of cotton with isopropylic alcohol, in order to avoid the contamination with traces of grease or other impurities (Figure 10 A). Inside the printer, the transparent borosilicate glass can be observed underneath of the vat, under which there is the ultraviolet (UV) light projector, which will perform light curing. The liquid resin tank was placed over this borosilicate glass. Before starting the printing process, it is recommended to evaluate that the resin is completely clear, with no residue adhering to the bottom of the container in which it is located. A spatula can be used for this purpose (Figure 10 B). The platform was positioned in the 3D printer, the enclosure was closed and the printing process started (Figure 10 C).

After the printing chamber was closed, the resin started the gradual heating process (Figure 10 D). Only after this phase is completed does printing actually begin. During printing, the display shows the name of the case, the temperature of the resin (30.3 degrees Celsius), the number of the layer being printed (1/294) and the remaining time until production is completed (1 hour and 15 minutes) (Figure 10 - E, F).

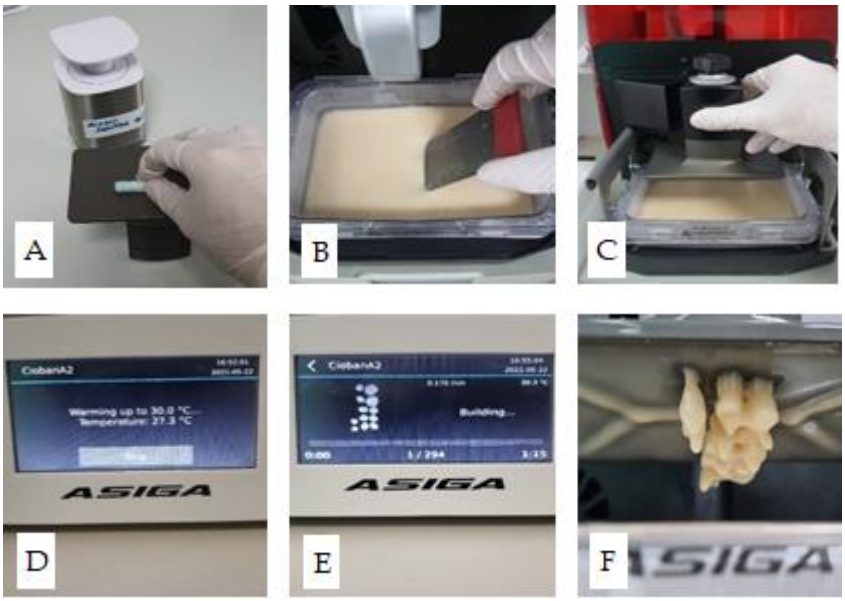

Figure 10. A - Cleaning the printer workbench with sanitary alcohol; B- Checking the purity of the resin in the liquid resin tank; C- Placing the workbench in the printer; D- The heating of the resin; E- Start of printing process; F- Printed provisional restorations attached to the workbench

At the end of the printing process, the provisional restorations were attached to the platform inside the printer, and once the platform was removed from the printer, the resin supports could be removed also and the conventional post-processing steps begun (Figure 11 A, B, C). The provisional restorations can be removed off the workbench with the help of a spatula, kept in close contact with the workbench, in order to avoid damage of the restorations.

Immediately after being removed from the platform, the printed provisional restorations were treated with isopropyl alcohol for 2 minutes (Figure 11 D). Finally, after being dried very well with compressed air, the printed provisional restorations were removed from the isopropyl alcohol and placed in the light curing chamber (Figure 11 E). The final light curing took place in an Otoflash (Bego GmbH, Bremen, Germany) post curing light pulsing unit, under nitrogen protection (N2) and at 2000 pulses (Figure 11 F).

The last stage was the fit adjustment and finishing of the printed provisional restorations obtained. They crowns were placed on the removable dies, and their shape and contacts with neighbouring and antagonist teeth and restorations were checked (Figure 11 F). The needed adjustments were performed with the help of small diamond dental burs, after which other finishes were made with various diamond discs, brushes and polishing paste.

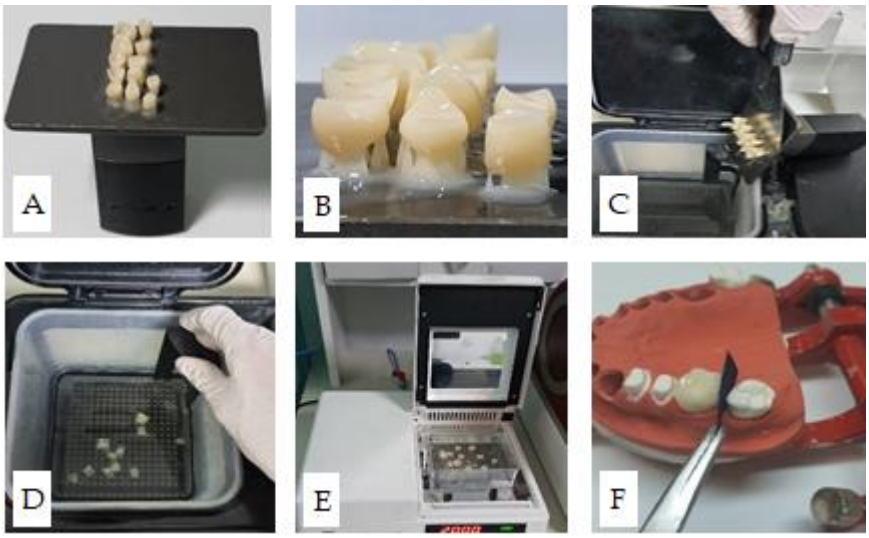

Figure 11. A - Printed provisional crowns attached to the platform; B- Detailed view of the printed provisional crowns; C- Removing the provisional crowns from the platform; D- Rinsing in isopropyl alcohol; E- Final light curing; F- Verification of the proximal contacts

At the end, the marginal fit of the provisional crowns on the abutments, the occlusion and the colour were checked for the printed provisional crowns and, also, the way in which the printed provisional crowns restored the morphology and functional integrity of the maxillary dental arch until the application of the final prosthetic restoration (Figure 12. A-D).

After handing over the case to the dental office, the patient's feedback was positive. It should also be noted that the printed provisional crowns did not need other adjustments in terms of contacts and shape, ensuring satisfactory comfort for the patient.

Figure 12. A - Frontal occlusion; B- Provisional crowns - occlusal view; C- Provisional crowns - left side view; D- Provisional crowns - right side view

DISCUSSIONS

Conventional processes for obtaining provisional crowns are expensive, both in terms of production (materials) and time (steps). 3D printing has made a significant contribution in this area, greatly simplifying the production process of provisional crowns [9]. It should be noted that 3D printing still has a number of limitations, such as the need to use support structures during the printing process and post-processing operations. There is a need to eliminate the additional support structures mentioned above, the excess material or to increase the mechanical strength of the structures generated by additive manufacturing. The rapid advancement of 3D printing technology will eliminate these considerations over time, by improving printer resolution and powder size [10]. Temporary restorations made with DLP and SLA technologies provide adequate flexural strength. 3D printed provisional crowns have improved than the conventional ones [11]. The continuous evolution of the printing parameters (thickness, mechanical strength, colour, accuracy, resolution, adaptability, materials) makes 3D printing the best option for manufacturing provisional crowns [12].

CONCLUSIONS

The DLP based 3D printing technology used in this study for the production of provisional fixed restorations demonstrated a predictable and simplistic digital workflow. In addition to this, we achieved a significant time reduction, both for the dental office and laboratory, by comparison with the traditional workflow, eliminating a number of technical steps through the advancements of 3D printing. The temporary restorations obtained with the technical 3D printing protocol described in this study, met the intended aesthetic and functional characteristics and were well integrated by the patient.

Acknowledgments

All 3 authors have the same contribution in this study.

REFERENCES

1. Bhargav A, Sanjairaj V, Rosa V, Feng LW, Fuh Yh J. Applications of additive manufacturing in dentistry: A review. J Biomed Mater Res B Appl Biomater. 2018 Jul;106(5):2058-2064.
2. Tahayeri A, Morgan M, Fugolin AP, Bompolaki D, Athirasala A, Pfeifer CS, Ferracane JL, Bertassoni LE. 3D printed versus conventionally cured provisional crown and bridge dental materials. Dent Mater. 2018 Feb;34(2):192-200.
3. Jaroslow B, Lambertson C, Frye C, Weatherby S. A dental technician's guide to 3D printing. Dental Technology Solutions, WhipMix, 2017, 50-62.
4. Hisham HH, Shafiee SA, Patel AA, Bhavik A.3D printable conductive materials for the fabrication of electrochemical sensors: A mini review. Electrochemistry Communications. 2018;96(1): 27–371.
5. Wu D, Zhao Z, Zhang Q, Qi HJ, Fang D. Mechanics of shape distortion of DLP 3D printed structures during UV post-curing. Soft Matter. 2019 ;15(30):6151-6159.
6. Sing SL, Yeong, WY. Laser powder bed fusion for metal additive manufacturing: perspectives on recent developments. Virtual and Physical Prototyping.2020: 15(3); 359–370.
7. Methani MM, Revilla-León M, Zandinejad A. The potential of additive manufacturing technologies and their processing parameters for the fabrication of all-ceramic crowns: A review. J Esthet Restor Dent. 2020 Mar;32(2):182-192.
8. Jockusch J, Özcan M. Additive manufacturing of dental polymers: An overview on processes, materials and applications. Dent Mater J. 2020 Jun 5;39(3):345-354.
9. Barazanchi A, Li KC, Al-Amleh B, Lyons K, Waddell JN. Additive Technology: Update on Current Materials and Applications in Dentistry. J Prosthodont. 2017 Feb;26(2):156-163.
10. Kessler A, Hickel R, Reymus M. 3D Printing in Dentistry-State of the Art. Oper Dent. 2020;45(1):30-40.
11. Park SM, Park JM, Kim SK, Heo SJ, Koak JY. Flexural Strength of 3D-Printing Resin Materials for Provisional Fixed Dental Prostheses. Materials (Basel). 2020;13(18):3970.
12. Tahayeri A, Morgan M, Fugolin AP, Bompolaki D, Athirasala A, Pfeifer CS, Ferracane JL, Bertassoni LE. 3D printed versus conventionally cured provisional crown and bridge dental materials. Dent Mater. 2018 Feb;34(2):192-200.

Custom ocular prosthesis - experience of an anaplastology laboratory in western Romania

Pricop M.O.[1], Talpoş Ş.[1], Urechescu H.[1], Cosoroabă R.M.[2], Popovici R.A.[2], Todor L.[3]

[1]*Oro-maxillofacial department, Faculty of Dental Medicine, Victor Babes University of Medicine and Pharmacy, Timisoara, Romania*
[2]*Discipline of Management, Legislation and Communication in Dentistry, Faculty of Dental Medicine, Victor Babes University of Medicine and Pharmacy, Timisoara, Romania*
[3]*Department of Dental Medicine, Faculty of Medicine and Pharmacy, University of Oradea, Romania*

Correspondence to:
Name: Şerban Talpoş
Address: Bd. Take Ionescu 5, Timisoara, Romania
Phone: +40722434390
E-mail address: talpos.serban@umft.ro

Abstract

The oldest ocular prosthesis was discovered in Iran, made for a woman who lived between 2900-2800 BC. Over time, techniques for making ocular prosthesis have improved and new materials have emerged to perfect the look. Today, the techniques for making an ocular prosthesis are sophisticated and the physiognomic results can achieve perfection.

This is a case report of a patient with left eye loss and details the stages of making an ocular prosthesis in an anaplastology laboratory in Timisoara. The technique describes the fabrication of an ocular prosthesis with materials that are inexpensive, readily available and regularly used in maxillofacial prosthetics. The prosthesis, although non-functional, provides good integration into the patients' physiognomy and the aesthetic effect is high. Ocular prosthesis restores patients' self-confidence and prevents social embarrassment.

Keywords: ocular prosthesis, technique, experience

INTRODUCTION

An ocular prosthesis creates an illusion of a normal eye and its surrounding tissues, and maintains the volume of its socket [1]. The accurate duplication of color, contour, size and orientation, similar to a natural eye, is important in order to obtain realism and symmetry [2]. The methods of fabricating ocular prostheses have progressed over the years to provide superior cosmetic replacement of the enucleated or eviscerated eye [3].

The oldest ocular prosthesis was discovered in Iran, belonged to a woman, and dates back to approximately 2900-2800 BC. The prosthesis has a hemispherical shape and a diameter of 2.5 cm. It was made of a very light material, probably bitumen paste. The surface of the artificial eye is covered with a thin layer of gold, engraved with a central circle (representing the iris). Tiny holes are drilled on both sides of the eye, through which a gold wire could hold the eyeball in the desired position (Figure 1) [4]. Later, BC and AD, such prostheses were made by Egyptian and Roman priests. The modern era of prosthetics begins around 1600 AD, with the achievements of Italian, French and German doctors in collaboration with local artisans. In 1943 production of acrylic ocular prostheses began in the U.S. [4]. Acrylic ocular prostheses proved to be superior, non-fragile, with enhanced aesthetic possibilities such as determining corneal and pupil dimensions and painting conjunctival vessels [5].

Nowadays, techniques for making ocular prostheses vary from simple to complicated. The ocular prostheses can be prefabricated or custom made, the latter offering better fit and aesthetics (Figure 1).

Figure 1. From the oldest eye prosthesis to custom made ocular prostheses in the anaplastology laboratory

A multidisciplinary approach including an ophthalmologist, oral-maxillofacial surgeon and maxillofacial prosthetist should be considered for an aesthetic and stable outcome [4].

The etiology of ocular and orbital defects is diverse:

- Congenital eye diseases
- Puncture with sharp objects (glass, needles, nails)
- Surgical procedures in cases of irreparable trauma
- Surgical interventions required by tumors (basal cell carcinoma, squamous cell carcinoma, retinoblastoma, malignant melanoma, etc.) [4].

Surgical procedures performed by ophthalmologists or oral-maxillofacial surgeons in these clinical situations are of several types:

- Evisceration is the surgical procedure that involves removal of intraocular contents while leaving an intact sclera (usually performed by ophthalmologist).
- Enucleation is the surgical procedure that involves removal of the globe while leaving all other surrounding structures (usually performed by ophthalmologist).

Exenteration is the surgical procedure that involves the removal of all tissues inside the eye socket, including the conjunctiva, eyeball, orbital fat, muscles, vessels and nerves, and partial or total eyelids (usually performed by oral-maxillo-facial surgeon) [6, 7, 8].

MATERIAL AND METHODS

Making an ocular prosthesis is complex and requires a succession of clinical and laboratory stages. Below we describe in detail the technique of making an ocular prosthesis in the anaplastology laboratory.

Consultation. Case examination

A 65-year-old male patient reported to the anaplastology laboratory with a defect in his left eye. The defect was caused by trauma due to a tree branch puncture five months ago. On inspection, the sclera and iris were absent, with orbital fat and intact eyelids observed. The muscle function of both the upper and lower eyelid seemed normal. No inflammation was present. As in many such situations encountered at the laboratory, the only option available to the patient was an ocular prosthesis (Figure 2).

Figure 2. Case examination

Figure 3. Impression of the defect

After obtaining the informed consent, the patient will be registered in the laboratory records, noting personal data, history of the disease, other diseases he suffers from (anamnesis). Clinical examination of the eyeball defect area is performed. It is checked if there is enough space for an eye prosthesis and if the inferior conjunctival fornix is capable of retaining this prosthesis.

To start making the ocular prosthesis, a minimum of 6 weeks must pass after the eyeball removal surgery. After this time the shape of the eye defect is stable and no longer undergoes major changes in terms of shape or volume [4].

The tissues must be normal in appearance, free of sutures, ulceration and inflammation, which could affect the fitting or wearing of the ocular prosthesis. If this is not the case, the patient should be referred to an ophthalmologist or maxillo-facial surgeon and the prosthesis should be postponed until the situation has improved [1].

Impression of the defect. Measurements and comparisons

Before the impression is made, the healthy eye is examined and measured: iris diameter, iris color and appearance, color of the sclera, density and arrangement of the scleral vasculature [9]. Prepare the materials and instruments needed for the impression: low-flavor alginate (especially menthol), bowl, spatula, water, tweezers, 10 ml syringe, bib, examination gloves. Remove the dressing or old eye prosthesis if present. With the patient lying on his back, the area to be examined is cleaned.

The alginate is prepared in a creamy consistency and is injected with the help of the syringe into the eye cavity, taking care to fill both conjunctival fornices (upper and lower)

without bubbles (Figure 3). Alginate hardening must be rapid in order to avoid discomfort to the patient, and not to irritate the orbital tissues. After the alginate has hardened, the eyelids are receding and the impression extracted. Until the model is cast, the impression should be kept in a moist environment.

The impression area is cleaned and the old prosthesis is reinserted or the eyelid dressing is restored.

Making the working model.

Disinfect the impression and remove excess material that has flowed back through the eyelid slit. The model will be cast in hard plaster (Moldano). The posterior part of the impression (the one that recorded the eyeball defect) is filled with plaster and turned over a pile of plaster on the table. After hardening, the plaster is insulated and the model lid, also made of hard plaster, is poured over it. Finish the model resulting from the final socket and separate the 2 components. Note the patient's name on the model (Figure 4).

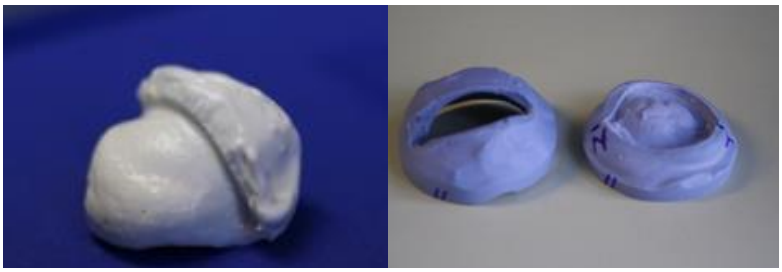

Figure 4. The impression and the working model

Making the wax-up and the acrylic model of the ocular prosthesis.

Isolate the model by immersion in water for a few minutes. Melted wax is introduced through the eyelid slit of the model until it is filled. After curing the wax, the 2 components of the model are removed and the upper lid is removed. Smooth out the excess wax of the model and create maximum wax convexity at the position of the future iris (Figure 5).

The wax-up at the bottom of the model is impressed with the putty silicone. A funnel-shaped hole will be made in the upper part of this impression. Remove the wax-up from the model. The silicone cap is waxed onto the lower portion of the model (after sealing the lower portion of the model with Pectizol). Then, a white self-curing acrylate fluid paste is poured through the created hole by vibration. After curing, the acrylate is removed from the model and the silicone cap, processed and polished to a high gloss so that there are no irritating areas. This acrylic model will be adapted to the patient until a suitable physiognomic appearance is achieved and it is well integrated and tolerated. The acrylic mock-up will also be used to position the iris of the future eyeball prosthesis.

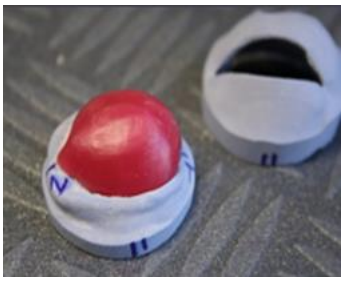

Figure 5. The wax-up of the ocular prosthesis

Making the iris: making the iris disc, painting it, fixing the pupil, pressing, curing transparent acrylate. Unpacking, processing, polishing.

A circle with a larger diameter than the iris of the patient's healthy eye is drawn on an acrylic plate. The circle is cut out with a milling cutter, then shaped into a round shape and given the appropriate diameter by clamping in a chuck and milling on a fine file. The diameter will be measured frequently until the required size is reached. The resulting disc is glued onto a holder that can be held comfortably in the hand.

Oil paints, the color of the patient's iris, will be applied to the surface of the disc. The paints are homogenized in advance with a light-curing varnish (Palaseal-Kulzer), which speeds up the curing of the different layers. When the painting is complete, a pupil made of black cardboard cut to the average diameter of the patient's pupil, is fixed in the center of the disc. The pupil is fixed with transparent self-curing acrylate.

The finished painted disc is detached from the support with which it was held. A Moldano plaster is inserted into a flask, allowed to harden and a shallow cavity is created, similar in shape to the iris and slightly larger in size. On the opposite side of the flask (also containing hard plaster) a shallow cavity, shaped like a calotte, is created.

The disc is fixed to the underside of the mold and glued with cyanoacrylate. Re-insulate the mold with Pectizol, insert, press and cure the transparent heat-curing acrylate. After the heat treatment, the artificial iris is unpacked, processed, finished and polished (Figure 6).

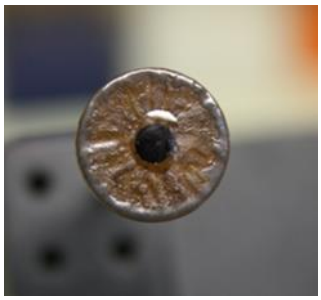

Figure 6. Painting the iris disc

Mock-up and iris try-in: Try-in of the mock-up and its adaptation. Determination of iris position, preparation for insertion, wax fixing, try-in, position adjustment. Retouching the shape of the palpebral aperture.

Check the patient's adaptation of the acrylic model by inserting it into the eyeball defect. The patient's comfort is the first priority in order to remove any areas of irritation. Then the eyelid opening is assessed, which should be similar to that of the healthy eye. If this is not the case, the necessary adjustments are made: acrylate is reduced or wax is added to the surface of the model.

Finally, the center of the pupil is marked with a dot. Around this point a space will be created in the model where the artificial iris will be inserted. This space should be wider than the iris, so that the iris position can be corrected. The iris should be in the same vertical plane and symmetrical to the midline of the iris of the healthy eye. Fixing the iris in the desired position is done with a special white wax. After the test, the iris mock-up is removed, and the patient's old prosthesis is reinserted into the defect, or the palpebral region is bandaged.

Making the mold: finishing the wax-up, acrylic guide, packing. Removal of the wax-up from the mold, cleaning, mold isolation. Fixing the iris in the unique position.

A small amount of self-polymerizing, non-retentive pyramid-shaped acrylate is applied to the surface of the iris (previously fixed in the wax-up during the test). Finish the surface of the wax-up by adding wax.

Packing the acrylic mock-up obtained in a flask of suitable size, using hard plaster. The lower part of the mold cover the back of the model up to the equator. After the

hardening, isolate the surface of the plaster, put the lid on the flask and pour the upper portion, also in hard plaster. In this part of the mold will be found the pyramidal extension of the ocular prosthesis.

After the plaster plug, the flask is removed, the model is removed, the mold is cleaned and the surface of the plaster is isolated. The marginal surface of the iris is roughened with a burr to facilitate the adhesion of the acrylate to the final eye shield. The iris is fixed with adhesive in the resulting pyramidal recess in the upper portion of the mold. The mock-up used for the trial is discarded.

Pressing, polymerization of acrylate. Scleral processing, vascularization, transparency.

Prepare heat-curing acrylate paste in the color of the patient's sclera. In the coke phase the acrylate paste is placed in the mold and pressed (Figure 7). The polymerization process follows the regime recommended by the acrylate manufacturer. After polymerization, the eyeball is removed from the mold without destroying the mold.

The outer surface of the eyeball is machined, removing the acrylic pyramidal guide and excess sclera on the iris, and approximately 0.5 to 1 mm of the thickness of the sclera to make space for the transparent layer. The edge of the iris remains covered with a thin layer of sclera over an area of 0.3-0.5 mm from the edge inwards.

The textile fibers are then added, mimicking the vascularization on the surface of the healthy eye's sclera. The fibers are impregnated in a light-curing varnish (Palaseal - Kulzer).

Re-isolate the surface of the mold and re-insert the eyeball thus processed. Prepare a small amount of transparent acrylate, which is then baked into the mold over the artificial eye. The flask is pressed and polymerization is carried out. The polymerization regime is different from that applied to the sclera layer and is specific to transparent acrylate.

Figure 7. Pressing and polymerization of acrylate

Processing, finishing, polishing.

Once polymerization is complete, the ocular prosthesis is removed from the mold. The acrylic protrusion on the iris and irregularities on the surfaces of the prosthesis are processed. Finish with great care, no rough or sharp areas allowed. Then polish, the resulting external surface being convex, without bumps, and the internal surface respecting the relief of the globe defect (Figure 8).

Figure 8. Completed ocular prosthesis

Insertion of the ocular prosthesis. Adjustments. Training the patient.

After the ocular prosthesis is completed, it is inserted into the defect and compared with the healthy eye. Check the patient's comfort and appearance. In the case of eyelid slit incongruity, the surface of the prosthesis in that area is thinned to allow proper closure of the eyelid (Figure 9). Adjustments and finishing of irritated areas are also done. The ocular prosthesis is refinished and polished.

This is followed by the final insertion of the ocular prosthesis and instruction of the patient in its use, maintenance and cleaning, and the timing of future control.

Figure 9. Insertion of the ocular prosthesis

RESULTS

We present below the results obtained by the same method in three other patients who came to the laboratory for an ocular prosthesis (Figures 10-12).

Figure 10. Post-traumatic loss of iris and sclera in the left eye

Figure 11. Post-traumatic sclera and iris defect of the left eye

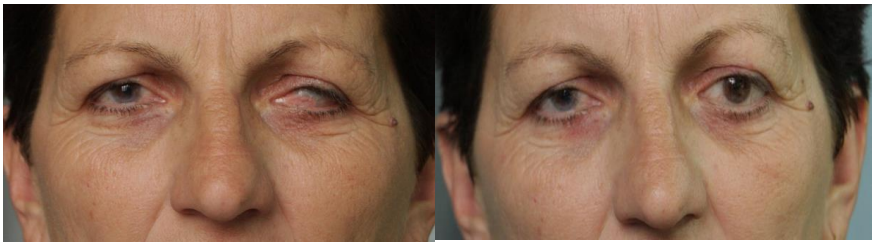

Figure 12. Post-traumatic sclera and iris defect of the left eye

DISCUSSIONS

The steps involved in making an ocular prosthesis are similar to those involved in making most dental prostheses. The work involves the technician working directly with the patient over several days. A minimum of 3-4 sessions with the patient and many intermediate technical steps are required.

Custom-made ocular prostheses are well adapted to the orbit, as the manufacture of the prosthesis is based on the anatomy of the ocular defect, thus offering fitting advantages, and the position of the iris is similar to that of the natural eye [10].

Intimate contact between the ocular prosthesis and the tissue bed contributes to a more balanced distribution of the pressure of the prosthesis on the surrounding tissues. In addition, the voids in the prefabricated dentures are minimized in custom-made prosthesis. Thus, dust and other small foreign bodies, which can irritate the mucous membrane and act as a potential source of infection, will be in smaller quantities [1, 10].

CONCLUSIONS

The own technique of manufacturing a custom-made ocular prosthesis described in the paper allows for good aesthetics and intimate adaptation of the prosthesis to the tissue bed. A well-made custom ocular prosthesis has a natural appearance and increased adjustability and also can maintain its orientation when the patient performs various eye movements.

The disfigurement resulting from the loss of an eye can have psychological and social consequences. An ocular prosthesis is absolutely necessary in these patients with various ocular defects and helps to restore aesthetic appearance and social reintegration. Ocular prosthesis, although it does not restore lost sight, remains the only aesthetic solution to resolve these cases.

The cosmetic and functional results of a customized ocular prosthesis accelerate the patient's return to a normal lifestyle.

REFERENCES

1. Cain JR. Custom Ocular Prosthetic. J Prosthet Dent. 1982;48:690–4.
2. Taicher S, Steinberg HM, Tubiana I, Sela M. Modified stock-eye ocular prosthesis. J Prosthet Dent. 1985;54:95–8.
3. Da Breo S. Surgical and prosthetic considerations in the management of orbital tumors. J Prosthet Dent. 1992;67:106–12.
4. Taylor TD, Clinical maxillofacial prosthesis. London: Quintenssense publication; 1998. pp. 265–77.
5. Bartlett SO, Moore DJ. Ocular prosthesis: A physiologic system. J Prosthet Dent. 1973;29:450–9.
6. Raflo GT. Enucleation and evisceration. In: Tasman W, Jarger E, editors. Duane's Clinical Ophthalmology. Philadelphia PA: Lippincott Williams and Wilkins; 1995. pp. 1–25.
7. Perman KI, Baylis HI. Evisceration, enucleation and exenteration. Otolaryngol Clin North Am. 1988;21:171–82.
8. Lubkin V, Sloan S. Enucleation and psychic trauma. Adv Ophthalmic Plast Reconstr Surg. 1990;8:259–62.
9. Mathews MF, Smith RM, Sutton AJ, Hudson R. The ocular impression: A review of the literature and presentation of an alternate technique. J Prosthodont. 2000;9:210–21.
10. Patil SB, Meshramkar R, Naveen BH, Patil NP. Ocular prosthesis: A brief review and fabrication of an ocular prosthesis for a geriatric patient. Gerontology. 2008;25:57-62.

Applications of basil extracts on diseases of the oral cavity

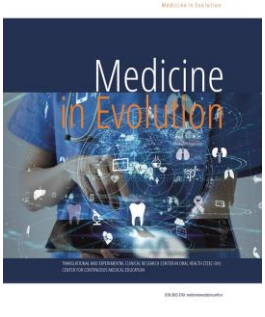

Faur A.[1], Dinu S.C.[2], Todor L.[3], Porumb A.[3], Todor S.A.[4], Cosoroabă R.M.[5], Popovici R.A.[5], Raica M.[1]

[1]*Victor Babes University of Medicine and Pharmacy, Faculty of Medicine, Department of Microscopic Morphology/Histology Angiogenesis Research Center Timisoara, Romania*
[2]*Department of Pediatric Dentistry, Faculty of Dental Medicine, "Victor Babeş" University of Medicine and Pharmacy, Timişoara, Romania*
[3]*Department of Dental Medicine, Faculty of Medicine and Pharmacy, University of Oradea, Romania*
[4]*Dentist doctor, private medical office, Oradea, Romania*
[5]*Department 1, Faculty of Dental Medicine, Victor Babes University of Medicine and Pharmacy, Timisoara, Romania*

Correspondence to:
Name: Liana Todor
Address: Department of Dental Medicine, Faculty of Medicine and Pharmacy, University of Oradea, Romania, December 1st Square no.10, 410068 Oradea, Bihor County, Romania
Phone: +40 723517100
E-mail address: liana.todor@gmail.com

Abstract

Nature offers us a great organic wealth, various types of plants growing in different parts of the world. Medicinal plants are cultivated or spontaneously grown plant species that, due to their chemical composition, have pharmaceutical properties, being used to alleviate various diseases. The holy basil, Ocimum sanctum Linn or Tulsi, has been used since ancient times to treat various ailments.

In this article we will talk about the use of Tulsi in oral diseases, , such as caries, gingivitis, periodontitis, oral cancer, oral candidiasis.

Keywords: Ocimum sanctum Linn, pharmaceutical properties, oral cavity

INTRODUCTION

Ocimum species representatives are very important for their therapeutic potential, being used against abdominal cramps, gastroenteritis, dysentery and diarrhea. The leaf extract has been used in the treatment of wounds, acne and vitiligo. Basil has traditionally been used to treat health problems such as anxiety, severe pain, stings, pyrexia, infectious diseases, myalgias, coughs, constipation, warts, helminths and kidney dysfunction [1-3]. It is also used as a deodorant, being considered an aphrodisiac [4].

The most important representatives of the Ocimum species are: Ocimum basilicum, Ocimum sanctum, Ocimum gratissimum, Ocimum canum, Ocimum kilimandscharicum, Ocimum americanum and Ocimumm icranthum [5].

Ocimum sanctum Linn, also known as Holy Basil or Tulsi, has been used since ancient times in Europe and Asia, especially in India, as a medicinal plant. The name "Tulsi" in Sanskrit means "the only one". Tulsi is considered to be one of the most sacred and sacred plants documented in Ayurvedic medicine [6,7].

Aim and objectives

The purpose of this review is to present the use of Tulsi in oral diseases, such as caries, gingivitis, periodontitis, oral cancer, oral candidiasis.

THERAPEUTIC PROPERTIES OF BASIL IN THE ORAL CAVITY

Basil (Ocimum basilicum), the most cultivated plant in the world, contains active components that recommend it to be used as an antimicrobial and natural antioxidant [8].

Experiments have shown that Tulsi (Figure 1) has anti-inflammatory, antipyretic, analgesic, antidiabetic, anti-stress, hepatoprotective, hypolipidemic, immunomodulatory, chemopreventive, radiation protection and free radical scavenging properties.

In the oral cavity, basil has antibacterial properties on periodontal pathogens (Aggregatibacter actinomycetemcomitans, Porphyromonas gingivalis) [9,10]. The ethanolic extract of Ocimum sanctum has anti-caries properties due to its antimicrobial activity against Streptococcus mutans [11,12].

Tulsi extracts also have antiviral [13] and antifungal properties against oral pathogenic fungi (Candida) [14,15].

Preclinical studies have shown that Tulsi and some of its phytochemicals (eugenol, rosmarinic acid, apigenin, myrethenal, luteolin, β-sitosterol, carnosic acid) prevented chemically induced oral, lung, skin and liver cancer by increasing antioxidant activity, induction of apoptosis, alteration of gene expression and inhibition of angiogenesis and metastasis [16].

Figure 1. Tulsi Plant – Holy Basil

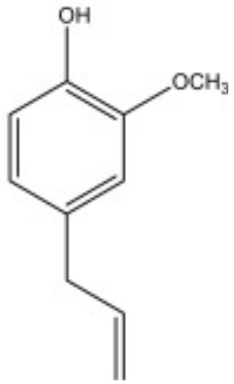

Figure 2. Eugenol

Tulsi leaf ethanolic extract is used for its anti-invasive effect on cancer cells [17]. The active phenolic compounds identified in it, rosmarinic acid, caffeic acid and apigenin, could be used as alternative therapeutic agents in malignant tumors [18].

Eugenol (1-hydroxy-2-methoxy-4-allylbenzene) (Figure 2), the active ingredient in Ocimum sanctum, is thought to be responsible for the therapeutic effects of Tulsi [19].

DISCUSSIONS

Many studies have been performed to evaluate the antimicrobial activity of Ocimum sanctum (tulsi) extract on bacteria that frequently colonize the subgingival area (A. actinomycetemcomitans, P. gingivalis), and those in dental caries (Streptococcus mutans). Ethanol extract of Tulsi prepared by the cold extraction method and diluted with an inert solvent, dimethylformamide, was used.

Jayanti et al. concluded that an 8% concentration of O. sanctum extract showed maximum antimicrobial activity against A. actinomycetemcomitans and P. gingivalis [10]. Mallikarjun et al. concluded that at 5% and 10% concentrations, Tulsi extracts showed antimicrobial activity against A. actinomycetemcomitans, similar to doxycycline. P. gingivalis and P. intermedia were resistant to Tulsi extract [20]. Eswar et al. observed that the antimicrobial potential against A. actinomycetemcomitans of Ocimum sanctum Linn extract was maximal at a concentration of 6% [21].

Dr. Devang Bharatkumar Khambholja incorporated Tulsi extract into the Guided Tissue Regeneration Membrane (GTR) to inhibit the growth of bacteria (Streptococcus sp. and Rhodococcus sp.) [22].

Agarwal et al. observed that Tulsi ethanolic extract had the highest zone of inhibition over S. mutans at a concentration of 4% [11].

Kochikar Pai et al used the ethanolic extract of Ocimum sanctum prepared by the hot extraction method, diluted with an inert solvent, dimethyl sulfoxide. The maximum activity against microorganisms responsible for dental caries (S. mutans and S. sanguis) was observed with the 10% extract [12].

There are studies comparing and evaluating the anti-karyogenic properties of different plant extracts against different karyogenic microorganisms. Thus Glycyrrhiza glabra (licorice) followed in descending order by Ocimum sanctum (Tulsi), Terminalia chebula (Harad), Tinospora cordifolia (Guduchi) have a strong antibacterial efficacy against Streptococcus mutans and Lactobacillus acidophilus [23].

Numerous studies have shown that several species of Ocimum sanctum (OS) extract have therapeutic properties and, in some cases, antitumor properties. The antiproliferative

effects of OS extract have been studied in cases of breast cancer, oral cancer and human fibrosarcoma [18].

Various researchers have studied the cytotoxic and anti-proliferative effects of extracts of two types of Tulsi on cancer cells (Rama Tulsi with open leaves and Krishna Tulsi with dark leaves). Aqueous and dry extracts have shown an important cytotoxicity on the studied cell lines, being effective as anti-proliferative agents that cause apoptosis in the cell line of oral cancer [24,25].

The presence of a large number of phytoconstituents in Tulsi (eugenol, rosmarinic acid, apigenin, myrethenal, luteolin, β-sitosterol, carnosic acid) could explain its beneficial effects, including in the prevention and treatment of cancer [16,26]. Tulsi has chemopreventive and radiation-protective properties. The aqueous extract of Ocimum sanctum and its flavonoids, orintin and vicenin, protect mice against γ-radiation-induced diseases and mortality and selectively protect normal tissues from the tumoricidal effects of radiation. Other phytoconstitutes: eugenol, rosmarinic acid, apigenin and carnosic acid, prevent radiation-induced DNA damage [16].

Uma Devi et al. showed that two water-soluble flavonoids, Orientin (Ot) and Vicenin (Vc), extracted from the leaves of Ocimum sanctum Linn provide remarkable protection against radiation [27].

The alkaloids present in Ocimum Sanctum, Flavanoids, Glycocides, Linolols, Eugenol, Cineol can be used as astringent, edema reliever, pain reliever and hemostatic for the treatment of oral submucosal fibrosis (OSMF). Srivastava et al. showed in a study that an adhesive made of 1 g of tulsi and 1 g of turmeric mixed with glycerin, applied topically 3-4 times a day, led to a statistically significant improvement in both the burning sensation and the opening of the mouth in patients with OSMF [28].

Candida albicans has recently shown resistance to many synthetic drugs, which has led to the need for new antifungal drugs with fewer side effects. Many studies have suggested that some plant species have promising antifungal compounds. Ocimum sanctum essential oil and its two components eugenol and linalool, have a strong antifungal activity by releasing secondary metabolites against candida albicans and candida tropicalis. Ethanolic extracts and ethyl acetate from Tulsi leaves obtained by the cold extraction method were used, and the antifungal activity was compared with that of fluconazole [29]. Ocimum sanctum essential oil is promising as an antifungal agent in combination treatments for candidiasis [30-33].

Aqueous extracts and oils from Ocimum sanctum have been compared, as an anti-candida activity, with those of other medicinal plants, with Tulsi essential oil proving to be the most effective [34]. Other researchers have synthesized silver nanoparticles using aqueous leaf extract of Ocimum sanctum (Tulsi) as a reducing agent, and found antimicrobial activity in Candida albicans as well [35].

Researchers are studying the use of Tulsi by incorporation into toothpaste or mouthwash, by studying the effects of declining periodontal indices, which are comparable to those of chlorhexidine [36 - 38].

A study by Gupta et al. showed a significant reduction in plaque, inflammation and gingival bleeding when a mouthwash of Ocimum sanctum was used for 15 to 30 days, which was as effective as chlorhexidine [39].

CONCLUSIONS

Ocimum sanctum extract, in concentrations between 5-10%, is recommended as an adjunct to mechanical therapy in the prevention and treatment of periodontal diseases, as well as for inhibiting the growth of bacteria responsible for carious lesions.

Tested Tulsi extracts show promising antibacterial activity and low cytotoxicity. Additional tests should be performed to eradicate the biofilm and examine the activity against other dental pathogens and the oral microbiome to confirm the potential of these extracts as antibacterial agents.

The Tulsi plant, widely grown in India, can be used for its anticancer properties for treating oral cancer. Not only will this be cost effective, but it will have fewer or no side effects.

Mouthwash with Ocimum sanctum proves to be effective due to its ability to lower periodontal indexes, being much more cost-effective than chlorhexidine and easily accessible.

Synthetic drugs have many side effects, so more attention has been paid to natural remedies, which are safe and effective. Today, the main focus is on herbal remedies, which has led to the screening of many plants for their potential antimicrobial activity. The same can be used clinically as an alternative to the drugs used in dentistry, for the treatment of diseases of the oral cavity.

REFERENCES

1. Akgül A. Volatile Oil Composition of Sweet Basil (Ocimum Basilicum L.) Cultivating in Turkey (Short Communication) Food Nahr. 1989;33:87–88.
2. Simon J.E., Quinn J., Murray R.G. Basil: A Source of Essential Oils. Advances in new crops; Proceedings of the First National Symposium "New Crops: Research, Development, Economics"; Indianapolis, IN, USA. 23–26 October 1988;484–489.
3. Lachowicz K.J., Jones G.P., Briggs D.R., Bienvenu F.E., Palmer M.V., Ting S.S.T., Hunter M. Characteristics of Essential Oil from Basil (Ocimum Basilicum L.) Grown in Australia. J. Agric. Food Chem. 1996;44:877–881.
4. Handbook of Arabian Medicinal Plants. [(accessed on 28 April 2021)]; Available online: https://www.routledge.com/Handbook-of-Arabian-Medicinal-Plants/Ghazanfar/p/book/9780849305399.
5. Antonescu Mintas AI, Miere Groza F, Fritea L, Ganea M, Zdrinca M, Dobjanschi L, Antonescu A, Vicas SI, Bodog F, Sindhu RK, Cavalu S. Perspectives on the Combined Effects of Ocimum basilicum and Trifolium pratense Extracts in Terms of Phytochemical Profile and Pharmacological Effects. Plants (Basel). 2021 Jul 7;10(7):1390.
6. Pattanayak P, Behera P, Das D, Panda SK. Ocimum sanctum linn. A reservoir plant for therapeutic applications: An overview. Pharmacogn Rev. 2010; 4:95–105.
7. Cohen MM. Tulsi-Ocimum sanctum: A herb for all reasons. J Ayurveda Integr Med. 2014;5:251-9.
8. Hamad GM, Darwish AMG, Abu-Serie MM, El-Sohaimy SA. Antimicrobial, Antioxidant and Anti-inflammatory Characteristics of Combination (Cassia fistula and Ocimum basilicum) Extract as Natural Preservative to Control & Prevent Food Contamination. Journal of Food and Nutrition Research. 2017; 5(10):771-780.
9. Carrol DH, Chassagne F, Dettweiler M, Quave CL. Antibacterial activity of plant species used for oral health against Porphyromonas gingivalis. PLoS One. 2020 Oct 8;15(10):e0239316.
10. Jayanti I, Jalaluddin M, Avijeeta A, Ramanna PK, Rai PM, Nair RA. In vitro Antimicrobial Activity of Ocimum sanctum (Tulsi) Extract on Aggregatibacter actinomycetemcomitans and Porphyromonas gingivalis. J Contemp Dent Pract. 2018 Apr 1;19(4):415-419.
11. Agarwal P, Nagesh L, Murlikrishnan. Evaluation of the antimicrobial activity of various concentrations of Tulsi (Ocimum sanctum) extract against Streptococcus mutans: an in vitro study. Indian J Dent Res. 2010 Jul-Sep;21(3):357-9.
12. Kochikar Pai R, Bhat SS, Salman A, Chandra J. Use of an Extract of Indian Sacred Plant Ocimum sanctum as an Anticariogenic Agent: An in vitro Study. Int J Clin Pediatr Dent. 2015 May-Aug;8(2):99-101.
13. Ghoke SS, Sood R, Kumar N, Pateriya AK, Bhatia S, Mishra A, Dixit R, Singh VK, Desai DN, Kulkarni DD, Dimri U, Singh VP. Evaluation of antiviral activity of Ocimum sanctum and Acacia

arabica leaves extracts against H9N2 virus using embryonated chicken egg model. BMC Complement Altern Med. 2018 Jun 5;18(1):174.
14. Zaidi KU, Shah F, Parmar R, Thawani V. Anticandidal synergistic activity of Ocimum sanctum and fluconazole of azole resistance strains of clinical isolates. J Mycol Med. 2018 Jun;28(2):289-293.
15. Gopalkrishna AH, Seshagiri M, Muddaiah S, Shashidara R. In vitro antifungal activity of different components of Centratherum anthelminticum and Ocimum sanctum seed oils and their synergism against oral pathogenic fungi. J Dent Res Dent Clin Dent Prospects. 2016 Spring;10(2):92-8.
16. Baliga MS, Jimmy R, Thilakchand KR, Sunitha V, Bhat NR, Saldanha E, Rao S, Rao P, Arora R, Palatty PL. Ocimum sanctum L (Holy Basil or Tulsi) and its phytochemicals in the prevention and treatment of cancer. Nutr Cancer. 2013;65 Suppl 1:26-35.
17. Karthikeyan K, Ravichandran P, Govindasamy S. Chemopreventive effect of Ocimum sanctum on DMBA-induced hamster buccal pouch carcinogenesis. Oral Oncol. 1999 Jan;35(1):112-9.
18. Utispan K, Niyomtham N, Yingyongnarongkul BE, Koontongkaew S. Ethanolic Extract of Ocimum sanctum Leaves Reduced Invasion and Matrix Metalloproteinase Activity of Head and Neck Cancer Cell Lines. Asian Pac J Cancer Prev. 2020 Feb 1;21(2):363-370.
19. Prakash P, Gupta N. Therapeutic uses of Ocimum sanctum Linn (Tulsi) with a note on eugenol and its pharmacological actions: a short review. Indian J Physiol Pharmacol. 2005 Apr;49(2):125-31.
20. Mallikarjun S, Rao A, Rajesh G, Shenoy R, Pai M. Antimicrobial efficacy of Tulsi leaf (Ocimum sanctum) extract on periodontal pathogens: An in vitro study. J Indian Soc Periodontol. 2016 Mar-Apr;20(2):145-50.
21. Eswar P, Devaraj CG, Agarwal P. Anti-microbial Activity of Tulsi {Ocimum Sanctum (Linn.)} Extract on a Periodontal Pathogen in Human Dental Plaque: An Invitro Study. J Clin Diagn Res. 2016 Mar;10(3):ZC53-6.
22. Devang Bharatkumar Khambholja et.al. Efficacy of Tulsi (Ocimum sanctum) Extract Incorporated onto Guided Tissue Regeneration (GTR) Membrane against Periodontal Pathogens. International Journal of Health Sciences & Research. 2019 Feb; 9(2):68-76
23. Rai A, Tripathi AM, Saha S, Dhinsa K, Jain B, Yadav G. Comparison of Antimicrobial Efficacy of Four Different Plant Extracts against Cariogenic Bacteria: An In Vitro Study. Int J Clin Pediatr Dent. 2020 Jul-Aug;13(4):361-367.
24. Harsha M, Mohan Kumar KP, Kagathur S, Amberkar VS. Effect of Ocimum sanctum extract on leukemic cell lines: A preliminary in-vitro study. J Oral Maxillofac Pathol. 2020;24(1):93-98.
25. Shivpuje P, Ammanangi R, Bhat K, Katti S. Effect of Ocimum sanctum on Oral Cancer Cell Line: An in vitro Study. J Contemp Dent Pract. 2015 Sep 1;16(9):709-14.
26. Bhattacharyya P, Bishayee A. Ocimum sanctum Linn. (Tulsi): an ethnomedicinal plant for the prevention and treatment of cancer. Anticancer Drugs. 2013 Aug;24(7):659-66.
27. Uma Devi P, Ganasoundari A, Vrinda B, Srinivasan KK, Unnikrishnan MK. Radiation protection by the Ocimum flavonoids orientin and vicenin: Mechanisms of action. Radiat Res 2000;154:455-60.
28. Srivastava A, Agarwal R, Chaturvedi TP, Chandra A, Singh OP. Clinical evaluation of the role of tulsi and turmeric in the management of oral submucous fibrosis: A pilot, prospective observational study. J Ayurveda Integr Med. 2015 Jan-Mar;6(1):45-9.
29. Samatha M, Reddy KH, Subrahamanyam G. Antifungal activity of solvent extracts of Piper betle and Ocimum sanctum Linn on Candida albicans: An in vitro comparative study. J Oral Maxillofac Pathol. 2019 Sep-Dec;23(3):333-337.
30. Amber K, Aijaz A, Immaculata X, Luqman KA, Nikhat M. Anticandidal effect of Ocimum sanctum essential oil and its synergy with fluconazole and ketoconazole. Phytomedicine. 2010 Oct;17(12):921-5.
31. Khan A, Ahmad A, Akhtar F, Yousuf S, Xess I, Khan LA, Manzoor N. Ocimum sanctum essential oil and its active principles exert their antifungal activity by disrupting ergosterol biosynthesis and membrane integrity. Res Microbiol. 2010 Dec;161(10):816-23.

32. Pozzatti P, Scheid LA, Spader TB, Atayde ML, Santurio JM, Alves SH. In vitro activity of essential oils extracted from plants used as spices against fluconazole-resistant and fluconazole-susceptible Candida spp. Can J Microbiol. 2008 Nov;54(11):950-6.
33. Zaidi KU, Shah F, Parmar R, Thawani V. Anticandidal synergistic activity of Ocimum sanctum and fluconazole of azole resistance strains of clinical isolates. J Mycol Med. 2018 Jun;28(2):289-293.
34. Khan A, Ahmad A, Manzoor N, Khan LA. Antifungal activities of Ocimum sanctum essential oil and its lead molecules. Nat Prod Commun. 2010 Feb;5(2):345-9.
35. Aazam ES, Zaheer Z. Growth of Ag-nanoparticles in an aqueous solution and their antimicrobial activities against Gram positive, Gram negative bacterial strains and Candida fungus. Bioprocess Biosyst Eng. 2016 Apr;39(4):575-84.
36. Penmetsa GS, Pitta SR. Efficacy of Ocimum sanctum, Aloe vera and chlorhexidine mouthwash on gingivitis: A randomized controlled comparative clinical study. Ayu. 2019 Jan-Mar;40(1):23-26.
37. Hosamane M, Acharya AB, Vij C, Trivedi D, Setty SB, Thakur SL. Evaluation of holy basil mouthwash as an adjunctive plaque control agent in a four day plaque regrowth model. J Clin Exp Dent. 2014 Dec 1;6(5): e491-6.
38. Nadar BG, Usha GV, Lakshminarayan N. Comparative Evaluation of Efficacy of 4% Tulsi Extract (Ocimum sanctum), Fluoridated and Placebo Dentifrices against Gingivitis and Plaque among 14-15 years School Children in Davangere City, India - A Triple Blinded Randomized Clinical Trial. Contemp Clin Dent. 2020 Jan-Mar;11(1):67-75.
39. Gupta D, Bhaskar DJ, Gupta RK, Karim B, Jain A, Singh R, Karim W. A randomized controlled clinical trial of Ocimum sanctum and chlorhexidine mouthwash on dental plaque and gingival inflammation. J Ayurveda Integr Med. 2014 Apr;5(2):109-16.

The importance of clinical examination in determining the benignity or malignancy of parotid tumors

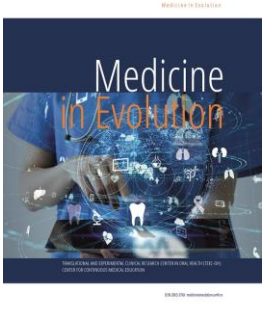

Urechescu H.[1], Talpoș Ș.[1], Cosoroabă R.M.[2], Popovici R.A.[2], Dinu S.C.[3], Pricop M.[1]

[1]Department of Maxillofacial Surgery, Faculty of Dentistry, Victor Babes University of Medicine and Pharmacy, Timisoara, Romania
[2]Discipline of Management, Legislation and Communication in Dentistry, Faculty of Dental Medicine, Departament 1, Victor Babes University of Medicine and Pharmacy, Timisoara, Romania
[3]Department of Pediatric Dentistry, Faculty of Dental Medicine, "Victor Babeş" University of Medicine and Pharmacy, Timişoara, Romania

Correspondence to:
Name: Talpoş Şerban
Address: Bd. Take Ionescu, nr.5, Timisoara, Romania
Phone: +40722434390
E-mail address: talpos.serban@umft.ro

Abstract

Parotid tumors are a common disease in the population not only as a primary disease but also in association with other diseases. There are a number of clinical signs and symptoms that may direct the examiner to a potential diagnosis of a benign or malignant tumor. The study is retrospective and consists in analysing the cases of parotid tumors treated during a year in the Maxillofacial Department. Clinical signs and symptoms that may indicate the malignancy or benign nature of the tumor were analysed and compared with the histopathological result obtained after surgical removal of the tumor. The aim is to determine the degree of correlation between the clinical signs and the type of tumor. Although the final diagnosis is determined by histopathological examination, clinical examination of any tumor is essential because it may lead to certain investigations and to the establishment of a specific treatment plan.

Keywords: Parotid tumor, clinical examination, benign, malignant

INTRODUCTION

The parotid gland is the largest of the major salivary glands, including the submandibular and sublingual glands. It is located in the retromandibular fossa. [1] It has superficial and deep lobes, separated by the facial nerve. The facial nerve and its branches pass through the parotid gland. [2] The superficial lobe lies lateral to the facial nerve and overlies the lateral surface of the masseter muscle. The deep lobe lies medial to the facial nerve and is situated between the mastoid process of the temporal bone and the mandibular ramus. [1]

The prevalence of parotid tumors is 70-85% compared to other major salivary glands. Most parotid tumors are well-defined and palpable mases and are located in the superficial lobe. 80% of these tumors are benign but parotid glands still account for almost half of all malignant salivary gland tumors. The incidence is estimated at 0.5 to 3.0 per 100,000 per year, accounting for about 5% of all head and neck malignancies. [3-6]

The latest World Health Organization (WHO) classification has attempted to simplify the classification but there are still more than 30 types of salivary gland tumors. [7] Malignant tumors of the parotid gland are represented by mucoepidermoid carcinoma, adenoid cystic carcinoma, acinic cell carcinoma, polymorphous adenocarcinoma, squamous cell carcinoma, lymphomas. Carcinomas can further be classified as high grade, low grade, or mixed. Benign tumors are mainly represented by pleomorphic adenoma followed by Warthin tumor. [8]

Fine-needle aspiration biopsy (FNA) is the primary diagnostic tool for parotid gland lesions. The role of FNA in the diagnosis of benign and malignant parotid tumor has some controversy regarding aspiration technique, adequacy of the specimen, cytological expertise, and limitations of the interpretation. For example, false-positive results can occur and lead to misdiagnosis of malignant lesions.

Regarding the imaging investigations, the ultrasound scan can provide information about the site, size and the presence of any significant cervical lymphadenopathy. It can be combined with FNA, which improves the accuracy rate. Also, ultrasound scan can distinguish malignant from benign disease in many situations. Computed tomography (CT) and magnetic resonance imaging (MRI) are other imaging investigations that can be used. MRI scanning of a parotid tumor is useful in the assessment and delineation of anatomical structures, extension into the deep lobe, and relation to the facial nerve. [9] However, if the result of paraclinical tests are at variance with other findings, then clinical judgment should prevail.

Pain, overlying skin ulceration, facial nerve palsy, adherence to deep planes, rapid growth in size or local lymph nodes swelling are clinical signs of malignancy. Medical history is important in patients with parotid lumps, as infectious, autoimmune or inflammatory processes may appear as neoplasms.

Aim and objectives

The aim of the study is to establish the importance of clinical signs in differentiating the benign or malignant character of a parotid tumor and to determine how much we can rely on the clinical examination when evaluating such a lesion.

MATERIAL AND METHODS

The present paper consists in a retrospective analysis of patients hospitalized in the Department of Maxillofacial Surgery Timisoara during a pre-pandemic year (2019). For the selection of patients, the database of the Timisoara Municipal Emergency Clinical Hospital, Maxillofacial Surgery Department was analysed.

Patient selection was performed using parotid tumor-specific diagnostic codes. After selecting the patients, the observation sheets were identified and analysed. A database was created in Microsoft Excel that contained the name, sex, age, primary diagnosis, clinical signs specific to parotid tumors, number of days of hospitalization, postoperative histopathological diagnosis, and benign or malignant nature of the tumor established following postoperative histopathological diagnosis. We recorded 7 clinical signs that are associated with malignancy in parotid tumors: tumor growth, consistency, ulceration of the covering skin, the presence of skin vascular pattern, bone invasion, facial nerve palsy, local or regional lymphadenopathy (Figures 1, 2, 3, 4).

Statistical processing along with graphs was performed in SPSSv17 and Microsoft Excel. In the case of nominal variables, the frequency tables were drawn up together with the "pie" type graphs. The associations and comparisons between these types of variables were made with the Chi2 test. For the numerical variables, the descriptive statistics were calculated, normality tests were performed and histogram, boxplot and column graphs were made. Comparisons between numerical series were performed with the non-parametric Mann-Whitney test in the case of comparisons between 2 series of values with non-gaussian distribution or between 2 series of ordinal values.

RESULTS

After analysing the observation sheets, a group of 28 patients was obtained, 64.3% (18) being female and 35.7% (10) being male (Table 1). The postoperative histopathological diagnosis showed that 64.3% (18) of the patients had a benign tumor and 35.7% (10) had a malignant tumor (Table 2). Regarding tumor growth, 67.9% (19) showed a slow growth and 32.1% (9) showed a rapid growth (Table 3). Tumor consistency was hard in 21.4% (6) of cases and soft in 78.6% (22) of cases (Table 4). 3.6% (1) of the cases showed skin vascular pattern (Table 5). Also, 3.6% (1) of the cases presented facial nerve palsy (Table 6). Regarding the growth of lymph nodes, 7.1% (2) of the cases presented local lymphadenopathy (Table 7). None of the cases showed ulceration of the covering skin or bone invasion (clinically detectable).

Table 1. Sex distribution

		Frequency	Percent	Valid Percent	Cumulative Percent
Valid	F	18	64,3	64,3	64,3
	M	10	35,7	35,7	100,0
	Total	28	100,0	100,0	

Table 2. Benign and malignant tumor distribution

		Frequency	Percent	Valid Percent	Cumulative Percent
Valid	Benign	18	64,3	64,3	64,3
	Malign	10	35,7	35,7	100,0
	Total	28	100,0	100,0	

Table 3. Tumor growth

		Frequency	Percent	Valid Percent	Cumulative Percent
Valid	Slow	19	67,9	67,9	67,9

	Rapid	9	32,1	32,1	100,0
	Total	28	100,0	100,0	

Table 4. Tumor consistency

		Frequency	Percent	Valid Percent	Cumulative Percent
Valid	Hard	6	21,4	21,4	21,4
	Soft	22	78,6	78,6	100,0
	Total	28	100,0	100,0	

Table 5. The presence of skin vascular pattern

		Frequency	Percent	Valid Percent	Cumulative Percent
Valid	Present	1	3,6	3,6	3,6
	Absent	27	96,4	96,4	100,0
	Total	28	100,0	100,0	

Table 6. Facial nerve palsy

		Frequency	Percent	Valid Percent	Cumulative Percent
Valid	Present	1	3,6	3,6	3,6
	Absent	27	96,4	96,4	100,0
	Total	28	100,0	100,0	

Table 7. Local or regional lymphadenopathy

		Frequency	Percent	Valid Percent	Cumulative Percent
Valid	Present	2	7,1	7,1	7,1
	Absent	26	92,9	92,9	100,0
	Total	28	100,0	100,0	

Figure 1. Left parotid tumor with slow growth and soft consistency

Figure 2. Right parotid tumor with slow growth, soft consistency and no facial nerve palsy

Figure 3. Left parotid tumor with skin vascular pattern

Figure 4. Left parotid tumor with facial nerve palsy

The association between the type of tumor and the sex of the patients is insignificant (Chi2 test, p = 0.725) (Table 8). The proportion of malignant tumors is significantly increased for those with rapid growth (Chi2 test, p <0.001) (Table 9). The proportion of malignant tumors is significantly increased for those with hard consistency (Chi2 test, p <0.001) (Table 10). The association between the type of tumor and the presence of the skin vascular pattern is insignificant (Chi2 test, p = 0.172) (Table 11), the situation being the same regarding the association between the tumor type and the presence of facial nerve palsy (Chi2 test, p = 0.172) (Table 12) and the presence of local and regional lymphadenopathy (Chi2 test, p = 0.119) (Table 13).

Age is significantly increased in patients with malignant tumor (Mann-Whitney test, p = 0.009). No significant association was established between the number of days of hospitalization and the type of tumor (Mann-Whitney test, p = 0.382) (Table 14).

Table 8. Association between tumor type and sex of the patient

			Sex		Total
			F	M	
Tumor type	Malign	Count	6	4	10
		% within Type	60,0%	40,0%	100,0%
	Benign	Count	12	6	18
		% within Type	66,7%	33,3%	100,0%
Total		Count	18	10	28
		% within Tip	64,3%	35,7%	100,0%

Table 9. Association between tumor type and tumor growth rate

			Tumor growth		Total
			Slow	Rapid	
Tumor type	Malign	Count	1	9	10
		% within Type	10,0%	90,0%	100,0%
	Benign	Count	18	0	18
		% within Type	100,0%	,0%	100,0%
Total		Count	19	9	28
		% within Tip	67,9%	32,1%	100,0%

Table 10. Association between tumor type and tumor consistency

			Tumor consistency		Total
			Hard	Soft	
Tumor type	Malign	Count	6	4	10
		% within Type	60,0%	40,0%	100,0%
	Benign	Count	0	18	18
		% within Type	,0%	100,0%	100,0%
Total		Count	6	22	28
		% within Tip	21,4%	78,6%	100,0%

Table 11. Association between tumor type and skin vascular pattern

			Skin vascular pattern		Total
			Present	Absent	
Tumor type	Malign	Count	1	9	10
		% within Tip	10,0%	90,0%	100,0%
	Benign	Count	0	18	18
		% within Tip	,0%	100,0%	100,0%
Total		Count	1	27	28
		% within Tip	3,6%	96,4%	100,0%

Table 12. Association between tumor type and facial nerve palsy

			Facial nerve palsy		Total
			Present	Absent	
Tumor type	Malign	Count	1	9	10
		% within Tip	10,0%	90,0%	100,0%
	Benign	Count	0	18	18
		% within Tip	,0%	100,0%	100,0%
Total		Count	1	27	28
		% within Tip	3,6%	96,4%	100,0%

Table 13. Association between tumor type and local and regional lymphadenopathy

			Lymphadenopathy		Total
			Present	Absent	
Tumor type	Malign	Count	2	8	10
		% within Tip	20,0%	80,0%	100,0%
	Benign	Count	0	18	18
		% within Tip	,0%	100,0%	100,0%
Total		Count	2	26	28
		% within Tip	7,1%	92,9%	100,0%

Table 14. Association between tumor type and age / tumor type and number of days of hospitalization

	Tumor type	N	Mean	Std. Deviation	Std. Error Mean
Age	Benign	18	55,50	12,650	2,982
	Malign	10	71,20	13,448	4,253
Days of hospitalization	Benign	18	6,89	2,083	,491
	Malign	10	6,10	3,479	1,100

DISCUSSIONS

Although the final diagnosis is determined by histopathological examination, clinical examination of any tumor is essential.

According to statistics, the incidence of malignancies is higher among elderly patients, but this cannot be considered a rule, as these tumors have also been observed in young people.

Pain, facial nerve palsy, adherence to deep planes, rapid growth and hard consistency are signs of malignancy. A malignant tumor can also ulcerate the covering skin and invade bone structures. None of the 28 patients in the study had skin ulceration or bone invasion, and the skin vascular pattern was present in a single tumor, although only 18 were benign and the remaining 10 were malignant. This highlights the fact that not all malignancies also have clinical signs of malignancy. There are situations in which the clinical examination may mislead us due to the absence of clinical signs of malignancy. One of the reasons could be the early stage of the malignant tumor when the tumor is small and without invasion or local changes.

A very useful aspect is the consistency of the tumor and its growth in the orientation towards a presumed diagnosis. The share of fast-growing and hard-growing tumors was significantly higher in malignancies.

Regarding local or regional lymphadenopathy, only 2 tumors had it associated, although this is a sign of malignancy especially in the advanced stages.

CONCLUSIONS

Early diagnosis of malignant parotid tumors is very important for the prognosis of the disease. Clinical examination can provide important information in diagnosing this type of lesion as soon as possible. There are a number of clinical signs that may be associated with malignancy in parotid tumors. These are represented by rapid tumor growth, hard consistency, ulceration of the covering skin, the presence of skin vascular pattern, bone invasion, facial nerve palsy, local or regional lymphadenopathy. The presence of one or more of these signs should warn of the possible malignancy of the tumor. The absence of these clinical signs in no way precludes the possibility that the tumor is malignant. Further investigation is absolutely necessary in the case of any parotid tumor. The histopathological diagnosis remains the definite diagnosis.

REFERENCES

1. Bialek EJ, Jakubowski W, Zajkowski P, Szopinski KT, Osmolski A. US of the major salivary glands: anatomy and spatial relationships, pathologic conditions, and pitfalls. Radiographics. 2006 May-Jun;26(3):745-63.
2. Borle RM, Jadhav A, Bhola N, Hingnikar P, Gaikwad P. Borle's triangle: A reliable anatomical landmark for ease of identification of facial nerve trunk during parotidectomy. J Oral Biol Craniofac Res. 2019 Jan-Mar;9(1):33-36.
3. Chan W.H., Lee K.W., Chiang F.Y., Ho K.Y., Chai C.Y., Kuo W.R.: Features of parotid gland diseases and surgical results in southern Taiwan. KaohsiungJ. Med. Sci. 2010; 26: 483–492.
4. Fonseca F.P., de Carvalho M.V., de Almeida O.P., Rangel A.L., Takizawa M.C., Bueno A.G., Vargas P.A.: Clinicopathologic analysis of 493 cases of salivarygland tumours in a Southern Brazilian population. Oral Surg. Oral Med. Oral Pathol. Oral Radiol. 2012; 114: 230–239
5. Lee Y.M., Choi H.J., Kim J.W., Kim J.H.: Parotid gland tumours in a Korean population. J. Craniofac. Surg. 2012; 23: 205–209.

6. Stryjewska-Makuch G, Kolebacz B, Janik MA, Wolnik A. Increase in the incidence of parotid gland tumors in the years 2005-2014. Otolaryngol Pol. 2017 Apr 30;71(2):29-34.
7. Paul M. Speight, A William Barrett, Salivary gland tumours: diagnostic challenges and an update on the latest WHO classification, Diagnostic Histopathology, Volume 26, Issue 4, 2020, 147-158
8. Sood S, McGurk M, Vaz F. Management of Salivary Gland Tumours: United Kingdom National Multidisciplinary Guidelines. J Laryngol Otol. 2016 May;130(S2) 142-S149.
9. Zengel P, Notter F, Clevert DA. VTIQ and VTQ in combination with B-mode and color Doppler ultrasound improve classification of salivary gland tumors, especially for inexperienced physicians. Clin Hemorheol Microcirc. 2018;70(4):457-466.

Meine Zukunft in Deutschland.

Der Start als Zahnarzt in Deutschland beginnt mit uns.

Ob eigene Praxis oder angestellter Zahnarzt
Mit unseren Kenntnissen und Erfahrungen stehen wir Ihnen in allen Fragen zur Verfügung. Wir helfen Ihnen beim Umgang mit Behörden, dem Erlangen einer Kassenzulassung, der Standort- und Praxissuche, der Beschaffung des Startkapitals und Finanzierungen jeglicher Art.

Als führendes Dental-Labor in Deutschland in den Bereichen **CNC-Fräsung**, **digitale Fertigung**, **3D-Druck** und **Intraoral-Scannen** bieten wir ein großes und hoch- modernes Portfolio an dentalen Leistungen an. Nehmen Sie Kontakt zu uns auf. **Wir kümmern uns um Ihre Formalitäten.**

HARTL GmbH
DENTALE TECHNOLOGIEN

Renthof 1
34117 Kassel
Deutschland

Fon: +49 561 - 560 24
+49 561 - 570 390
Email: hartl@web.de

Cephalometric analysis of the upper airway in adult Caucasians with skeletal Class I and Class II malocclusion

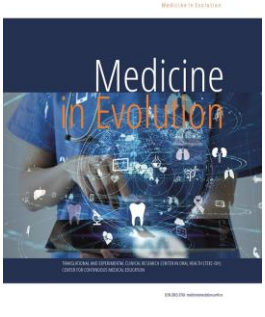

Popa G.[1], Bratu D.C.[1], Podariu A.C.[2], Dragoş B.[3], Luca M.M.[4], Pop S.I.[5]

[1]*Department of Orthodontics and Dento-Facial Orthopedics, Orthodontic Research Center, Faculty of Dental Medicine, "Victor Babeş" University of Medicine and Pharmacy, Timişoara, Romania*
[2]*Department of Preventive, Community Dentistry and Oral Health, Faculty of Dental Medicine, "Victor Babeş" University of Medicine and Pharmacy, Timişoara, Romania*
[3]*Research Center in Dental Medicine Using Conventional and Alternative Technologies, Faculty of Dental Medicine, "Victor Babeş" University of Medicine and Pharmacy, Timişoara, Romania*
[4]*Department of Pediatric Dentistry, Pediatric Dentistry Research Center, Faculty of Dental Medicine, "Victor Babeş" University of Medicine and Pharmacy, Timişoara, Romania*
[5]*Department of Orthodontics, Faculty of Dental Medicine, George Emil Palade University of Medicine, Pharmacy, Science, and Technology, Târgu Mureş, Romania*

Correspondence to:
Name: Bratu Dana Cristina
Address: Department of Orthodontics and Dento-Facial Orthopedics, Faculty of Dental Medicine, 9 Revoluției din 1989 Boulevard, Timişoara, Romania
Phone: +40 744835314
E-mail address: danacristinabratu@yahoo.com

Abstract

Aim and objectives: The aim of our study was to evaluate the nasopharyngeal and oropharyngeal anteroposterior space width in adult Caucasians with skeletal Class I and Class II malocclusion, using several linear cephalometric measurements.

Material and methods: Our retrospective study included a total of 60 lateral cephalometric radiographs from adult patients (31 females and 29 males), with skeletal Class I and skeletal Class II malocclusion, aged 18 to 34 years. The skeletal pattern was assessed using Steiner's ANB angle. The pharyngeal width measurements included the width of the nasopharynx, upper pharyngeal airway width (UPAW), middle pharyngeal airway width (MPAW) and lower pharyngeal airway width (LPAW).

Results and conclusions: The mean values of UPAW and MPAW in the skeletal Class II male subgroup were significantly lower than the mean values in the female subgroup. The mean values of LPAW in the skeletal Class I male subgroup were significantly higher than the mean values in the female subgroup. The mean values of MPAW and LPAW in the skeletal Class I male subgroup were significantly higher than the mean values in skeletal Class II male subgroup.

Keywords: upper airway, skeletal Class I, skeletal Class II, cephalometric analysis

INTRODUCTION

The pharynx, a segment of the upper airways, is a muscular tube divided into three anatomical regions, according to their location: the nasopharynx, oropharynx, and hypopharynx (laryngopharynx).

The nasal cavities extend posteriorly with an elongated space, the nasopharynx, which is delimited by the base of the skull and the posterior surface of the soft palate. The hypertrophy of the adenoid tonsils, located on the posterosuperior wall of the nasopharynx, is one of the most frequent causes for the constriction of the upper respiratory tract. The middle part of the pharynx, the oropharynx, is the space located behind the oral cavity, inferior to the soft palate region and above the superior border of the epiglottis. The hypopharynx is the most inferior region of the pharynx and is delimited caudally by the inferior border of the cricoid cartilage.

The relationship between the respiratory function and the growth and development of the craniofacial structures has long been debated in the literature, but with contradictory results. There are authors that didn't find any correlation between the characteristics of the craniofacial complex and the pharyngeal region [1–4], while other authors found significant relationships between these structures [5–8].

Being able to identify the predisposition to respiratory disorders based on the craniofacial skeletal patterns, or the predisposition to malocclusion based on the alterations in the respiratory function (e.g., oral breathing, sleep apnea) or on the factors that cause upper airway obstruction (e.g., hypertrophied adenoids, infections, allergies), could provide the clinicians with the proper tools for early diagnosing these anomalies [1,9–11].

When compared to CBCT scans, two-dimensional radiographic images cannot offer data about the depth or the volume of the anatomic structures. Even with these limitations, lateral cephalograms continue to be a useful standard complementary exam for analyzing the craniofacial and the pharyngeal airway morphology, because they are accessible, reliable and require exposure to very low doses of radiation [8,12].

Aim and objectives

The aim of our study was to evaluate the nasopharyngeal and oropharyngeal anteroposterior space width in adult Caucasians with skeletal Class I and Class II malocclusion, using several linear cephalometric measurements.

MATERIAL AND METHODS

Our retrospective study included a total of 60 lateral cephalometric radiographs from adult patients (31 females and 29 males), with skeletal Class I and skeletal Class II malocclusion, aged 18 to 34 years. The patients were selected from the database in our private dental office and from the Department of Orthodontics and Dento-Facial Orthopedics, Faculty of Dental Medicine, "Victor Babeş" University of Medicine and Pharmacy Timişoara. All the patients agreed to participate in medical research and they all signed an informed consent. The patients were included in the study according to the following criteria: Romanian Caucasian adult patients, without upper airway obstruction, with no respiratory disorders, with posterior dental arch integrity (no extractions, with the exception of the third molars), without prior orthodontic treatment or orthognathic surgery.

Investigation method

The radiographs were digitally analyzed using the AudaxCeph 5 Essentials orthodontic software suite. We used a custom cephalometric analysis for linear and angular

measurements, with the following skeletal cephalometric landmarks: N (nasion), Point A, Point B, ANS (anterior nasal spine), PNS (posterior nasal spine), S (sella) and Ba (basion).

The skeletal pattern of each patient was assessed using Steiner's ANB angle, which is obtained by subtracting the value of SNB angle from the value of SNA angle. The patients were divided in two groups: skeletal Class I group (ANB = 2° ± 2°) and skeletal Class II group (ANB > 4°). A cephalometric tracing with the angular measurements is illustrated in Figure 1.

For the analysis of the width of the nasopharynx (PNSp-Ad), we used two constructed landmarks (PNSp and Ad), which resulted from the intersection of the radiographic contour of the soft tissue of the nasopharynx and a line connecting PNS with the midpoint (M) of the sella-basion line (S-Ba). PNSp was defined as the intersection point between the PNS-M line and the anteroinferior region of the radiographic contour of the nasopharynx. Ad (adenoid point) was defined as the intersection point between the PNS-M line and the posterosuperior area of the radiographic contour of the nasopharynx. The upper pharyngeal airway width (UPAW), the border between the nasopharynx and the oropharynx, was defined by the intersection of the posterior extension of the palatal plane (ANS-PNS) and the radiographic contour of the oropharynx; one intersection point is located on the posterior surface of the soft palate and the other, on the posterior pharyngeal wall. In order to characterize the middle pharyngeal airway width (MPAW), we chose to measure the narrowest width between the posterior surface of the soft palate and the posterior pharyngeal wall, along a line parallel with the palatal plane. The lower pharyngeal airway width (LPAW) was measured along a line parallel with the palatal plane, between the posterior pharyngeal wall and a point located at the intersection of the contour of the mandible and the base of the tongue. All the landmarks and linear measurements are illustrated on the cephalometric tracing in Figure 2.

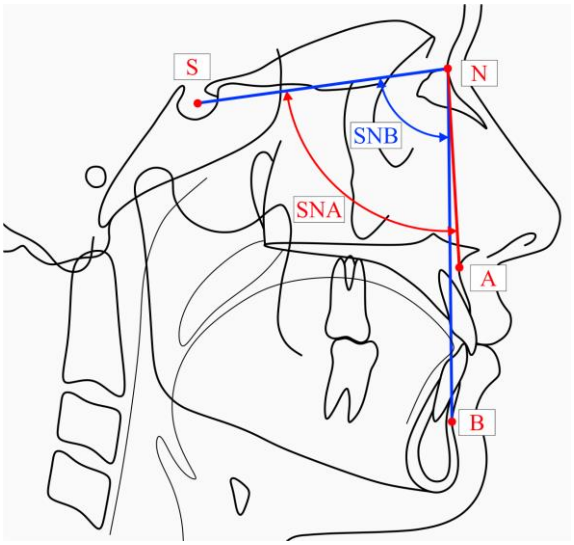

Figure 1. Cephalometric tracing illustrating the angular measurements SNA and SNB

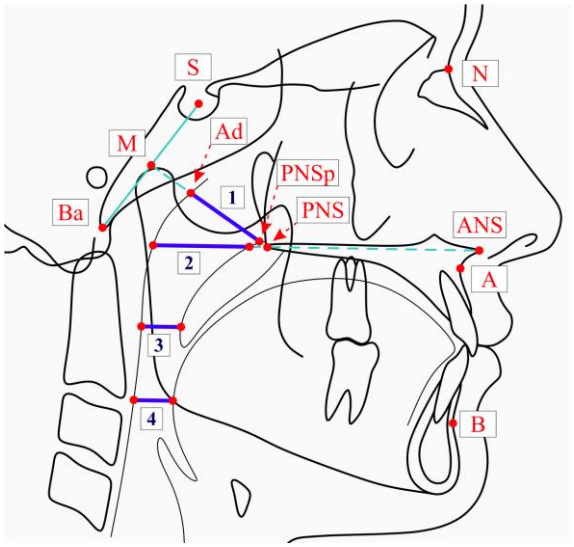

Figure 2. Cephalometric tracing illustrating the linear measurements: 1 – PNSp-Ad; 2 – UPAW; 3 – MPAW; 4 – LPAW

Statistical analysis

The data were statistically analyzed using the IBM SPSS Statistics for Windows software package (IBM SPSS Statistics for Windows, Version 24.0. Armonk, NY: IBM Corp). Descriptive statistics were generated for all the measured variables. Independent-samples t-tests were used to test for differences in the examined variables between males and females with the same sagittal skeletal pattern, and between males and females belonging to different skeletal groups (Class I vs Class II). We considered the independent-samples t-test to be statistically significant at $p < 0.05$.

One outlier was identified in the MPAW Class I male group, as assessed by inspection of boxplots. We decided to include the outlier in the data set, because the outlier was not extreme and it did not affect the outcome of the study. The measured variables were normally distributed, as assessed by Shapiro-Wilk's test ($p > 0.05$). There was homogeneity of variances for all the measured variables, as assessed by Levene's test for equality of variances ($p > 0.05$), with only two exceptions. There was no homogeneity of variances for PNSp-Ad and MPAW when comparing all the patients (males and females overall) in skeletal Class I group and Class II group, therefore a Welch t-test was used to analyse the data.

RESULTS

The sample distribution by age and gender (31 females and 29 males) in skeletal Class I group and skeletal Class II group is shown in Figure 3 and Figure 4.

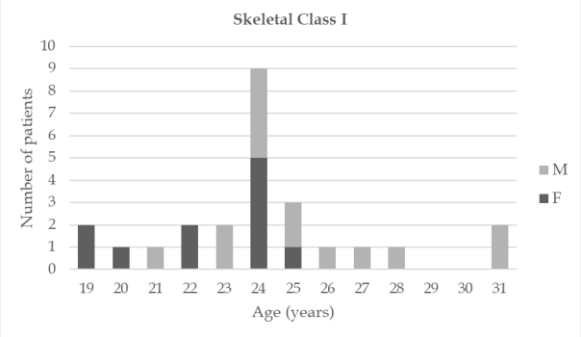

Figure 3. Sample distribution by age and gender in skeletal Class I group (M – males; F – females)

Figure 4. Sample distribution by age and gender in skeletal Class II group (M – males; F – females)

The descriptive statistics and the results of the independent-samples t-test are presented in Table 1. The independent-samples t-test was used to determine if there were differences in the pharyngeal width measurements between males and females belonging to the same group (skeletal Class I group and Class II group, respectively).

Table 1. Comparison of the pharyngeal width measurements between males and females belonging to the same group (Class I group and Class II group, respectively) and the results of the independent-samples t-test

Variables	Skeletal Class	Males				Females				t-test						
		N	Mean	SD	SEM	N	Mean	SD	SEM	*t*	df	*p*	Mean Diff.	SED	95% CI	
															Lower	Upper
PNSp-Ad (mm)	I	14	19.91	3.08	0.82	11	18.83	2.76	0.83	0.91	23.00	0.373	1.08	1.19	-1.38	3.54
	II	15	19.83	2.01	0.52	20	20.18	2.35	0.53	-0.47	33.00	0.643	-0.35	0.76	-1.89	1.18
UPAW (mm)	I	14	19.78	2.70	0.72	11	20.32	2.68	0.81	-0.50	23.00	0.623	-0.54	1.08	-2.78	1.70
	II	15	18.91	2.50	0.65	20	21.71	2.65	0.59	-3.17	33.00	0.003**	-2.81	0.88	-4.60	-1.01
MPAW (mm)	I	14	9.25	1.24	0.33	11	8.77	1.82	0.55	0.78	23.00	0.443	0.48	0.61	-0.79	1.74
	II	15	6.82	2.05	0.53	20	9.37	2.18	0.49	-3.51	33.00	0.001**	-2.55	0.73	-4.03	-1.07
LPAW (mm)	I	14	12.66	2.44	0.65	11	9.49	1.68	0.51	3.67	23.00	0.001**	3.17	0.86	1.38	4.95
	II	15	10.74	1.85	0.48	20	11.44	3.06	0.69	-0.79	33.00	0.438	-0.70	0.89	-2.52	1.12

N – sample size; SD – Std. Deviation; SEM - Std. Error Mean; df – degrees of freedom; Mean Diff. – Mean Difference; SED - Std. Error Difference; 95% CI – 95% Confidence Interval of the Difference; **p < 0.005.

The mean values of UPAW and MPAW in the skeletal Class II male subgroup were significantly lower than the mean values in the female subgroup ($p = 0.003$ and $p = 0.001$, respectively).

The mean values of LPAW in the skeletal Class I male subgroup were significantly higher than the mean values in the female subgroup ($p = 0.001$).

Table 2 shows the differences between the pharyngeal width measurements for the male subgroups belonging to different skeletal groups (Class I vs Class II) and the female subgroups belonging to different skeletal groups (Class I vs Class II).

Table 2. Comparison of the measured variables between males belonging to different skeletal groups and females belonging to different skeletal groups and the results of the independent-samples t-test

Variables	Gender (Class I vs Class II)	*t*	df	*p*	Mean Diff.	SED	95% CI	
							Lower	Upper
PNSp-Ad (mm)	M	0.09	27.00	0.930	0.08	0.96	-1.88	2.05
	F	-1.44	29.00	0.162	-1.35	0.94	-3.27	0.57
UPAW (mm)	M	0.90	27.00	0.374	0.87	0.97	-1.11	2.86
	F	-1.39	29.00	0.174	-1.39	1.00	-3.43	0.65
MPAW (mm)	M	3.82	27.00	0.001**	2.42	0.64	1.12	3.73
	F	-0.78	29.00	0.441	-0.60	0.77	-2.19	0.98
LPAW (mm)	M	2.40	27.00	0.023*	1.92	0.80	0.28	3.56
	F	-1.94	29.00	0.062	-1.94	1.00	-3.99	0.10

M – males; F – females; df – degrees of freedom; Mean Diff. – Mean Difference; SED - Std. Error Difference; 95% CI – 95% Confidence Interval of the Difference; *p < 0.05; **p < 0.005.

The mean values of MPAW and LPAW in the skeletal Class I male subgroup were significantly higher than the mean values in skeletal Class II male subgroup (p = 0.001 and p = 0.023, respectively).

There were no statistically significant differences between the patients (males and females overall) belonging to skeletal Class I group and the patients (males and females overall) belonging to skeletal Class II group (Table 3).

Table 3. Overall comparison of the measured variables between all the patients in skeletal Class I group and all the patients in skeletal Class II group and the results of the independent-samples t-test. A Welch t-test was used to analyse the variables PNSp-Ad and MPAW

Variables	Skeletal Class I				Skeletal Class II				t-test						
	N	Mean	SD	SEM	N	Mean	SD	SEM	*t*	df	*p*	Mean Diff.	SED	95% CI	
														Lower	Upper
PNSp-Ad (mm)	25	19.44	2.94	0.59	35	20.03	2.19	0.37	-0.85	42.11	0.398	-0.59	0.69	-1.99	0.81
UPAW (mm)	25	20.02	2.65	0.53	35	20.51	2.91	0.49	-0.67	58.00	0.505	-0.49	0.74	-1.96	0.98
MPAW (mm)	25	9.04	1.51	0.30	35	8.28	2.45	0.41	1.48	56.91	0.146	0.76	0.51	-0.27	1.78
LPAW (mm)	25	11.27	2.64	0.53	35	11.14	2.60	0.44	0.19	58.00	0.852	0.13	0.69	-1.24	1.50

N – sample size; SD – Std. Deviation; SEM - Std. Error Mean; df – degrees of freedom; Mean Diff. – Mean Difference; SED - Std. Error Difference; 95% CI – 95% Confidence Interval of the Difference.

DISCUSSIONS

In the literature, there are several different approaches of assessing the upper airway morphology and dimensions. There are studies using either 2D or 3D imaging techniques, with a variety of proposed landmarks and reference planes, which creates some difficulty in properly comparing the reported findings. Discrepancies between sample sizes and ethnic groups are other potential sources of contradictory results.

Nasopharyngeal dimensions were examined in many studies, both in Class I and Class II malocclusion. In one of these studies, Kim, Hong, Hwang and Park reported that the nasopharyngeal region had a similar or a wider width in subjects with Class II malocclusion, while the oropharyngeal area was narrower [13].

Alves et al. found that Class II patients had a narrower pharyngeal width, especially in the oropharynx at the level of the mandible and at the tip of the uvula, and also in the nasopharyngeal region at the level of the hard palate [2].

In a study that analyzed both the sagittal and vertical skeletal patterns, de Freitas et al. found that the type of malocclusion did not influence the upper and the lower pharyngeal airway widths in Class I and Class II patients [14].

Similar results were found by Memon, Fida and Shaikh [15] who concluded that the type of sagittal malocclusion had no effect on the upper pharyngeal width. Chauhan, Autar, Pradham and Yadav [16], found no significant differences in the measured pharyngeal anteroposterior dimensions between Class I and Class II Division I patients.

When we analyzed the sagittal skeletal groups in our study, without considering the patients' gender, we found similar results, with no statistically significant differences between the skeletal Class I group and the skeletal Class II group. When we compared the data for possible sexual dimorphism, our findings revealed that the mean values of the upper and middle pharyngeal airway widths in the skeletal Class II male subgroup were significantly lower than the mean values in the female subgroup.

Regarding the lower pharyngeal airway width, Küçükkaraca et al. compared Class II Division 1 and Division 2 groups with Class I malocclusion; the authors reported that the lower airway in Class I malocclusion was narrower than in Class II [17].

In our study we found that the mean values of the lower pharyngeal airway width in the skeletal Class I male subgroup were significantly higher than the mean values when compared both to the Class I female subgroup and the skeletal Class II male subgroup.

The main limitation of 2D radiographic images is that they cannot offer any information about the volume of the upper respiratory tract, therefore we intend to extend our research in the future to include a larger sample size and CBCT scans in order to better characterize the morphology of the pharyngeal structures.

CONCLUSIONS

The mean values of UPAW and MPAW in the skeletal Class II male subgroup were significantly lower than the mean values in the female subgroup. The mean values of LPAW in the skeletal Class I male subgroup were significantly higher than the mean values in the female subgroup. The mean values of MPAW and LPAW in the skeletal Class I male subgroup were significantly higher than the mean values in skeletal Class II male subgroup. There were no statistically significant differences between the patients (males and females overall) belonging to skeletal Class I group and the patients (males and females overall) belonging to skeletal Class II group.

REFERENCES

1. Indriksone I, Jakobsone G. The upper airway dimensions in different sagittal craniofacial patterns: a systematic review. Stomatologija. 2014;16(3):109–17.
2. Alves M, Franzotti ES, Baratieri C, Nunes LKF, Nojima LI, Ruellas ACO. Evaluation of pharyngeal airway space amongst different skeletal patterns. Int J Oral Maxillofac Surg. 2012 Jul;41(7):814–9.
3. Grauer D, Cevidanes LSH, Styner MA, Ackerman JL, Proffit WR. Pharyngeal airway volume and shape from cone-beam computed tomography: relationship to facial morphology. Am J Orthod Dentofacial Orthop. 2009 Dec;136(6):805–14.
4. Oh KM, Hong JS, Kim YJ, Cevidanes LSH, Park YH. Three-dimensional analysis of pharyngeal airway form in children with anteroposterior facial patterns. Angle Orthod. 2011 Nov;81(6):1075–82.
5. Diwakar R, Kochhar AS, Gupta H, Kaur H, Sidhu MS, Skountrianos H, Singh G, Tepedino M. Effect of Craniofacial Morphology on Pharyngeal Airway Volume Measured Using Cone-Beam

Computed Tomography (CBCT)—A Retrospective Pilot Study. Int J Environ Res Public Health. 2021;18(9):5040.
6. Lopatienė K, Dabkutė A, Juškevičiūtė V. Vertical and sagittal morphology of the facial skeleton and the pharyngeal airway. Stomatologija. 2016;18(1):21–5.
7. Swathi K, Maragathavalli G. Cephalometric assessment of the width of pharyngeal airway space and correlation with skeletal malocclusion- A retrospective study. J Pharm Sci Res. 2019;11(6):2263–6.
8. Kaur S, Rai S, Kaur M. Comparison of reliability of lateral cephalogram and computed tomography for assessment of airway space. Niger J Clin Pract. 2014;17(5):629–36.
9. Ryu HH, Kim CH, Cheon SM, Bae WY, Kim SH, Koo SK, Kim MS, Kim BJ. The usefulness of cephalometric measurement as a diagnostic tool for obstructive sleep apnea syndrome: a retrospective study. Oral Surg Oral Med Oral Pathol Oral Radiol. 2015 Jan;119(1):20–31.
10. Nadja e Silva N, Lacerda RHW, Silva AWC, Ramos TB. Assessment of upper airways measurements in patients with mandibular skeletal Class II malocclusion. Dental Press J Orthod. 2015 Sep;20(5):86–93.
11. Silva VG, Pinheiro LAM, Silveira PL da, Duarte ASM, Faria AC, Carvalho EGB de, Zancanella E, Crespo AN. Correlation between cephalometric data and severity of sleep apnea. Braz J Otorhinolaryngol. 2014;80(3):191–5.
12. Borges P de TM, da Silva BB, Moita Neto JM, Borges NE de S, Li LM. Cephalometric and anthropometric data of obstructive apnea in different age groups. Braz J Otorhinolaryngol. 2015 Jan 1;81(1):79–84.
13. Kim YJ, Hong JS, Hwang YI, Park YH. Three-dimensional analysis of pharyngeal airway in preadolescent children with different anteroposterior skeletal patterns. Am J Orthod Dentofacial Orthop. 2010;137(3):306.e1-306.e11.
14. de Freitas MR, Alcazar NMPV, Janson G, de Freitas KMS, Henriques JFC. Upper and lower pharyngeal airways in subjects with Class I and Class II malocclusions and different growth patterns. Am J Orthod Dentofacial Orthop. 2006 Dec;130(6):742–5.
15. Memon S, Fida M, Shaikh A. Comparison of Different Craniofacial Patterns with Pharyngeal Widths. J Coll Physicians Surg Pakistan. 2012;22(5):302–6.
16. Chauhan A, Autar R, Pradhan KL, Yadav V. Comparison of pharyngeal airway dimension, tongue and hyoid bone position based on ANB angle. Natl J Maxillofac Surg. 2015;6(1):42.
17. Küçükkaraca E, Üçüncü N. Sınıf II Div 1 ve Sınıf II Div 2 Malokluzyonlu Bireylerde Havayolunun Değerlendirilmesi [Aiway Evaluation in Class II Div 1 and Class II Div 2 Malocclusion Individuals]. Turkiye Klin Orthod Top. 2019;5(3):23–8.

Hemisection: A conservative management of an abutment mandibular molar tooth - Case report

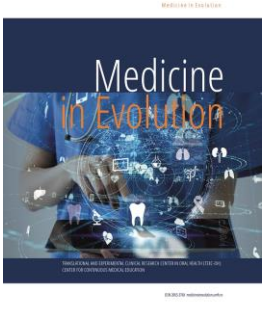

Todor L.[1], Bonta D.F.[1], Todor S.A.[2], Porumb A.[1], Cosoroaba R.M.[3], Popovici R.A.[3], Pricop M.O.[4]

[1]*Department of Dental Medicine, Faculty of Medicine and Pharmacy, University of Oradea, Romania*
[2]*Dentist doctor, private medical office, Oradea, Romania*
[3]*Department 1, Faculty of Dental Medicine, Victor Babes University of Medicine and Pharmacy, Timisoara, Romania*
[4]*Department 2, Faculty of Dental Medicine, Victor Babes University of Medicine and Pharmacy, Timisoara, Romania*

Correspondence to:
Name: Dan Florin Bonta
Address: Department of Dental Medicine, Faculty of Medicine and Pharmacy, University of Oradea, Romania, December 1st Square no.10, 410068 Oradea, Bihor County, Romania
Phone: +40766611693
E-mail address: bontadan2006@yahoo.com

Abstract

Hemisection of the mandibular molars is an option for surgical treatment when a vertical coronal fracture has occurred and a root is healthy.

This article illustrates a case in which the damaged terminal abutment was part of a fixed prosthesis. The loss of a distal abutment can result in the patient wearing a removable partial denture. Hemisection and fixed prosthetic rehabilitation gave a satisfactory result. This treatment option should always be considered before tooth extraction and implant therapy.

Keywords: hemisection, mandibular molar, abutment, fixed prosthesis

INTRODUCTION

Hemisection at the level of a molar (Figure 1) is the removal of a root together with the corresponding part of the crown, and is practiced to preserve the structure of the tooth and alveolar bone, and perform the fixed prosthetic restoration. Hemisection can be considered as an alternative treatment option to extraction and implant therapy [1-5].

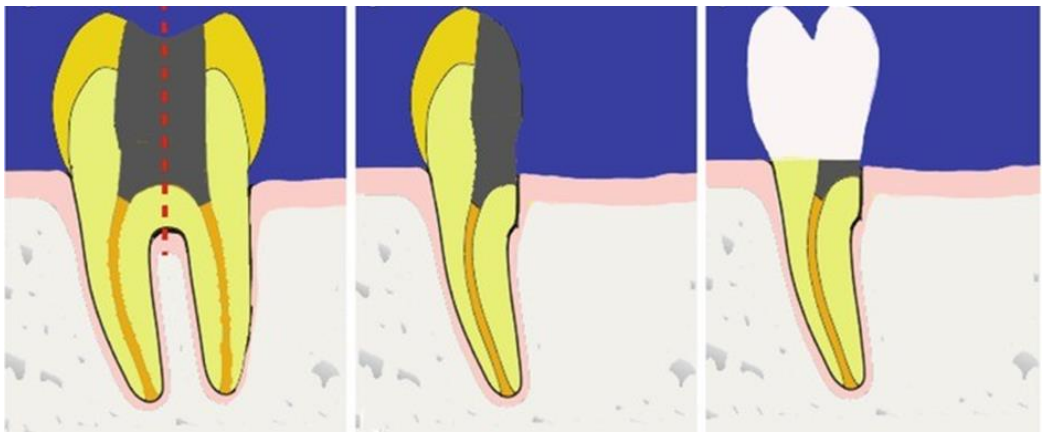

Figure 1. Hemisection of a molar

A mandibular molar may have affected the forked area or one of the roots as a result of carious lesions, periodontal disease or coronary fractures [6,7]. Efforts to save parts of the teeth date back more than 100 years [8]. Currently, endodontic and periodontal treatments provide the means to save molars with furcation problems that would otherwise be subject to extraction. After periodontal therapy adequate bone support for root stabilization should be available. Endodontic therapy should provide a long-term prognosis. After treating caries, an adequate tooth structure must remain after hemisection [9].

CASE REPORT

The 48-year-old patient presented to the dental office for pain at the level of the molar 47. The clinical examination shows that the molar 47 is one of the abutments of a fixed prosthetic reconstruction. Radiological examination shows that the molar 47 has a vertical coronal fracture that affects the forked area (Figure 2). The molar has no periapical lesions.

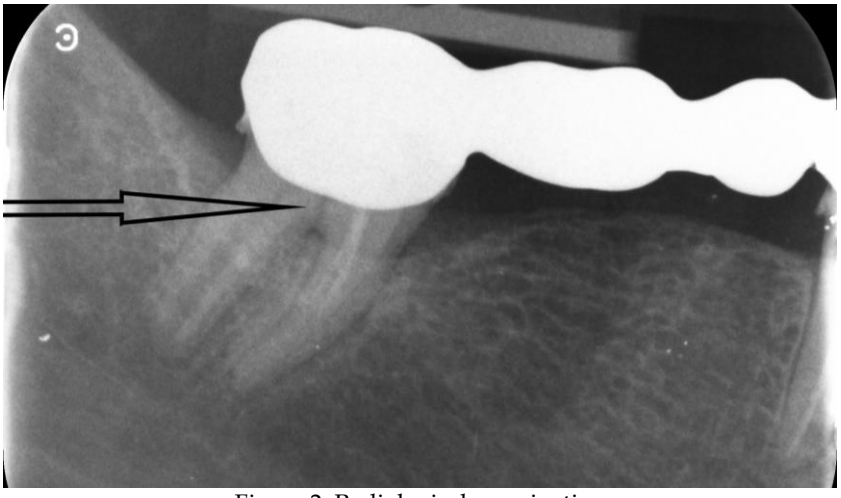

Figure 2. Radiological examination

After discussing treatment options and obtaining the patient's consent, it was decided to hemisection with preservation of the mesial roots (Figure 3) and a new fixed restoration. It was decided to keep the mesial roots due to the higher prosthetic value and in order to reduce the distance between the dental abutments.

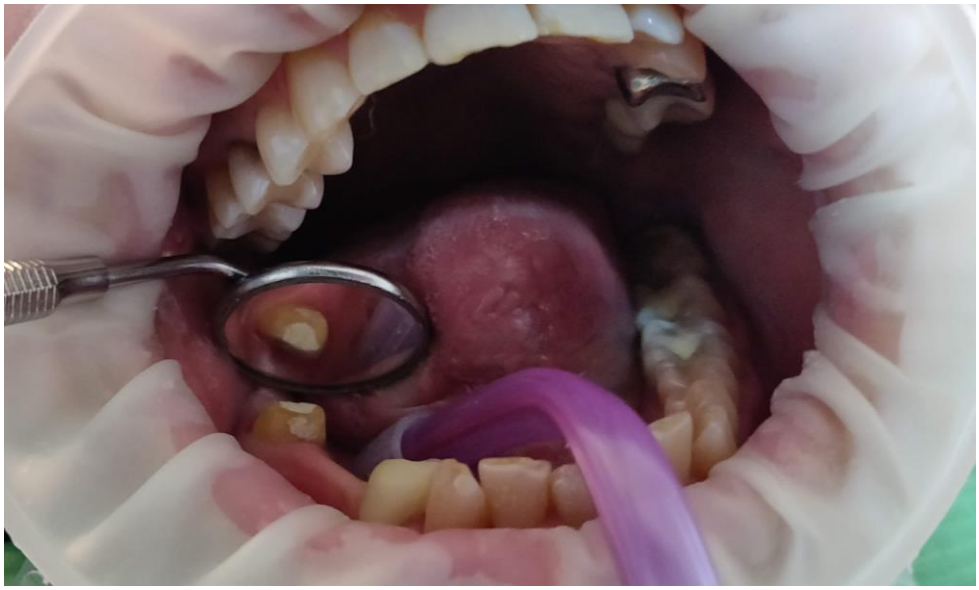

Figure 3. Removal by hemisection of the distal root

Until the alveolar bone heals a temporary fixed partial denture is made. Four months after the hemisection, a new radiological examination is performed (Figure 4) showing bone healing at the alveolar and cervical level, and the absence of any periapical reaction.

Figure 4. Radiological examination four months after hemisection

The final prosthetic restoration of zirconium is decided. The prosthesis was made using CAD-CAM technology (Figures 5-7).

The patient was monitored and a clinical examination was performed at three and six months. After one year, the final restoration is functional, with no detectable mobility or visible bone loss.

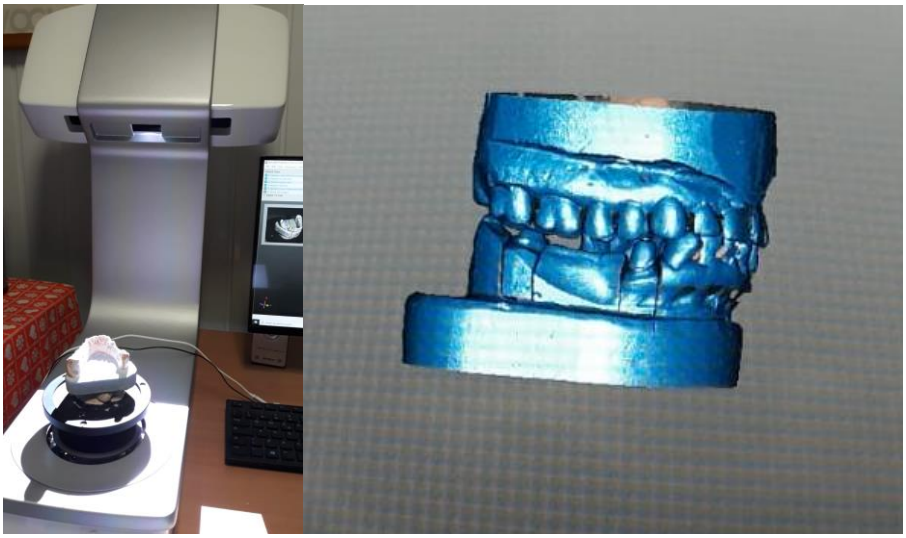

Figure 5. Scanning the model

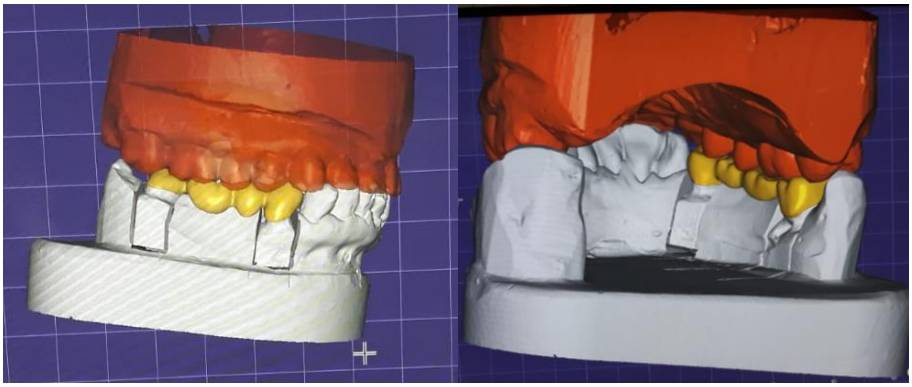

Figure 6. Computer-aided design of the final prosthetic rehabilitation

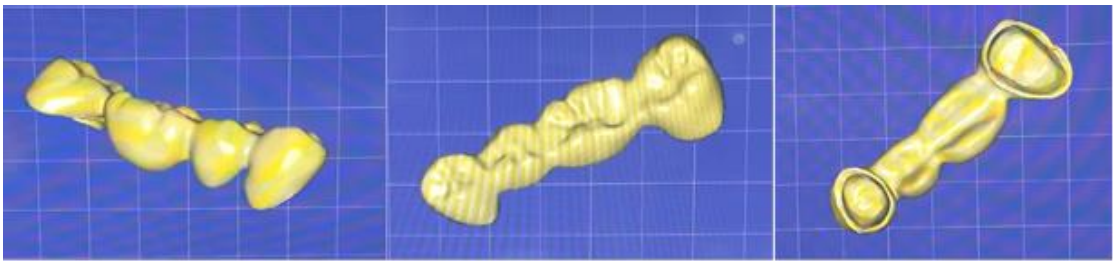

Figure 7. Computer-aided design of fixed prosthesis (vestibular, occlusal-lingual, mucosal view)

DISCUSSIONS

For mandibular molars affected at the forked area, the decision to perform a hemisection or to remove it and place an implant is often complicated. There are retrospective studies of patients who have received treatment by hemisection, molar resection or implant therapy. The highest degree of failure is when there are single terminal abutments [10]. In patients with periodontitis, hemisect mandibular molars are more prone to complications than implants [11].

A molar with forked area involvement often involves an interdisciplinary approach (endodontics, periodontics, prosthetics) to diagnose and plan treatment [9]. By hemisection it is no longer necessary to lose a molar with forked area problems [5,12].

There are few long-term studies on the success of hemisection treatment in trying to preserve molars that are distal abutments. The average failure rate is 13.1%, often compared to the results of implant studies [13].

CONCLUSIONS

When faced with a molar with damage to the forked area, the dentist must decide between a number of treatment options: hemisection, root resection, extraction and placement of the implant. Hemisection and prosthetic rehabilitation of this case gave a satisfactory result.

Hemisection is a relatively simple, inexpensive treatment with a high chance of success in a proper selection of the case.

REFERENCES

1. Babaji P, Sihag T, Chaurasia VR, Senthilnathan S. Hemisection: A conservative management of periodontally involved molar tooth in a young patient. J Nat Sci Biol Med. 2015 Jan-Jun;6(1):253-5.
2. Sharma S, Sharma R, Ahad A, Gupta ND, Mishra SK. Hemisection as a Conservative Management of Grossly Carious Permanent Mandibular First Molar. J Nat Sci Biol Med. 2018 Jan-Jun;9(1):97-99.
3. Varma K M, Chittem J, Satish R K, Kumar M SR, Sajjan GS. A novel approach for restoration of hemisectioned mandibular second molar with modified tunnel restoration: a case report. J Clin Diagn Res. 2014 Oct;8(10):ZD07-9.
4. Silverstein LH, Moskowitz ME, Kurtzman D, Shatz PC, Gornstein RA. Prosthetic considerations with periodontal root resective therapy, Part 2. Hemisections. Dent Today. 1999 Sep;18(9):86-9.
5. Hürzeler MB, Strub JR. Combined therapy for teeth with furcation involvement used as abutments for fixed restorations. Int J Prosthodont. 1990 Sep-Oct;3(5):470-6.
6. Sharma S, Tewari RK, Mishra SK, Kharade PP. Conservative management of grossly carious mandibular first molar with a hemisection approach: a case report. Gen Dent. 2015 Jul-Aug;63(4):19-21.
7. Saad MN, Moreno J, Crawford C. Hemisection as an alternative treatment for decayed multirooted terminal abutment: a case report. J Can Dent Assoc. 2009 Jun;75(5):387-90.
8. Green EN. Hemisection and root amputation. J Am Dent Assoc. 1986 Apr;112(4):511-8.
9. Bohnenkamp DM, Garcia LT. Fixed restoration of sectioned mandibular molar teeth. Compend Contin Educ Dent. 2004 Nov;25(11):920-4.
10. Fugazzotto PA. A comparison of the success of root resected molars and molar position implants in function in a private practice: results of up to 15-plus years. J Periodontol. 2001 Aug;72(8):1113-23.
11. Zafiropoulos GG, Hoffmann O, Kasaj A, Willershausen B, Deli G, Tatakis DN. Mandibular molar root resection versus implant therapy: a retrospective nonrandomized study. J Oral Implantol. 2009;35(2):52-62.
12. Kinsel RP, Lamb RE, Ho D. The treatment dilemma of the furcated molar: root resection versus single-tooth implant restoration. A literature review. Int J Oral Maxillofac Implants. 1998 May-Jun;13(3):322-32.
13. Bühler H. Survival rates of hemisected teeth: an attempt to compare them with survival rates of alloplastic implants. Int J Periodontics Restorative Dent. 1994 Dec;14(6):536-43.

Therapeutical related quality of life in oncologic patient

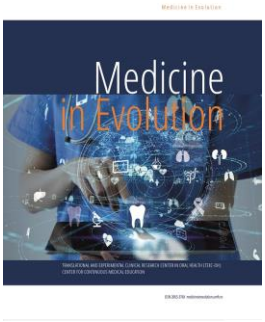

Balean O.I.[1,2], Jumanca D.[1,2], Sava-Rosianu R.[1,2], Dumitrescu R.C.[1,2]

[1]1 Department of Preventive Dentistry, Faculty of Dental Medicine, Victor Babes, University of Medicine and Pharmacy, 14A Tudor Vladimirescu Ave., 300173 Timisoara, Romania;
[2]Translational and Experimental Clinical Research Center in Oral Health (TEXC-OH), 14A Tudor Vladimirescu Ave., 300173 Timisoara, Romania

Correspondence to:
Name: Sava-Rosianu Ruxandra
Address: splaiul Tudor Vladimirescu 14A, Timisoara
Phone: +40 740315848
E-mail address: sava-rosianu.ruxandra@umft.ro

Abstract

Cancer, a word that is becoming more and more common nowadays, is an abnormal cell proliferation followed by its spread to the rest of the body. The aim of the paper is to assess the quality of life of patients with cancer. We follow both the etiological factors of the diseases, also the side effects of the performed therapy and the correlation of the obtained data from the completion of a questionnaire containing 19 questions. The average age for females is 52 years, compared to 48 years for males. Of the study group 71% had difficulty closing / opening the oral cavity, 32% stated that their pathology was in stage III (32%), the highest percentage of oncological treatment was occupied by chemotherapy and radiotherapy Regarding the risk factors that could cause malignancies, 59% of the study group stated that they were smokers. Pain or discomfort when chewing are present quite often in 36% of respondents and 18% very often. Correlating a patient's health history, observed clinical changes, and the relative risk associated with prompt use of appropriate and proven diagnostic methods will ensure that physicians provide patients with an optimal level of management for a possible long-term satisfactory outcome.

Keywords: cancer, head, neck, quality of life

INTRODUCTION

Oral cancer is an extremely relevant issue for global public health. It is ranked in the top 10 neoplastic diseases, is the sixth most common malignancy worldwide, and despite advances in research and therapy, survival has not improved significantly in recent years, posing a continuing challenge to biomedical science [1]. Oral cancer metastasis is a complex process that involves detachment of tumor tissue cells, regulating cell motility and invasion, proliferation and evasion through the lymphatic system or blood vessels, a continuous chain that leads to a negative influence on quality of life.

Cancer is caused by a mutation of a normal gene. The scientific name for mutant genes is called oncogenes. Studies have shown that more mutations are needed to cause cancer. Old or physiologically malfunctioning cells self-destruct and are replaced by other young new cells. As for cancer cells, they do not self-destruct but continue to divide producing millions of new cancer cells [2].

Oral cancer patients undergoing treatment suffer from a wide range of side effects, both physical and psychological.

Treatment side effects, both short-term and long-term, can affect the quality of life for the cancer survivor [3].

These complications require special attention for their prevention and treatment, pre-treatment assessment and stabilization of the disease are needed for each patient, counseling patients before and during radiation therapy is important to help them become aware of oral complications and prevent them. [4]

Acute effects usually develop at the beginning of the radiation treatment period and persist 2-3 weeks after the end of treatment, while late effects may become apparent at any time after the end of treatment, ranging from weeks to years. The changes in pH and salivary flow are due to damage to the glandular tissue, leading to fibrosis, degeneration, acinar atrophy and cell necrosis producing dry mouth (xerostomia) and clinically reversible hyposalivation, local diseases caused by bacteria and fungi, halitosis and high discomfort when using mobile prostheses, changes in taste (dysgeusia), functional impairment when swallowing, speech and other complications of hard tissues. [4].

Oral mucositis is a condition characterized by ulcerative lesions of the mucous membranes of patients undergoing radiation or chemotherapy. Oral mucositis is currently considered to be the most severe complication of anticancer therapy, affecting 40-80% of patients undergoing chemotherapy and almost all those undergoing radiotherapy at the cephalic extremity. The incidence of oral mucositis ranges from 40 to 76% in patients undergoing chemotherapy and can reach 90% in patients receiving radiation therapy to the head and neck. These values increase when there is an association between chemotherapy and radiation therapy [4,5].

Oral lesions lead to a considerable decrease in the quality of life for these patients due to dysphagia (difficulty feeding) with solid and liquid food, dysarthria (poor coordination of speech muscles) and odynophagia (pain or burning sensation on swallowing); In addition, the lesions may be a gateway for opportunistic infections. [6]

Poor oral hygiene and inadequate prosthetic restorations can exacerbate oral ulcers. [4,5]

Most oral cancers are found in advanced stages (stage III or IV), usually when they have metastasized to another area, most often in the lymph nodes of the throat. Being difficult to detect, the patient has no symptoms and has a high risk of producing secondary tumors.

Aim and objectives

The aim of the paper is to assess the quality of life of patients with cancer. We follow both the etiological factors of the diseases and the side effects of the performed therapy and the correlation of the obtained data from the completion of a questionnaire containing 19 questions.

The study aims to correlate the obtained results by age groups, sex, location of the tumor and its stage, associating these results with vicious habits that are considered risk factors. We look which side effects have a greater predisposition to appear and how the quality of life has been influenced.

MATERIAL AND METHODS

The study was performed on a group of 277 patients aged 18-78 years.

Inclusion criteria: diagnosed patients with stage I, II, III or IV malignancy, a condition that must be located in the head-neck, have undergone or are undergoing treatment consisting of radiotherapy, chemotherapy, immunotherapy, surgical treatment or combinations thereof.

Exclusion criteria: patients with malignancies other than head-neck, patients with neck cancer but have not received any of the above treatments.

Taking into account the inclusion and exclusion criteria, only patients who were included in the study completed the questionnaire. Some patients completed the questionnaire online based on a platform, while another part of the patients completed the physical questionnaire in collaboration with the Oncohelp Medical Center Timisoara.

The patient questionnaire was a 19-questions questionnaire. It was piloted on 20 patients to see if the patients understood the asked questions. Subsequently, the questionnaire was widely applied. It includes relevant questions to assess the quality of the patients' life with oncological disease following or undergoing treatment consisting of chemotherapy, radiotherapy, immunotherapy, surgical treatment or the combination of these, highlight whether or not there have been changes in the oral cavity due to the treatment of the disease. What are these changes and how have they influenced the quality of life in terms of pain and physical disability, functional limitation, psychological discomfort and social disability. The questions had multiple answers attached. Study participants signed the patient's agreements.

After receiving the results from the questionnaires, their statistics were made using the Microsoft Excel program, for each question depending on the answer, but also associations between certain questions in order to highlight important data.

RESULTS

Following the statistical analysis, the average age data for females who were included in the study is 52 years, and for males is 48 years, the share by gender of patients was predominant female 58%, and males were 42%.

Depending on the environment they come from, it was established that 69% of the respondents are from urban areas, and 31% are from rural areas.

Depending on the location of the predominant tumor, malignant tumors are found in the tongue (25%), followed by the nasopharynx (14%), oropharynx, larynx, buccal floor and submandibular glands (10%), tonsils (8%), parotid gland (7%), eyes (2%) and brain (3%).

Tumor location by sex predominates in males for cancer of the tonsils, parotid gland, lingual floor, eyes, brain. (Fig. 1)

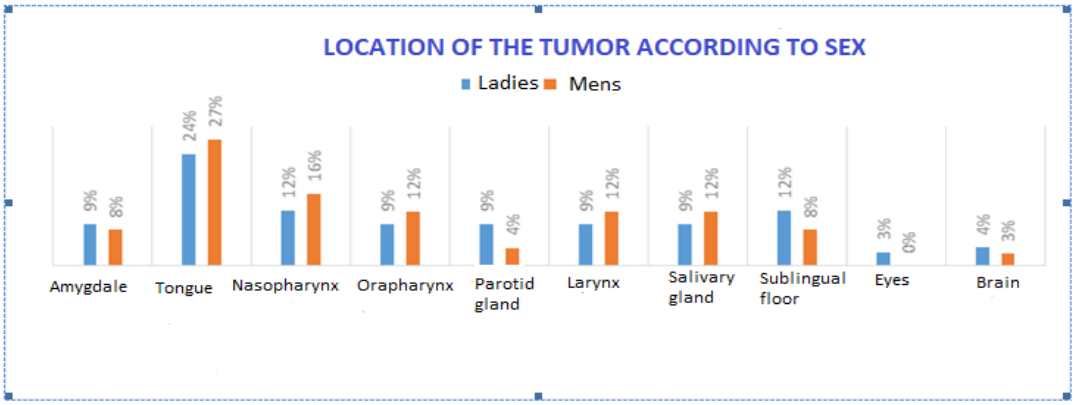

Figure 1. Tumor location by sex

Most respondents stated that their pathology was in stage III (32%), followed by stage IV (31%), stage II (27%), and in the incipient stage-stage I only 10% were discovered.

Regarding the oncological treatment, the highest percentage was occupied by chemotherapy and radiotherapy, followed by chemotherapy, radiotherapy and surgical treatment (15%) and radiotherapy with surgical treatment (14%).

Regarding the risk factors that could cause malignancies, 59% of the study group stated that they were smokers. Depending on the frequency of alcohol consumption, 34% drank alcohol occasionally, 24% frequently, 18% rarely, and 24% never drank alcohol. Diseases of the oral cavity were present even before the starting of treatments for most of the surveyed patients (68%), instead the quality of life of cancer patients decreases when starting the treatment. Pain or discomfort when chewing are present quite often in 36% of respondents, 18% very often and 29% occasionally. (Fig. 2) 69% of patients developed difficulties in opening and closing the oral cavity after treatment.

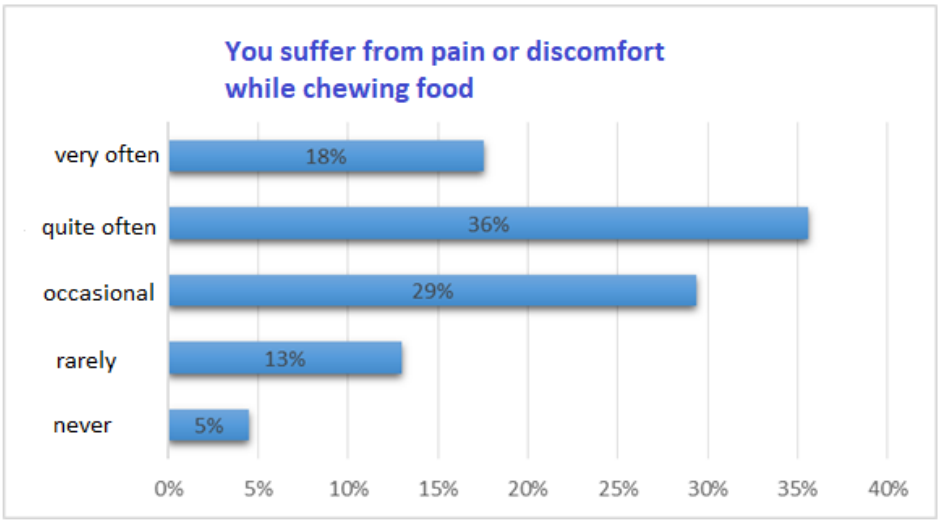

Figure 2. Discomfort during chewing

Of the patients who presented trismus (lockjaw), most were treated with radiation therapy or combinations of treatments which included radiotherapy. Of these, 71% had difficulty closing/opening the oral cavity (trismus), and 29% of patients did not have this condition. (Fig.3)

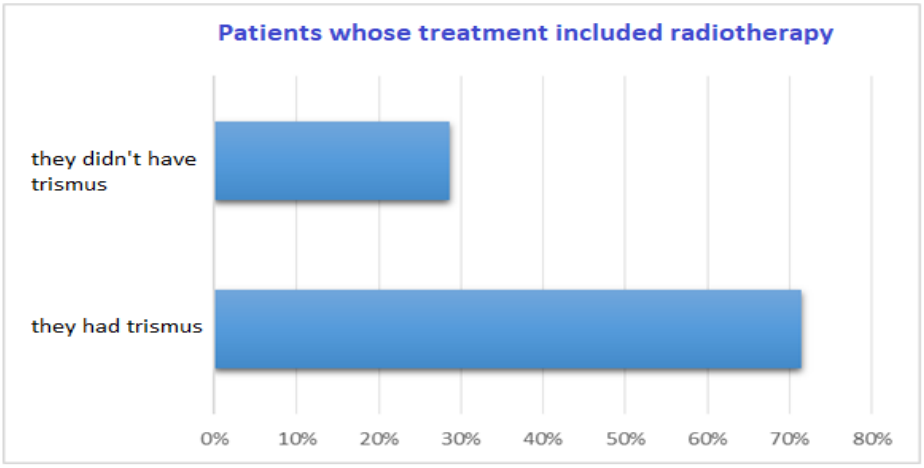

Figure 3. Correlation between radiotherapy and trismus

When asked about the diet, 37% answered "no" and the rest of the respondents, 63%, answered "yes" regarding the unsatisfactory diet due to problems in the oral cavity following cancer treatment.

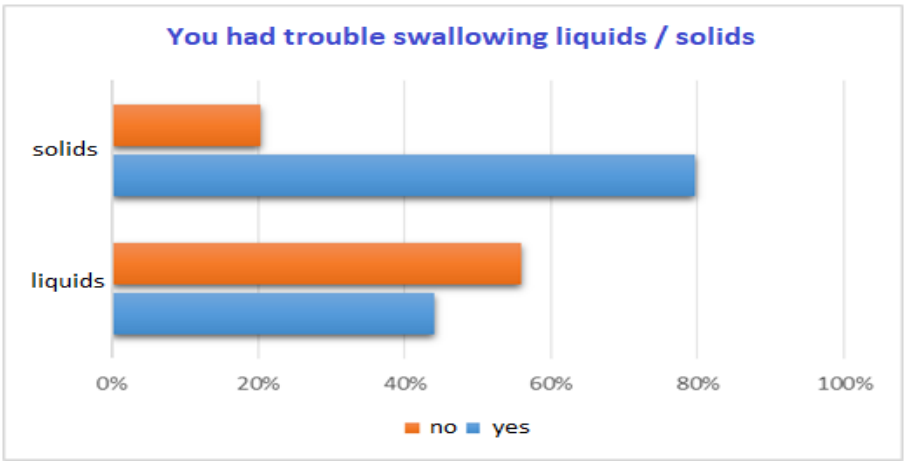

Figure 4. Difficulty swallowing solid / liquid foods

Regarding the ability to swallow solid and liquid foods, the greatest discomfort was given by swallowing solid foods (80%), followed by difficulties in swallowing liquid foods (44%). (Fig.4)

The quality of life of cancer patients decreases considerably predominantly, 75% state anxiety, with a less satisfactory life (75%) and embarrassed by the company of other people.

DISCUSSIONS

Cancer is by far one of the most common causes of death in developed and, respectively, developing countries. Of all cancers, squamous cell carcinoma of the head and neck has a frequency of 600,000 cases worldwide, with 40-50% annual mortality, and the burden is expected to double in developing countries until 2030 [7].

After recognizing the huge impact of head and neck cancer on patients' lives, research has focused on better investigation of their quality of life, as it is recognized that both diagnosis and treatment can have a significant impact on quality of life.

Quality of life is a broad, subjective, multidimensional, global concept that aims to provide a comprehensive picture of the patient's perception of himself. The World Health Organization (WHO) defines it as "an individual's perception of his or her position in life in the context of the patient's culture and value systems and of his or her goals, expectations, standards, and concerns." Another definition describes it as "the perceived discrepancy between the reality of what a person has and the concept of what the person wants, needs or expects." Sometimes specific treatments may not necessarily prolong life, but they can increase their quality. The importance of quality of life has been increasingly recognized and is reflected in its use as a measure of the outcome of cancer research, on an equal footing with the response rate and survival. [8]

The age and gender aspects of the participants in this investigation are consistent with the epidemiological profile of head and neck cancer found in the literature, men and women over the age of 45, exposed to at least one risk factor, such as highlighted dental problems before starting cancer therapy, smoking or alcohol.

Of all patients evaluated, 10% were eligible only for radiation therapy, 12% for chemotherapy combined with surgical treatment, 15% for chemotherapy combined with surgical treatment and radiation therapy, and 25% were treated with radiation therapy associated with chemotherapy, and in low percentages, associations between treatments. Technological advances in radiotherapy procedures and new chemotherapy protocols have favored the choice of these means of treatment. However, there is a risk of increased chemo-radiation-induced toxicity with painful and debilitating effects, which may necessitate discontinuation of treatment, compromising the patient's diagnosis.

Different treatment modalities for some head and neck tumors can lead to survival and similar disease control, however, treatment methods also have side effects such as the decreased quality of life, that also contribute to the diagnosis. In this context, the interest in the quality of life of these patients is directly associated with the day-to-day care practices in health centers.

Given the obtained results in the previous chapter, we can conclude that most of the surveyed patients had complications and their quality of life changed negatively.

From the previously obtained results we can conclude that most side effects occurred after the combined treatment of radiotherapy and chemotherapy. These side effects are represented in the oral cavity by occurring dysfunctions during swallowing, chewing, decreased saliva, alteration or even total loss of taste for indefinite periods and difficult speech. All these dysfunctions are interconnected, the decrease of the saliva quantity being the most important and having influence on the others.

In terms of physical dysfunction, as mentioned above, the results showed a decrease in performance, and in terms of social / emotional functions, the results showed that they also became unsatisfactory for patients, especially in the field of anxiety, in which patients have obtained a high percentage, most of them feeling embarrassed by the company of other people in their entourage.

Many research studies have focused on the impact of depression on treatment outcomes, such as mortality or disease progression, in cancer patients. However, depression is often underdiagnosed and therefore undertreated. Therefore, early identification or prediction of depression is crucial. [9,10,11,12]

As the literature shows, the risk factors for the occurrence of these cancers and not only, represented by tobacco and alcohol, had an increased share among the surveyed patients, respectively 59% and over 58% consume alcohol frequently / occasionally compared to those who never or rarely consume (42%).

Due to the fact that a fairly small number of the population regularly go for screenings and consultations, over 63% of the respondents had an advanced stage of the tumor, compared to 37% who had stage I or II.

Another observation is that patients had difficulty feeding after starting the appropriate treatment, the difficulties being more obvious during the diet with solid products compared to liquid products. Given that respondents mentioned changes in the amount of saliva, it goes without saying that eating solid products has been difficult.

Most patients reported trismus after radiotherapy treatment, as mentioned in the literature, this condition being highlighted in a large mass of patients treated with radiotherapy, compared to those treated with chemotherapy.

The quality of life decreased significantly for the patients included in the study, regardless of the treatment applied, each of them presented physical and emotional dysfunctions, concluding that their life has become less satisfactory, both due to the diagnosis and due to the side effects of the treatment. Researchers have shown increased levels of suffering in cancer patients after diagnosis, during active treatment and up to 4 years after treatment. [13,14,15]

CONCLUSIONS

The diagnosis of precancerous forms and oral cancer remains a challenge for the dentist profession, especially in the detection, evaluation and management of changes in the early stages.

Our focus on early changes and awareness of patients' harmful habits remains crucial to meeting this challenge. Correlating a patient's health history, observed clinical changes, and the relative risk associated with prompt use of appropriate and proven diagnostic methods will ensure that physicians provide patients with an optimal level of management for a possible long-term satisfactory outcome.

REFERENCES

1. Kittipong D, Somsri R, Watcharaporn T, Sompid K, Ajiravudh S, Mark D. Oral cancer: A multicenter study. Med Oral Patol Oral Cir Bucal. 2018 Jan; 23(1): e23–e29
2. Malay K, Ronak N,Tapan GM. Journal of Cancer Research and Therapeutics- April June 2016- Volume 12-Issue 2, 458-463
3. Jelena Karan, Denise Laronde. Treatment modalities of oral cancer. Canadian Journal of Dental Hygiene. February 2014; 48(19):13
4. S Devi , N Singh. Dental care during and after radiotherapy in head and neck cancer. Natl J Maxillofac Surg. 2014 Jul-Dec; 5(2): 117–125
5. Maria IdCC, Celso NC, Fernando MA, Beatriz JVA. Oral mucositis in cancer treatment: Natural history, prevention and treatment. Spandidos Publications. 2014, 337-340
6. Maria OM, Eliopoulos N , Muanza T (2017) Radiation Induced Oral Mucositis. Front. Oncol. 7:89, 2017
7. Anwar, N., Pervez, S., Chundriger, Q. (2020). Oral cancer: Clinicopathological features and associated risk factors in a high risk population presenting to a major tertiary care center in Pakistan. PLOS ONE, 15(8)
8. https://www.uptodate.com/contents/health-related-quality-of-life-in-head-and-neck-cancer#H559186648
9. Jacques B., Head and Neck Cancer: Multimodality Management, Springer International Publishing, 2016.
10. Alexandre Bozec, Philippe Schultz, Jocelyn Gal, Emmanuel Chamorey, Yann Chateau, Olivier Dassonville, Gilles Poissonnet, François Demard, Frédéric Peyrade, Esma Saada, Karen

Benezery, Axel Leysalle, Laure Santini, Lila Messaoudi, Nicolas Fakhry, Evolution and predictive factors of quality of life in patients undergoing oncologic surgery for head and neck cancer: A prospective multicentric study, Surgical Oncology, 2019 (28) 236-242

11. Takes, R.P., Halmos, G.B., Ridge, J.A. et al. Value and Quality of Care in Head and Neck Oncology. Curr Oncol Rep 22, 92 (2020). https://doi.org/10.1007/s11912-020-00952-5
12. Meier, J.K., Schuderer, J.G., Zeman, F. et al. Health-related quality of life: a retrospective study on local vs. microvascular reconstruction in patients with oral cancer. BMC Oral Health 19, 62 (2019). https://doi.org/10.1186/s12903-019-0760-2
13. Dominik Horn, Sven Zittel, Julius Moratin, Karl Metzger, Oliver Ristow, Johannes Krisam, Jens Bodem, Michael Engel, Christian Freudlsperger, Jürgen Hoffmann, Kolja Freier, Prospective feasibility analysis of salvage surgery in recurrent oral cancer in terms of quality of life, Oral Oncology, 2020(102)
14. Acharya S, Rahman S, Hallikeri K. A retrospective study of clinicopathological features of oral squamous cell carcinoma with and without oral submucous fibrosis. J Oral Maxillofac Pathol. 2019;23(1):162. doi:10.4103/jomfp.JOMFP_275_17
15. Claire E Wakefield, Joanna E Fardell, Emma L Doolan, Neil K Aaronson, Paul B Jacobsen, Richard J Cohn, Madeleine King, Participation in psychosocial oncology and quality-of-life research: a systematic review, The Lancet Oncology, 2017, 18(3), pages e153-e165.

Prosthetic rehabilitation of the upper arch using pressed layered and monolithic ceramics- technical steps

Baciu S.[1], Cotan C.K.[2], Stănus A.[3], Manole M.[1], Grecu A.G.[1], Sava S.[4]

[1]*Department of Propaedeutics and Aesthetics, Faculty of Dental Medicine, "Iuliu Haţieganu" University, Cluj-Napoca*
[2]*Dental technician, private practice, Cluj -Napoca*
[3]*Dental tehnician, private practice, Cluj-Napoca*
[4]*Department of Dental Materials, Facultu of Dental Medicine, "Iuliu Haţieganu" University, Cluj-Napoca*

Correspondence to:
Name: Manole Marius
Address: 32 Clinicilor str Cluj-Napoca
Phone: 0264-597256
E-mail address: mnole22@yahoo.com

Abstract

Aims and objectives: the present paper wants to highlight the essential parameters to be considered during the technical steps of the manufacturing process of pressed monolithic and layered full ceramic pressed crowns. Material and method: a complex clinical case was taken in consideration. The patient presented different shades of abutments that required different technical approaches for obtaining the expected aesthetic effects. Specific manufacturing steps were conducted. Results: highly aesthetic and functional reconstructions were obtained that fulfilled the patients demands.

Keywords: monolithic, layered, pressed ceramics, aesthetics, technical steps

INTRODUCTION

Social behaviour can be best understood as a function of people's perception of the world and the way they manipulate their images of the world (1). The aesthetic appearance of a person is closely related to both the facial appearance and the aspect of the dental arches. Prosthetic restorations play an essential role in the natural, pleasant aspect of a person, having to meet at the same time aesthetic functionality. Due to the development of the therapeutic procedures and more efficient evaluation, treatment, and diagnostic possibilities, ideal, optimal restorations can nowadays be manufactured.

Aim and objectives

This presentation is trying to shed light upon essential parameters in the reconstruction of the dental arches, using full ceramic restorations. In the first place, the right choice of material and technique is the key to a successful treatment. Secondly, the technician needs to consider individualization of a prosthetic work in terms of internal colour of the restoration. Before choosing the restorative material, the shade of the prosthetic abutment must be accurately evaluated. For obtaining an individualized match and a real blending in of the prosthetic reconstruction, it is advisable to establish from the beginning if the prosthetic substrate needs to be masked or not and, if necessary, how to accomplish this task (2). Depending on the choice, later different layering techniques of ceramics in different parts of the prosthetic reconstruction are likely to be required. In the third-place cement shade, ceramic thickness, and abutment material of the cast are parameters that must be considered, since they have a major influence on the final colour of full-ceramic restorations (3). The case presented below needed a complex rehabilitation of both arches. In the first stage the upper arch was reconstructed using the lost wax technique and pressed ceramics (lithium disilicate). The technical stages were different, depending on the rehabilitated area, namely monolithic reconstructions were used in the lateral area, and layered copings for the frontal group.

MATERIALS AND METHODS

The preoperative treatment was started by an intraoral scan and a digital smile design (DSD). for oral rehabilitation of the upper arch. The DSD was made according to aesthetic parameters and congruous to the golden rule (Figure 1, 2).

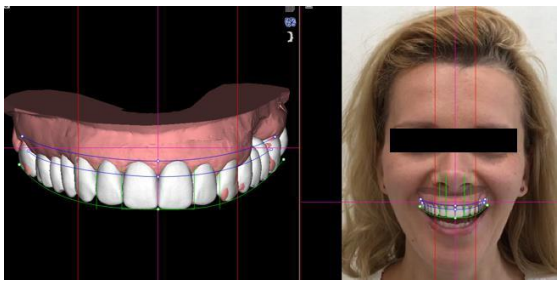

Figure 1. Intraoral scan design

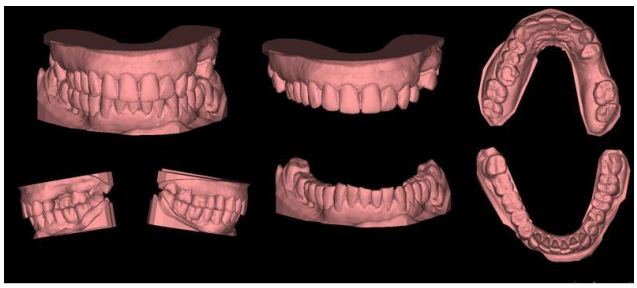

Figure 2. Digital smile

A digital wax-up was made, which was outlined with the help of a 3D printer (figure 3-5). The classical, analogue wax-up was avoided because in terms of number and disposition of occlusal contact points, modern procedures seem to have a significant importance in improved occlusal morphology (4).

Figure 3. Digital wax-up frontal view

Figure 4. Digital wax-up left lateral view

Figure 5. Digital wax-up right lateral view

The impression of the upper arch was taken with Impregum Penta H DuoSoft, the antagonists with Impregum Garant L DuoSoft (3M Espe) (Figure 6,7).

Figure 6. Impression upper arch

Figure 7. Impression - antagonists

Figure 8. intermediate stage in obtaining the analogue maxillary cast

Figure 9. The control cast frontal and later view

The impressions were poured using Rocky Mountain class 4 plaster. Two casts were poured into the maxillary impression: one with removable dies and one – a control cast without removable dies. The cast without removable dies was used for a precise defining of the contact points due to different mobility of dento-parodontal structures (5) vs removable die mobility, necessary in large oral rehabilitation, as in the present case. For mounting, an Artex CR articulator and an Artex face bow (Amman Girrbach) were used (figure 8-12).

Figure 10. Mounted casts

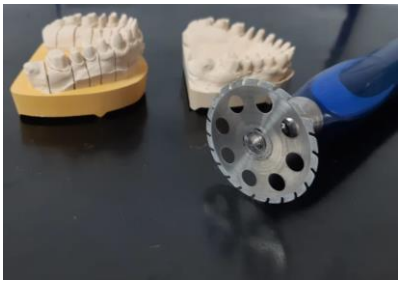

Figure 11. Obtaining the removable dies – maxillary cast

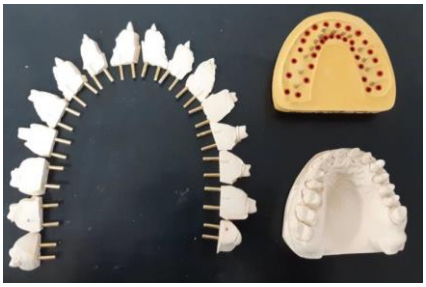

Figure 12. The casts prepared for the scanning

The working cast and the antagonists were scanned using the 3D Vinyl scanner (Smart Optics Sensortechnik GmbH). Scanning also included the mounted casts in the articulator obtaining the intermaxillary relationship. Data was thus converted from analogue to digital, followed by the design stage (Figure 13-19).

The images below show the scanned model with removable dies. Scanning of the soft tissue offers valuable information of the parameters describing the papilla-fill, height, width, and effect of papilla base width on the vertical papillary dimension (6). These parameters will, in turn, offer data about the interdental space and placement of the interproximal contacts, so that the final prosthetic reconstruction will insure an aesthetic outcome.

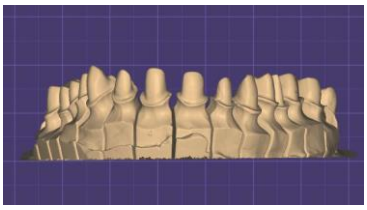

Figure 13. The digital cast with removable dies

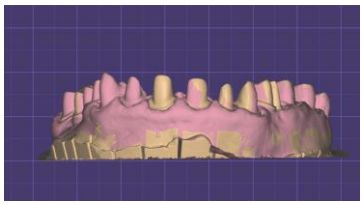

Figure 14. The digital cast with soft tissues included

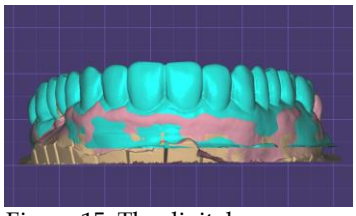

Figure 15. The digital wax up on the digital cast

Starting from the first premolar distally, monolithic reconstructions were used, while in the frontal area layered copings were used for better aesthetic results.

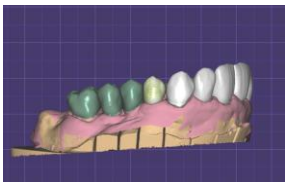

Figure 16. Biogeneric calculation and morphology left side

Figure 17. Biogeneric calculation and morphology right side

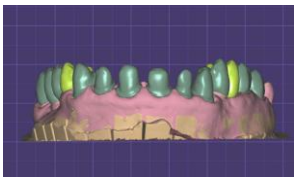

Figure 18. Predefined design of the copings- frontal group frontal view

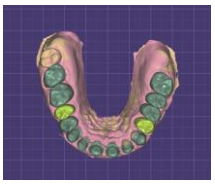

Figure 19. Predefined design of the copings – frontal group occlusall view

The wax patterns for the frontal were obtained by milling using ProArt CAD wax and CAD CAM technology (Figure 20-23).

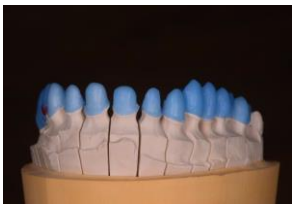

Figure 20. Milled copings in the frontal area

Figure 21. Milled full contour wax patterns in the lateral area- left upper arch

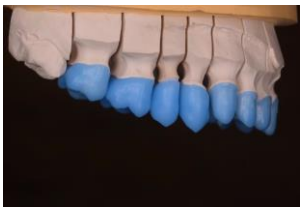

Figure 22. Milled full contour wax patterns in the lateral area- left upper arch

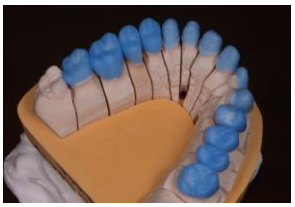

Figure 23. Occlusal view of the milled wax patterns used for rehabilitation of the upper arch

Wax patterns were checked on the working cast and prepared for investing and pressing using the e.max system (Ivoclar Vivadent) (Figure 24-26).

Figure 24. Wax patterns prepared for investing

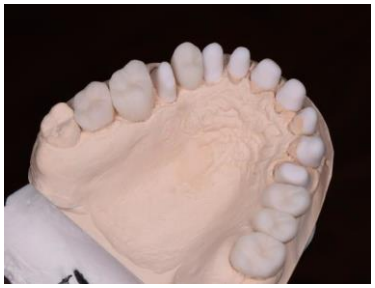

Figure 25. Pressed copings/ full contour reconstructions

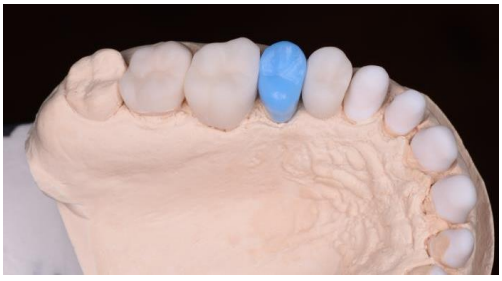

Figure 26. Wax pattern ready to be pressed- discoloured abutment 1.5

For pressing, in the frontal area MO 0 ingots were chosen. In the lateral, medium translucency (MO) was chosen for the discoloured abutment 2.4. that was rehabilitated going through the same manufacturing steps as for the frontal teeth, by pressing a coping that was afterwards layered. The rest of the lateral abutments were restored by using high translucency ingots (HT) for pressing monolithic reconstructions.

Casting rods (3 mm diameter and 0.6 cm length) were placed onto the occlusal surface (non-functional buccal cusp) of the wax patterns and were attached on the conformer's cylinder, at an incline of 450, avoiding sharp angles. 100 grams IPS PressVest Premium (Ivoclar Vivadent) powder was mixed manually with 16 ml of liquid and 11 ml of distilled water in the mixer's vacuum tank. A homogenous consistency was obtained by means of a vacuum mixer.

For the pigmented abutment (1.5.) an MO ingot was used so that even the thinnest parts of the crown the material was able to mask the substrate. In the lateral area the HT translucency ingot that we used, rendered the full contour restorations an appropriate translucency. The final staining and, glazing was done selectively, only limited to the aesthetically relevant zones (7).

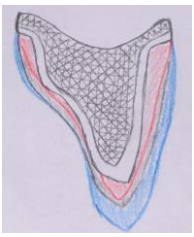

Figure 27. Scheme of the layers black-abutment, white-coping, red- deep dentin, dentin, blue-enamel transpa incisal 1, opal effect 1

Figure 28. Deep dentine B1

Figure 29. Dentine B1

Figure 30. Transition dentine

Figure 31. Transpa

Figure 32. Opal effect

In the frontal area, in order to obtain B1 final restorations, MO 0 ingots were used to obscure the A3.5 shade of the abutments. The copings were layered with e.max Ceram (Ivoclar Vivadent). For the cervical area Power dentine/ Deep dentin B1 was used. B1 dentine was used in the middle third of the teeth. A transition area between the middle third and the incisal third of each frontal tooth was obtained by mixing the dentin of B1 with Opal effect 4 and Transpa incisal 1. Over the transition layer only transparent ceramics was used for light absorption and translucency: Opal effect 1, Transpa incisal 1 (in the incisal half), Transpa blue (in the proximal areas of the tooth, to render a bluish tint to the tooth), and Opal effect 4 to obtain the halo effect. For light reflection Opal effect 4 was applied over the dentin, in the middle third of the restored front teeth (Figure 27-32). After the sintering, surface processing followed aiming to obtain the desired texture followed by polishing.

Figure 33. Sintered layers – frontal view

Figure 34. Sintered layers – lateral view

Figure 35. Dimanond burs used for surface texture

Figure 36. Discs and Polishing wheels

Glaze and stain were used to obtain the final glossy, smooth appearance of the restorations (Figure 33-45).

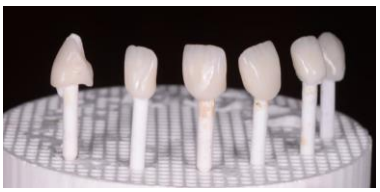

Figure 37. Glaze applied before sintering

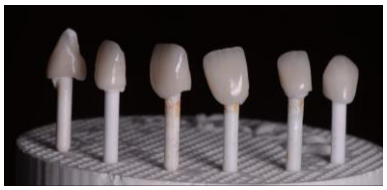

Figure 38. Sintered glaze buccal view

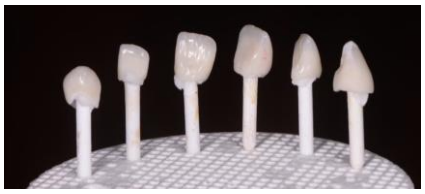

Figure 39. Sintered glaze oral view

Figure 40. The for upper incisors after glazing

Figure 41. Final aspect of the restoration abutment 1.5

Figure 42. Aspect of the restorations in the lateral are- left arch

Figure 43-45. Final aspect of the monolithic and of the layered restorations on the working cast frontal and lateral view

DISCUSSIONS

Lithium disilicate (LS2) is a glass-ceramic, sold by specialized commercials as ingots, ready to be heat pressed to obtain metal free restorations. This particle-filled glass material allows manufacturing of cores that are veneered using translucent fluorapatite ceramic (19–23% of fluorapatite crystals ($Ca_5(PO_4)_3F$) embedded in a glassy matrix) (8). As an alternative, monolithic reconstructions can be obtained using the pressing technique this type of reconstruction indicated for the areas where the mechanical and not the aesthetical demands prevail.

Zhao et al. (9) shows in his study, that the mechanical resistance of veneered copings registered lower fracture load values compared to monolithic restorations. Different researches (10-17) show that monolithic restorations have improved fracture strength and fatigue resistance, that enables their use in the posterior areas, for tooth supported single crowns, for 3-unit brides as well as for implant supported reconstructions. Not the same features and indications are available for layered restorations.

Lithium disilicate fixed reconstructions have showed to have wear and abrasiveness parameters highly related to the polishing procedures. The values are close to those of the enamel but higher than those found for noble alloy (gold) restorations (18). Specific, more aggressive surface characteristics have been reported after grinding, glaze coating and fluorapatite ceramic veneering. Thus, several studies (19-23) showed increased roughness and wear in antagonist teeth but also of the prosthetic restoration per se. Song et al (7) showed that glazing of monolithic posterior restorations is not indicated on the occlusal surfaces if aesthetic considerations do not prevail and that meticulous polishing procedures should compulsorily succeed any occlusal grinding.

Biocompatibility of lithium disilicate material was demonstrated over and over in vitro and in vivo studies (24-26). Lithium disilicate insures low plaque retention, as well as adhesion and proliferation of human epithelial cells and human gingival fibroblasts in the absence of any inflammatory reactions of the soft tissues.

CONCLUSIONS

Lithium disilicate is one of the most versatile metal free materials, widely used because of the high aesthetic requirements it possess, as well as for the improved mechanical performance and good bonding strength to dental tissues (27). It is a material often used for fixed implant or tooth supported single or plural dental reconstructions. Lithium disilicate ceramics can be utilized for tooth supported structures (inlay, onlay, overlay, tabletops, veneers, crowns, foxed partial dentures) as well as on implant-supported restorations (28)(29).

A 10-year study found an 83.5% survival rate of monolithic lithium disilicate single dental reconstructions (30).

In the lateral area for table-tops and occlusal veneers on premolars and molars lithium disilicate has shown obvious advantages, e.g.: adhesive bonding strength, low wear and abrasive potential and high load-at-fracture. The improved mechanical resistance at reduced thickness of the restoration (1–1.5 mm) which translates into reduced hard tissue preparation, enhances thus a biological approach (31-36).

REFERENCES

1. Kurt Lewi Kurt Lewin Ladd Wheeler (2008). Social and Personality Psychology Compass 2/4 2008: 1638–1650.
2. Czigola A, Abram E, Kovacs ZI, Marton K, Hermann P, Borbely J. Effects of substrate, ceramic thickness, translucency, and cement shade on the color of CAD/CAM lithium-disilicate crowns. J Esthet Restor Dent. 2019 Sep;31(5):457-464.
3. Chongkavinit P, Anunmana C. Optical effect of resin cement, abutment material, and ceramic thickness on the final shade of CAD-CAM ceramic restorations. J Prosthet Dent. 2021 Mar;125(3):517.
4. Abduo J, Bennamoun M, Tennant M, McGeachie J. Effect of prosthodontic planning on intercuspal occlusal contacts: comparison of digital and conventional planning. Comput Biol Med. 2015 May; 60:143-50.
5. Li LL, Chen H, Li WW, Wang Y, Zhou YS, Wang YB, Sun YC. [Investigation of posterior teeth displacement under normal bite force by an intraoral scanner]. Zhonghua Kou Qiang Yi Xue Za Zhi. 2020 Oct 9;55(10):743-749.
6. Belák Š, Žižka R, Starosta M, Zapletalová J, Šedý J, Štefanatný M. The influence of gingival phenotype on the morphology of the maxillary central papilla. BMC Oral Health. 2021 Jan 23;21(1):43.
7. Song XF, Ren HT, Yin L. Machinability of lithium disilicate glass ceramic in in vitro dental diamond bur adjusting process. J Mech Behav Biomed Mater. 2016 Jan; 53:78-92.
8. Fischer K, Bühler-Zemp P, Völkel T. Scientific Documentation IPS e.max CAD. Schaan, Liechtenstein: Ivoclar Vivadent; 2005.p.1–30.
9. Zhao K, Wei YR, Pan Y, Zhang XP, Swain MV, Guess PC. Influence of veneer and cyclic loading on failure behavior of lithium disilicate glass-ceramic molar crowns. Dent Mater. 2014;30(2):164–71.
10. Alsarani M, Souza G, Rizkalla A, El-Mowafy O. Influence of crown design and material on chipping-resistance of all-ceramic molar crowns: an in vitro study. Dent Med Probl. 2018;55(1):35–42.
11. Hamza TA, Sherif RM. Fracture resistance of monolithic glass-ceramics versus bilayered zirconia-based restorations. J Prosthodont. 2019;28(1):e259–64.
12. Silva NR, Thompson VP, Valverde GB, Coelho PG, Powers JM, Farah JW, Esquivel-Upshaw J. Comparative reliability analyses of zirconium oxide and lithium disilicate restorations in vitro and in vivo. J Am Dent Assoc. 2011;142(Suppl 2):4S–9S.

13. Choi JW, Kim SY, Bae JH, Bae EB, Huh JB. In vitro study of the fracture resistance of monolithic lithium disilicate, monolithic zirconia, and lithium disilicate pressed on zirconia for three-unit fixed dental prostheses. J Adv Prosthodont. 2017;9(4):244–51.
14. Schultheis S, Strub JR, Gerds TA, Guess PC. Monolithic and bi-layer CAD/ CAM lithium disilicate versus metalceramic fixed dental prostheses: comparison of fracture loads and failure modes after fatigue. Clin Oral Investig. 2013;17(5):1407–13.
15. Dogan DO, Gorler O, Mutaf B, Ozcan M, Eyuboglu GB, Ulgey M. Fracture resistance of molar crowns fabricated with monolithic all-ceramic CAD/CAM materials cemented on titanium abutments: an in vitro study. J Prosthodont. 2017;26(4):309–14
16. Monaco C, Rosentritt M, Llukacej A, Baldissara P, Scotti R. Marginal adaptation, gap width, and fracture strength of teeth restored with different all-ceramic vs metal ceramic crown systems: an in vitro study. Eur J Prosthodont Restor Dent. 2016;24(3):130–7.
17. Kim JH, Lee SJ, Park JS, Ryu JJ. Fracture load of monolithic CAD/CAM lithium disilicate ceramic crowns and veneered zirconia crowns as a posterior implant restoration. Implant Dent. 2013;22(1):66–70.
18. Lee A, Swain M, He L, Lyons K. Wear behavior of human enamel against lithium disilicate glass ceramic and type III gold. J Prosthet Dent. 2014; 112:1399–405
19. Figueiredo-Pina CG, Patas N, Canhoto J, Cláudio R, Olhero SM, Serro AP, Ferro AC, Guedes M. Tribological behaviour of unveneered and veneered lithium disilicate dental material. J Mech Behav Biomed Mater. 2016;53:226–38.
20. Preis V, Weiser F, Handel G, Rosentritt M. Wear performance of monolithic dental ceramics with different surface treatments. Quintessence Int. 2013;44:393–405.
21. Song XF, Ren HT, Yin L. Machinability of lithium disilicate glass ceramic in in vitro dental diamond bur adjusting process. J Mech Behav Biomed Mater. 2016;53:78–92.
22. Mörmann WH, Stawarczyk B, Ender A, Sener B, Attin T, Mehl A. Wear characteristics of current aesthetic dental restorative CAD/CAM materials: two-body wear, gloss retention, roughness and martens hardness. J Mech Behav Biomed Mater. 2013;20:113–25.
23. Peng Z, Izzat Abdul Rahman M, Zhang Y, Yin L. Wear behavior of pressable lithium disilicate glass ceramic. J Biomed Mater Res B Appl Biomater. 2016;104(5):968–78.
24. Ariaans K, Heussen N, Schiffer H, Wienert AL, Plümäkers B, Rink L, Wolfart S. Use of molecular indicators of inflammation to assess the biocompatibility of all-ceramic restorations. J Clin Periodontol. 2016;43(2):173–9.
25. Forster A, Ungvári K, Györgyey Á, Kukovecz Á, Turzó K, Nagy K. Human epithelial tissue culture study on restorative materials. J Dent. 2014; 42(1):7–14.
26. Tetè S, Zizzari VL, Borelli B, De Colli M, Zara S, Sorrentino R, Scarano A, Gherlone E, Cataldi A, Zarone F. Proliferation and adhesion capability of human gingival fibroblasts onto zirconia, lithium disilicate and feldspathic veneering ceramic in vitro. Dent Mater J. 2014;33(1):7.
27. Zarone F, Di Mauro MI, Ausiello P, Ruggiero G, Sorrentino R. Current Status on lithium disilicate and zirconia: a narrative review. BMC Oral Health. 2019 Jul 4;19(1):134.
28. Fabian Fonzar R, Carrabba M, Sedda M, Ferrari M, Goracci C, Vichi A. Flexural resistance of heat-pressed and CAD-CAM lithium disilicate with different translucencies. Dent Mater. 2017;33(1):63–70.
29. Fischer K, Bühler-Zemp P, Völkel T. Scientific Documentation IPS e.max CAD. Schaan, Liechtenstein: Ivoclar Vivadent; 2005. p. 1–30.
30. Rauch A, Reich S, Dalchau L, Schierz O. Clinical survival of chair-side generated monolithic lithium disilicate crowns:10-year results. Clin Oral Investig. 2018;22(4):1763–9.
31. Dhima M, Carr AB, Salinas TJ, Lohse C, Berglund L, Nan KA. Evaluation of fracture resistance in aqueous environment under dynamic loading of lithium disilicate restorative systems for posterior applications. Part 2. J Prosthodont. 2014;23(5):353–7.
32. Guess PC, Zavanelli RA, Silva NR, Bonfante EA, Coelho PG, Thompson VP. Monolithic CAD/CAM lithium disilicate versus veneered Y-TZP crowns: comparison of failure modes and reliability after fatigue. Int J Prosthodont. 2010;23(5):434–42.
33. Sasse M, Krummel A, Klosa K, Kern M. Influence of restoration thickness and dental bonding surface on the fracture resistance of full-coverage occlusal veneers made from lithium disilicate ceramic. Dent Mater. 2015;31(8):907–15.

34. Seydler B, Rues S, Muller D, Schmitter M. In vitro fracture load of monolithic lithium disilicate ceramic molar crowns with different wall thicknesses. Clin Oral Investig. 2014; 18:1165–71.
35. von Maltzahn NF, E Meniawy OI, Breitenbuecher N, Kohorst P, Stiesch M, Eisenburger M. Fracture strength of ceramic posterior occlusal veneers for functional rehabilitation of an abrasive dentition. Int J Prosthodont. 2018; 31(5):451–2.
36. Vianna ALSV, Prado CJD, Bicalho AA, Pereira RADS, Neves FDD, Soares CJ. Effect of cavity preparation design and ceramic type on the stress distribution, strain, and fracture resistance of CAD/CAM onlays in molars. J Appl Oral Sci. 2018; 26:e20180004.

Quantitative three-dimensional analysis of dental diagnostic models obtained by two additive manufacturing techniques

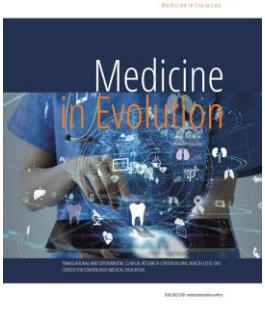

Burde A.V.[1], Baciu S.[1], Grecu A.G.[1], Manole M.[1], Sava S.[2]

[1]*Department of Propaedeutics and Aesthetic Dentistry, Faculty of Dental Medicine, "Iuliu Haţieganu" University of Medicine and Pharmacy Cluj-Napoca, Romania*
[2]*Department of Dental Materials and Ergonomics in Dentistry, Faculty of Dental Medicine, "Iuliu Haţieganu" University of Medicine and Pharmacy Cluj-Napoca, Romania*

Correspondence to:
Name: Baciu Sorana
Address: Clinicilor St, No. 32
Phone: +40745317441
E-mail address: soranav@yahoo.com

Abstract

Aim and objectives: Due to the low tensile strength of gypsum that causes susceptibility to fracture of dental diagnostic plaster casts, long-term storage of these models may become problematic and inconvenient for dental healthcare practitioners. The purpose of this study is to investigate the possibility of 3D printing these models, by testing the accuracy of dental diagnostic models produced by two additive manufacturing techniques. Material and methods: For this purpose, 20 conventional plaster models from randomly chosen subjects were selected and served as reference. The casts were digitized using a 3D scanner and virtual models were adjusted for 3D printing. The virtual models were reconstructed by using a material jetting (MJ) and reversed-stereolithography (SLA) 3D printer. The reconstructed models were digitized using a laboratory 3D scanner and the resulting mesh datasets were compared with the virtual models by using dedicated inspection software. Results: The trueness of printed models was 67.8 µm for the MJ printer and 86.7 µm for SLA printer, even though this difference was statistically significant ($p > 0.05$), all of the 3D printed models were clinically acceptable.

Keywords: 3D printing, SLA, material jetting, dental model

INTRODUCTION

In the field of dental medicine, plaster study- and working casts are used to provide a three-dimensional perspective of patients' dental arches and to allow the dental healthcare providers to analyze, diagnose, monitor and treat possible abnormalities.1 The necessity of long-term preservation of this type of patient related information is mandatory in many countries and regulated by legislative authority through the means of clinical practice guidelines and ethics codes.

Nonetheless, due to the low tensile strength of gypsum that causes susceptibility to fracture of plaster casts, along with the reduced abrasion resistance of the gypsum1,2 and the relatively large space required for archival of plaster models3, long-term storage of dental models may become problematic and inconvenient for dental healthcare practitioners4. A solution to solve these inconveniences is to digitalize the plaster models, store them in a virtual environment, and obtain physical copies of these models, if needed, through additive manufacturing systems.5–7 Through this state-of-the-art technology, dental models can be obtained without the use of conventional material by means of direct intraoral data capturing via an optical device.8 Digital dental models provide accuracy similar to conventional dental casts9 and can be successfully used for manufacturing dental restorations10 and orthodontic measurements.11 Through this method of production, models can be obtained via subtractive manufacturing in the form of CAD/CAM milling, which is relatively time consuming and wasteful, and additive manufacturing which tends to be main choice, due to the diversity of 3D printing techniques which exist and the low initial cost of such machines.12

Although digital models can be successfully used,13,14 conventional casts are still preferred when dealing with complex cases, when multiple materials are combined to create a restoration such as porcelain fused to metal, over-press crowns or bridges, or implant-based restorations. Furthermore, the production cost of printed models is prohibitively expensive when compared with plaster models, because of the high initial price of the printer and materials and also operating costs. 15 Low cost alternatives to professional 3D printers may represent an approach for the implementation of additive manufactured models, given the fact that numerous companies are creating dedicated materials for this application.

Aim and objectives

Studies which validate the accuracy of 3D models generated with low-cost 3D printers are sparse and mainly focus on a single additive manufacturing process,16 henceforth the purpose of this study is to investigate the accuracy of dental models produced by two additive manufacturing techniques using a professional 3D printer and entry-level alternative. The null hypothesis for this study was that there are no statistically significant differences between the reconstructed models manufactured with the two 3D printers included in this study.

MATERIALS AND METHODS

A monocentric study was designed and conducted on 20 conventional diagnostic casts belonging to 10 randomly chosen pseudo-anonymized patients. The exclusion criteria for the selection of the conventional casts were: (1) models which represented edentulous or partially edentulous ridges, (2) casts which contained fissures, fractures or air bubbles on the surface of the model, (3) casts with removable dies. The chosen models replicated dental arches with different dental pathologies, including dental anomalies with or without loss of substance and a variety of malocclusions (Figure 1). The conventional casts were digitized with a

laboratory 3D optical scanner (In-Eos, Sirona Gmbh, Bensheim, Germany), which scans the surfaces of a single arch at a time, by using blue light optical scanning.

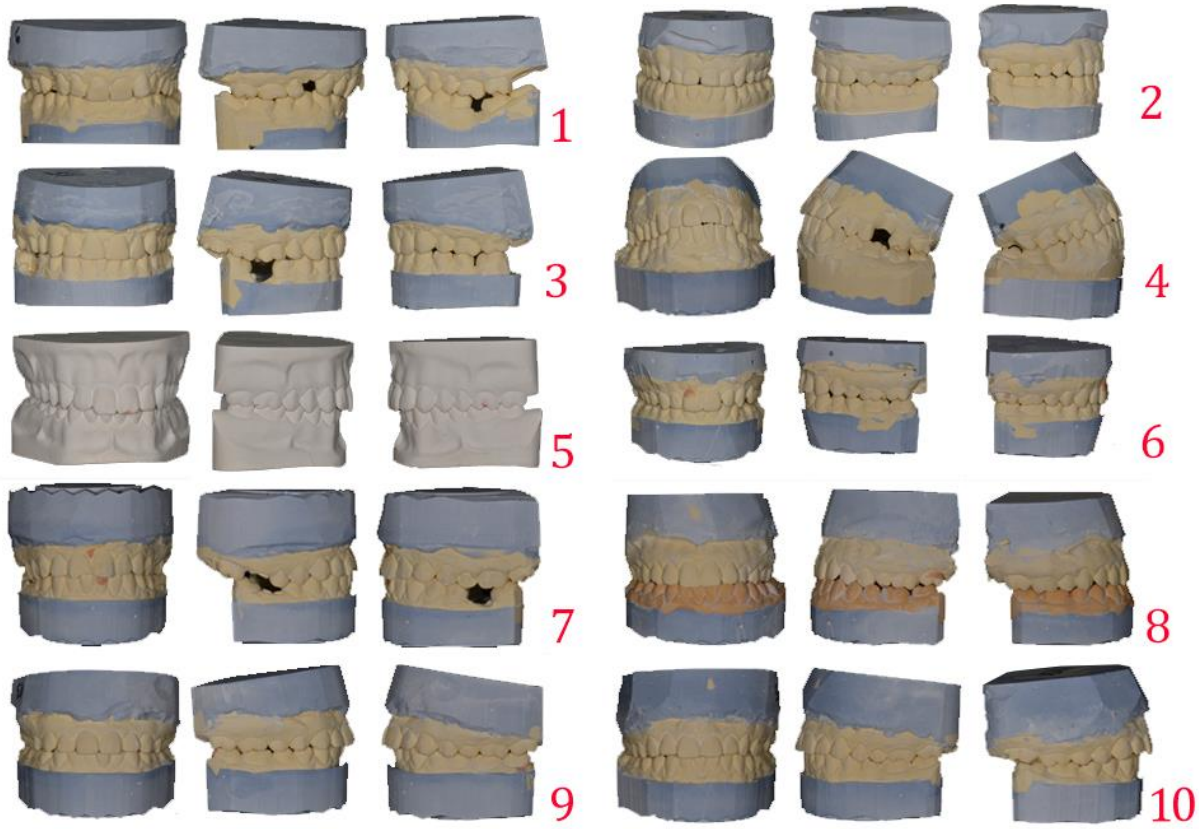

Figure 1. The 10 pairs of dental models used as a reference in this study

The resulting high-resolution point-cloud models were converted to standard tessellation library (.STL) models through the use of the Inlab SW15 (Sirona Gmbh, Bensheim, Germany) computer-aided design software and the resulting mesh models were adjusted further for additive manufacturing reconstruction by using the same dedicated software. In order to ensure a similar configuration, the virtual models were generated as solid models with a flat base.

These digital models will be used to manufacture the 3D printed models and will also serve as reference (REF dataset) when performing the 3D accuracy evaluation by digital superimposition.

The digital reference models were 3D printed by using a reversed-stereolithography printer (Form 3B+, Formlabs Gmbh, Berlin, Germany) and a material jetting printer (Objet 30 Dental Prime, Stratasys LTD, Rehovot, Israel).

In order to manufacture the models through reversed-stereolithography (SLA), the proprietary printing software called PreForm was used to import and orient the digital models flat on the printer platform, as well as to generate the printing strategy. Model V3 resin (Formlabs Gmbh, Berlin, Germany) was used to print the models at a layer thickness of 50 µm. Due to the relatively small size of the build plate, the models were printed flat on the build plate in 3 different batches, by using the same batch of resin, in order to avoid any dimensional error induced by the orientation of the models or by the required support. After printing was completed, post processing was performed by removing the supports, cleaning the excess resin with isopropyl alcohol by using a FormWash automated washing station (Formlabs Gmbh, Berlin, Germany) and a 30-minute exposure per model to UV in a FormCure automated post-curing chamber (Formlabs Gmbh, Berlin, Germany).

The models produced via material jetting (MJ) were manufactured by using a Objet 30 Dental Prime (Stratasys LTD, Rehovot, Israel) 3D printer. This printer has a resolution of 600 dpi on the X and Y axis dpi and 1600 dpi on the Z axis, combined with a layer thickness of 16 µm. We used the Draft mode to manufacture the models, using the Objet Studio software (Objet Geometries Ltd, Rehovot, Israel) to prepare the digital models for printing. This printing mode was chosen because the 36 µm resolution is the most similar setting to the layer height of the reversed-SLA printer. The VeroGlaze MED620 resin (Stratasys LTD, Rehovot, Israel) in combination with the FullCure SUP705 support resin (Stratasys LTD, Rehovot, Israel) were chosen for the production of the models. After printing, the support material was removed by water-jet washing.

After the production of the models, one experienced operator digitized the printed models with the same optical 3D scanner (InEos X5, Sirona Gmbh, Bensheim, Germany) and the 40 resulting mesh datasets (N=40: 20 SLA; 20 MJ) were reference digital models, by using a dedicated inspection software (Geomagic Qualify 13, Geomagic, Morrisville, USA), in order to evaluate three-dimensional accuracy by superimposition. For the purpose of obtaining equal evaluation boundaries for all of the models, the datasets were reduced to the field of interest (1-3 mm below the cervical line of the teeth).

As a result of the performed superimpositions, we analyzed the dimensional discrepancies between the REF dataset and 3D printed models (Figure 2). Thus, the root mean square (RMS) error was used to evaluate the congruence of the superimposed datasets. Color-coded maps were generated from this process to highlight the areas of deviation.

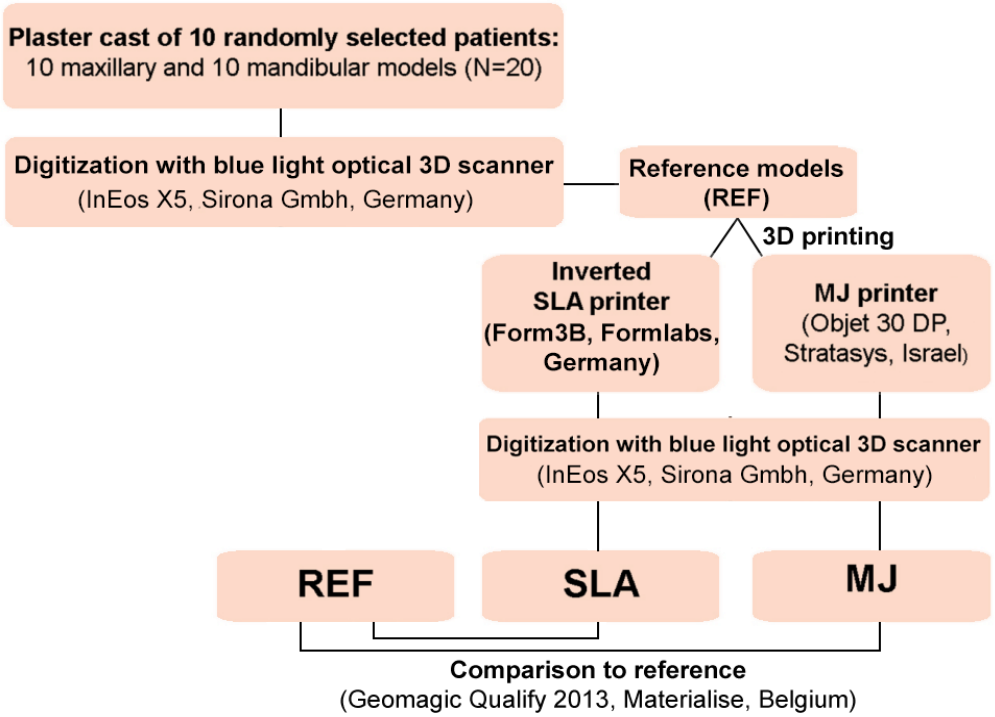

Figure 2. Overview on the general study workflow and methods of data creation

The statistical analysis was performed using the SPSS Statistics 20.0 statistical processing software (IBM SPSS Inc., Chicago, USA). Descriptive statistics and the Shapiro-Wilk test were used to assess normal distribution of the data. Paired t-tests were performed to evaluate statistically significant differences between the additive manufacturing systems (□=0.05). An a priori test of statistical power determination was performed to identify the minimum number of samples required (GPower 3.1.9.2, Kiel, Germany).

RESULTS

In order to compare the differences in accuracy between the two groups, the results of the a priori power test showed that 20 models per group are sufficient for an effect size of 0.5, an estimate of statistical power of 0.95 and an error level of α = 0.05.

The Shapiro-Wilk test demonstrated a normal distribution of data (p> 0.05). The mean values of the differences between the digital reference models and the digital models of the printed casts, the standard deviation and the descriptive statistics are presented in Table 1.

Table 1. Descriptive statistics of the mean three-dimensional deviations recorded between the CAD models and the printed models- RMS (µm)

Manufacturing method	Mean+SD	Min.	Max.	Range	95% Confidence Interval	
					Lower Bound	Upper Bound
SLA	86.7 ±5.44	79.85	99.86	20.1	84.4	89.2
MJ	67.8±5.67	59.84	78.71	18.86	65.3	70.3

Results of the paired-t test indicated that there is a significant medium difference between MJ (M = 67.8, SD = 5.7) and SLA (M = 86.8, SD = 5.4), t (19) = 37.1, p < .001. Thus, the inverted stereolithography printer was associated with a statistically significant smaller degree of accuracy in comparison with the material jetting printer included in this study. Cohen's d was estimated at 8.29, which indicates that the magnitude of the difference between the average of the differences and the expected average of the differences is large according to Cohen's guidelines. By evaluating the color-coded maps of comparisons between the digital models and the printed models, we can see that the deviations are predominantly horizontal for both additive manufacturing methods, as can be seen in Figure 3.

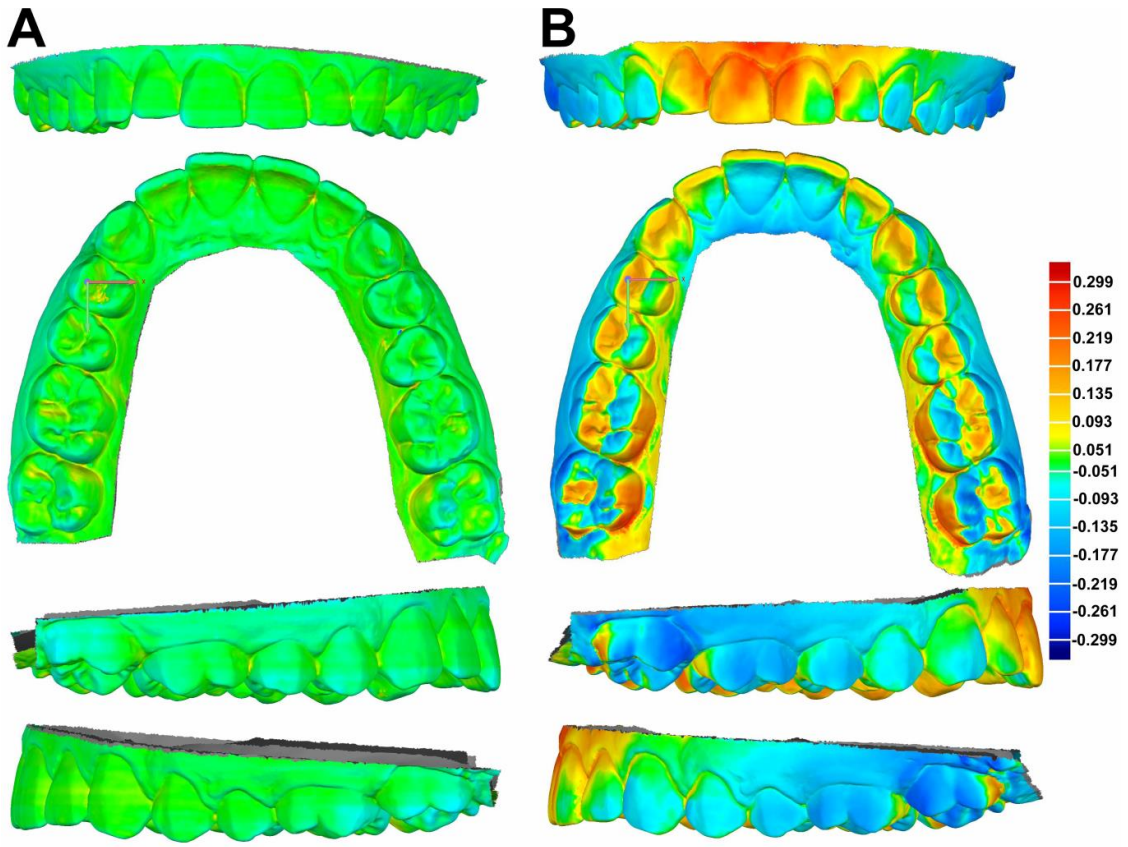

Figure 3. Qualitative analysis of the deviations recorded between the digital models and the printed models; A- model printed with MJ printer; B- model printed with SLA printer

The SLA group records the most horizontal contraction in the lateral area, as well as higher vertical distortion in the posterior area and a slight tendency of horizontal contraction on the oral surfaces of front teeth. Consistent with the information provided by the applied statistical analysis, the smallest deviations in the vertical and horizontal plane can be observed in the models obtained with the MJ printer.

DISCUSSIONS

The results of this study lead to the rejection of both null hypotheses, as the printed models had different levels of accuracy compared to the reference data sets and there are also statistically significant differences between the reversed-stereolithography and material jetting 3D printers.

In order to achieve the reconstruction of a digital model that was acquired through intraoral scanning, it is necessary to go through several production steps: intraoral data acquisition, digital data processing, actual manufacturing and post-processing.17 Each of these clinical and technical steps can induce a degree of deviation in the accuracy of the reconstructed model mainly through four types of error: (a) operator-induced error; (b) error induced by the printer; (c) material-induced error; and (d) environmental errors.

While subtractive manufacturing is an accurate production method for short-span models18, this method is relatively time-consuming and has a high rate of material consumption. It has been demonstrated that, in general, by using subtractive manufacturing, up to 90% of the material block is removed, depending on the type of restoration produced.19 As an alternative to milling, some additive manufacturing processes, such as material jetting, do not produce material waste because there is no need for supporting structures. In addition, the operator can modify the internal structure of the manufactured object by changing the in-filling degree and the type of filling structure.

In our study, the material jetting printer had the smallest dimensional deviation of the printed models. When selecting the in-fill level, the role of the model should be considered in order to optimize the print speed. For example, documentation models do not require the same mechanical properties as working models, which means that the in-fill volume can be lowered or the model could be printed hollow.

While printers based on material jetting can print patterns directly on the work platform without the need for placement of supports or a particular orientation on the platform, SLA-printed models require tilting on the work platform to prevent delamination caused by the surface tension of the resin. Tilting changes the orientation of the layers, which can change the roughness of the printed part.20

According to the result of the present study, SLA printed models had a smoother surface appearance, but the models exhibited horizontal and vertical contraction. This problem can be caused by the low layer thickness, polymerization shrinkage or post-processing inefficiency. Distortions and contraction can also be caused by defects existing in the polygon network of virtual models, which should be “water-tight”, without overlapping or incorrect orientation of the vertices.

CONCLUSIONS

Within the limitations of this in vitro study, we conclude that diagnostics models manufactured with MJ and SLA technologies are adequate for use in orthodontics or treatment planning. Although the differences between the diagnostic and reference models manufactured with SLA and MJ technologies were statistically significant, the dimensional

error of all printed models was found below 100 μm and therefore they are considered to be acceptable for clinical use.

REFERENCES

1. Quimby ML, Vig KW, Rashid RG, Firestone AR. The accuracy and reliability of measurements made on computer-based digital models. Angle Orthod 2004;74:298-303.
2. Brusco N, Andreetto M, Lucchese L, Carmignato S, Cortelazzo GM. Metrological validation for 3D modeling of dental plaster casts. Med Eng Phys 2007;29:954-66.
3. Arora M, Kohli S, Kalsi R. Influence of Custom Trays, Dual-Arch Passive, Flexed Trays and Viscosities of Elastomeric Impression Materials on Working Dies. J Clin Diagn Res 2016;10:ZC112-16.
4. Balamurugan T, Manimaran P. Evaluation of accuracy of direct transfer snap-on impression coping closed tray impression technique and direct transfer open tray impression technique: an in vitro study. J Indian Prosthodont Soc 2013;13:226-32.
5. Kulkarni MM, Thombare RU. Dimensional Changes of Alginate Dental Impression Materials-An In vitro Study. J Clin Diagn Res 2015;9:ZC98-ZC102.
6. Vojdani M, Torabi K, Ansarifard E. Accuracy of different impression materials in parallel and nonparallel implants. Dent Res J 2015;12:315-22.
7. Nagrath R, Lahori M, Agrawal M. A Comparative Evaluation of Dimensional Accuracy and Surface Detail Reproduction of Four Hydrophilic Vinyl Polysiloxane Impression Materials Tested Under Dry, Moist, and Wet Conditions-An In Vitro Study. J Indian Prosthodont Soc 2014;14:59-66.
8. Güth JF, Keul C, Stimmelmayr M, Beuer F, Edelhoff D. Accuracy of digital models obtained by direct and indirect data capturing. Clin Oral Investig 2013;17:1201-8.
9. Seelbach P, Brueckel C, Wöstmann B. Accuracy of digital and conventional impression techniques and workflow, Clin Oral Investig 2013; 17:1759-64.
10. Rödiger M, Heinitz A, Bürgers R, Rinke S. Fitting accuracy of zirconia single crowns produced via digital and conventional impressions-a clinical comparative study. Clin Oral Investig 2017;21:579-587.
11. Radeke J, von der Wense C, Lapatki BG. Comparison of orthodontic measurements on dental plaster casts and 3D scans. J Orofac Orthop 2014; 75:264-74.
12. Jeong YG, Lee WS, Lee KB. Accuracy evaluation of dental models manufactured by CAD/CAM milling method and 3D printing method. J Adv Prosthodont 2018; 10: 245–251.
13. Patzelt SBM, Bishti S, Stampf S, Att W. Accuracy of computer-aided design/computer-aided manufacturing–generated dental casts based on intraoral scanner data. J Am Dent Assoc 2014;145:1133–1140.
14. Koch G K, Gallucci GO, Lee SJ. Accuracy in the digital workflow: From data acquisition to the digitally milled cast. J Prosthet Dent 2016; 115: 749–754.
15. Lin L, Fang Y, Liao Y, Chen G, Gao C, Zhu P. 3D Printing and Digital Processing Techniques in Dentistry: A Review of Literature. Adv Eng Mater 2019; 21:1801013.
16. Kasparova M, Grafova L, Dvorak P, Dostalova T, Prochazka A, Eliasova H. Possibility of reconstruction of dental plaster cast from 3D digital study models. Biomed Eng Online 2013;12:49.
17. Patzelt SBM, Bishti S, Stampf S, Att W. Accuracy of computer-aided design/computer-aided manufacturing-generated dental casts based on intraoral scanner data. J Am Dent Assoc 2014;145:1133–40.
18. Koch GK, Gallucci GO, Lee SJ. Accuracy in the digital workflow: From data acquisition to the digitally milled cast. J Prosthet Dent 2016;115:749–54.
19. Uzun G. An overview of dental CAD/CAM systems. Biotechnol Equip 2008;22:530–5.
20. Alharbi N, Osman R, Wismeijer D. Effects of build direction on the mechanical properties of 3D-printed complete coverage interim dental restorations . J Prosthet Dent 2016;115:760-767.

Errata - Knowledge and behaviors regarding cariogenic nutrition in a group of adolescents from Bucharest

Sfeatcu R.[1], Radu A.C.[2], Pîrvu C.[3], Oancea R.[4], Bucur M.V.[5], Ilinca R.[6]

[1]Assoc. Professor, Oral Health and Community Dentistry Department, Faculty of Dental Medicine, "Carol Davila" University, Bucharest
[2]Student, Faculty of Dental Medicine, "Carol Davila" University, Bucharest
[3]Teaching Assistant, Research Methodology-Ergonomics Department, Faculty of Dental Medicine, "Carol Davila" University, Bucharest
[4]Professor, Preventive, Community Dentistry and Oral Health Department, Faculty of Dental Medicine, "Victor Babeş" University of Medicine and Pharmacy, Timisoara, Romania
[5]Teaching Assistant, Dental Prosthesis Technology Department, Faculty of Dental Medicine, "Carol Davila" University, Bucharest
[6]Teaching Assistant, Biophysics Department, Faculty of Dental Medicine, "Carol Davila" University, Bucharest

Correspondence to:
Name: Cristina Pîrvu
Address: Nitu Vasile Street no. 42, Bucharest
Phone: +40 721278028
E-mail address: cristina.pirvu@umfcd.ro

Abstract

The article entitled "Knowledge and behaviors regarding cariogenic nutrition in a group of adolescents from Bucharest", published in no. 4 of Medicine in evolution Journal, in 2021, has the following group of authors: Sfeatcu R.1, Radu A.C.2, Pîrvu C.3, Oancea R.4, Bucur MV. 5, Ilinca R.6. (The name of the last author has been corrected, instead of Radu I., Ilinca R. is correct).

ProMax 3D • PlanScan • ProFace

Unique 3D combination for open CAD/CAM

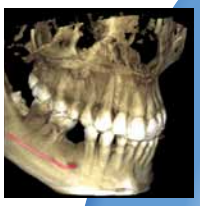

Digital perfection

Planmeca sets new standards with world's first dental unit integrated intraoral scanner for open connectivity to various CAD/CAM systems.

We would like to invite you to explore the dentistry in new dimensions – see the perfect combination of digital intraoral scan, CBVT and 3D facial photo datasets in one 3D image. This digital perfection enables you to study patient's complete anatomy in detail, plan and utilise open interface with modern CAD/CAM systems according to your needs. Now you can be one of the pioneering specialists, whether you are an implantologist, endodontist, periodontist, orthodontist or maxillofacial surgeon. The new era of dentistry is reality. It's your decision.

Planmeca Oy, Asentajankatu 6, 00880 Helsinki, Finland
tel. +358 20 7795 500, fax +358 20 7795 555, sales@planmeca.com, www.planmeca.com

PLANMECA

1971 - 2011

Planmeca ProMax 3D

All volume sizes

The Planmeca ProMax concept offers a full range of imaging volumes providing detailed information on patient anatomy. The comprehensive Planmeca ProMax platform complies with every need in dental radiology, offering digital panoramic, cephalometric, and 3D imaging as well as 3D face photo together with advanced imaging software.

At the heart of the concept is the robotic SCARA technology: the unique robotic arm enables any movement pattern required by existing or future program, eliminating all imaging restrictions. With the Planmeca ProMax concept superior maxillofacial radiography can be performed with a single platform, today and in the decades to come.

All volume sizes

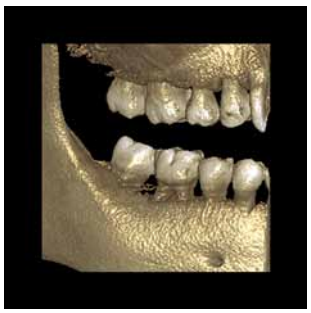

Planmeca ProMax 3D s
Ø42 x 42 mm–90 x 60 x 130 mm

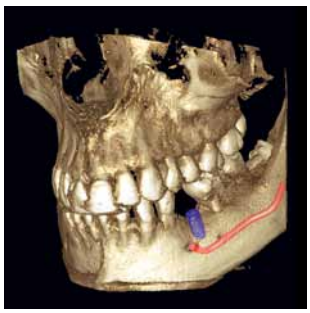

Ø34 x 42 mm–140 x 105 x 130 mm

Planmeca ProMax 3D

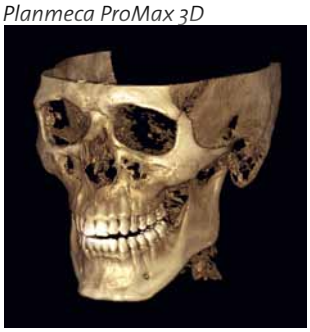

Planmeca ProMax 3D Mid
Ø34 x 42 mm–Ø160 x 160 mm

Planmeca ProMax 3D Max
Ø42 x 50 mm–Ø230 x 260 mm

Planmeca Oy, Asentajankatu 6, 00880 Helsinki, Finland
tel. +358 20 7795 500, fax +358 20 7795 555
sales@planmeca.com, www.planmeca.com

PLANMECA

Planmeca Romexis

Software refined

Available on the App Store

Planmeca Romexis is the software of choice for all dental imaging purposes. All patient's digital images – intraoral and extraoral X-ray images, 3D volumes, and photographs – are processed and stored in one easy-to-use system. Planmeca Romexis offers a complete set of tools for image viewing, enhancement, measurement, and implant planning, and fully integrates digital imaging with the patient's other clinical data.

Thanks to its powerful printing features, stunning printouts can be produced. Planmeca Romexis provides direct image capture from Planmeca X-ray units, interfaces with 3rd party devices via TWAIN, and is fully DICOM-compatible. Planmeca Romexis is a JAVA software that runs on Windows, Mac OS, and Linux operating systems, and embraces modern IT standards.

Planmeca Oy, Asentajankatu 6, 00880 Helsinki, Finland
tel. +358 20 7795 500, fax +358 20 7795 555
sales@planmeca.com, www.planmeca.com

PLANMECA

1971 - 2011

INSTRUCTIONS FOR AUTHORS

The journal publishes general reviews, studies and clinical, epidemiological, experimental and laboratory research, clinical case presentation, papers from the history of medicine, reviews, scientific and technical state-of-the-art articles, medical informations and opinions. Only papers which have not been published or sent for publishing in other journals are accepted. The authors are responsable for the opinions expressed in the papers. ***The paper must be edited both in Romanian and in English; the English version will be supervised by our collaborator Dana Brehar-Cioflec, MD, PhD; typed on white A_4 paper and on CD, DVD or Memory Stick***.

Manuscripts will not exceed:

- general reviews: 6-8 pages
- studies and researches: 5-7 pages
- case presentations: 2-4 pages
- reviews, scientific and technical state-of-the-art articles, medical informations and opinions: 1-2 pages.

The paper will be edited according to international editing rules for manuscripts. The title will be written in capital characters and it will be followed by the name and surname of the author (authors), followed by their place of work (place where the paper has been elaborated). Studies and researches will be followed by a brief abstract, followed by 3-4 key-words.

The body of the paper will be structured on the following chapters: introduction, aim, objectives, material and method, results and discussions, conclusions. The references will be presented alphabetically and in conformity to the Vancouver Convention, including:

- for articles: name of the authors and surname initials, title of the article in the original language, title of the journal according to the international abreviation system, year of issue, volume, number, pages;
- for books: name of the authors and surname initials, volume, publisher (editors), city of publishing, year of issue.

Citation of references inside the body of the paper will be put between brackets, Harward style (author, year) or Vancouver style (number in square brackets or superscript). Cited reference titles will be selected, maximum 6 for studies and case presentations and 12 for general reviews. Acceptance, rejection or the need of alterations in sent materials, or in inconography, will be comunicated to the authors in due time. For this, the authors will indicate the person and address for corespondence (phone number, e-mail address). Given the less pleasant experience of the editorial board with some articles being rejected because they did not meet publishing criteria, we decided to support those who intend to publish in this journal by detailing the way such a paper should be elaborated, as well as our requirements.

Except some particular aspects concerning this journal, the following details are general requirements asked or imposed by other journals as well. Conditions to be met in order to propose a paper for publishing. The main author has the responsability to make sure the article has been approved by all the other authors. The journal will have copyright

for papers accepted for publishing. The editorial board reservs the right to change the style and dimensions of an article (major changes will be discussed with the main author) and to decide the date of issue.

2. FIRST PUBLICATION

The editorial board will not consider a paper already reported in a published general review or described in a paper proposed to or accepted by another journal. This does not exclude papers which have been rejected by other journals. Also, papers which have been presented at a scientific meeting will be accepted for discussion if they have not been entirely or partially published in a similar publication. „Multiple" publishing of the same study is seldom justified. One of the possible justifications is publishing in a second language but only if the following conditions are met:

- Editors of both journals involved are fully informed;
- Priority of the initial publication will be respected by a minimum publishing interval of two weeks;
- For the second publication, a shortened version will suffice;
- The second version strictly reflects data and interpretations in the first;
- A footnote may state: „This article is based upon a study initially published in [title of the journal]".

3. PATERNITY

Paternity must reflect the common decision of the coauthors. Each author must have participated enough to take public responsability for the content. A paper with collective paternity must have a key person responsable for the article.

4. COPYRIGHT

In order to reproduce materials from other sources, written agreement from the copyright owner must be obtained:

- photographer – for unpublished photographs;
- hospital where the photographer (physician) is employed – for unpublished photographs performed during the employment period;
- initial publisher – for a table, picture or text which have previously been published elsewhere.

5. ETHICAL ASPECTS

Do not use name of patients, initials or hospital observation charts numbers. If a photograph of a body part which could allow direct or deductive recognition of the patient needs publishing, then the paper must be accompanied by the written consent of the patient and clinician, as well.

6. PRESENTING THE MANUSCRIPT

6.1. CONTENT OF THE PAPER - INDICATIONS FOR ORIGINAL ARTICLES

Paper title [Book Antiqua 20, bold, left alignment]

Surname N.[1], Surname N.[2] [Book Antiqua, 14, bold]

[1] *Author Affiliation (DEPARTMENT, FACULTY, UNIVERSITY, CITY/COMPANY) [10, italic]*
[2] *Author Affiliation (DEPARTMENT, FACULTY, UNIVERSITY, CITY/COMPANY) [10, italic]*

Correspondence to:
Surname Name: [10, italic]
Address: [10, italic]
Phone: +40 [10, italic]
E-mail address: [10, italic]

Abstract [Book Antiqua, 12, bold, justify alignment]

Recommendations for original studies

Original studies must include a structured abstarct of maximum 150 words, containing the following titles and informations: Aim and objectives; Material and methods; Results; Conclusions; Key words: give 3-5 key words; The abstract will be translated into an international circulation language.

Keywords: Innovation, technology, research projects, etc. [Book Antiqua 9].

INTRODUCTION [Book Antiqua, 11, bold, left alignment]

Introduction presentation of general aspects, in the context of the approached theme.

Introduction include **Aim and objectives –** Define the aim of the article. Briefly expose the rationale of the presented study or observation. Make strictly pertinent referals and do not exhaustively review the subject. Do not include data or conclusions from the paper.

There is a limitation of 4/6 pages. All pages size should be A4 (21 x 29,7cm). The top margins should be 2 cm, the bottom, right, margins should be 2cm and left margins should be 2,85 cm. All the text must be in one column and Book Antiqua font, including figures and tables, with single-spaced 10-point interline spacing.

Aim and objectives [Book Antiqua 11, bold italic, left alignment]

The text included in the sections or subsections must begin one line after the section or subsection title. Do not use hard tabs and limit the use of hard returns to one return at the end of a paragraph. Please, do not number manually the sections and subsections; the template will do it automatically.

[Book Antiqua, 11 point, normal, justified alignment].

MATERIAL AND METHODS [Book Antiqua, 11, bold, left alignment]

Describe the selection of observations or subjects for the experiment (including controls). Identify methods, equipments (with the name and address of the manufacturer in brackets) and give sufficient details on procedures. Give references for the selected methods, including statistical methods; offer details and brief descriptions for previously published methods which are not well known; describe new or substantially modified methods, justify their use and assess their limitations. Precisely identify all used drugs and chemicals, including generic names, dosage and administration ways. Describe statistical methods with sufficient details for reported results to be verified. Whenever possible, quantify discovered aspects and present them with appropriate measurement indicators for the uncertainty or error of measurement (such as confidence intervals). [Book Antiqua, 11 point, normal, justified alignment].

RESULTS [Book Antiqua, 11, bold, left alignment]

Present results in a logical succession as text, tables and illustrations. Emphasize or briefly describe only important observations. [Book Antiqua, 11 point, normal, justified alignment].

DISCUSSIONS [Book Antiqua, 11, bold, left alignment]

Underline new, important aspects of the study. Do not repeat in detail data which have been presented in previous sections. Include implications of revealed aspects and their limitations, including implications for future studies. Connect your observations to other relevant studies. Relate the results to the aim proposed for the study. [Book Antiqua, 11 point, normal, justified alignment].

CONCLUSIONS [Book Antiqua, 11, bold, left alignment]

Organize conclusions which emerge from the study. In the end state: a) contributions to be acknowledged but which do not justify paternity right; b) thanks for technical support;

c) thanks for financial or material support. [Book Antiqua, 11 point, normal, justified alignment].

REFERENCES [Book Antiqua, 11, bold, left alignment]

A numbered list of references must be provided at the end of the paper. The list should be arranged in the order of citation in the text of the publication, assignment or essay, not in alphabetical order(according to the Vancouver rules). List only one reference per reference number. It is very important that you use the correct punctuation and that the order of details in the references is also correct.

- Books - Standard format - #. Author of Part, AA. Title of chapter or part. In: Editor A, Editor B, editors. Title: subtitle of Book. Edition(if not the first). Place of publication: Publisher; Year. p. page numbers.
- Journal Articles - Standard format - #. Author of article AA, Author of article BB, Author of article CC. Title of article. Abbreviated Title of Journal. year; vol(issue): page number(s).
- E-Books - Standard format - #. Author A, Author B. Title of e-book [format]. Place: Publisher; Date of original publication [cited year abbreviated month day]. Available from: Source. URL.
- E-Journals - Standard format - #. Author A, Author B. Title of article. Abbreviated Title of Journal [format]. year [cited year abbreviated month day]; vol(no): page numbers [estimated if necessary]. Available from: Database Name (if appropriate). URL.

Internet Documents - Standard format - #. Author A, Author B. Document title. Webpage name [format]. Source/production information; Date of internet publication [cited year month day]. Available from: URL. [Book Antiqua, 10 point, normal, justified alignment].

[1] _____
[2] _____
[3] _____

6.2. CONTENT OF THE PAPER - INDICATIONS FOR CASE REPORTS

Content of the paper for case report will respect indications for original articles.

Themes may be selected from all medical fields. Manuscripts which offer a special gain for daily activity will have priority. The title must be clearly, precisely stated. It may be completed by a subtitle. It is advisable to include in the key words of the title the main message, the special element which may be observed from the case evolution. The content of a case report must be divided into three parts:

Introduction – It must include a maximum of 15 typed rows (half page). Here, the main medical problem is summarized in order to place the case in a specific domain.

Case report – It contains essential specific information on the case. In order to make a logical, chronological and didactical case report the following 5 chapters are needed:

I. Anamnesis;
II. Clinical examination data;
III. Laboratory data;
IV. Additional paraclinical investigations;
V. Treatment and evolution.

Discussions – The reason for the case report must be stated. The report must be patient-centered. Occasional deviations from typical (characteristic) evolutions, nosologically important facts must be presented in such a manner to expose the clinical picture as completely as possible. The case report must not appear as an appendix of a general review. Dimensions of a case report: maximum 6-8 typed pages, 30 rows of 60 characters/page.

6.3. MEASUREMENT UNITS, SYMBOLS, ABREVIATIONS

All measurements must be expressed in International System (IS) units. Abreviations must be fully explained when first used.

6.4. TABLES

Tables are noted with Roman figures and they will have a brief and concise title, concordant with their content.

6.5. ILLUSTRATIONS

Number all illustrations in Arabic figures in a single succession. Apply a label on the back side of every illustration, containing its number and an arrow indicating the upper side. Coloured illustrations may be accepted but it is the choice of the editors, according to particular technical abilities of each journal issue, or it may involve a fee in special cases.

6.6. EXPLANATIONS FOR DRAWINGS AND GRAPHS

Explanation for drawings and graphs must be clear and in readable dimensions, considering the necessary publishing shrinkage.

6.7. PHOTOGRAPHS

Offer glossy, good quality photographs. Any annotation, inscription, etc. must contrast with the ground. Microphotographs must include a scale marker.

6.8. ILLUSTRATION LEGENDS

Include explanations for each used symbol, etc. Identify the printing method for microphotographs.

7. COPIES FOR PUBLISHING

In order to accelerate publishing, the main author will send a set of printed sheets presenting the final version of the paper, as it will appear in the journal. It is really helpful that texts to be also sent on electronic support, diacritic characters mandatory.

8. REJECTION OF PAPERS

If a paper does not meet publishing conditions, whatever these may be, the editors will notify the first author on this fact, without the obligation of returning the material. Original photographs or the whole material will be returned only if the author comes to the editor and takes them.

Papers submitted for publishing will be addressed to:

Prof. Angela Codruta Podariu, DMD, PhD
Journal Medicine in evolution
Department of Preventive, Community Dental Medicine and Oral Health
Splaiul Tudor Vladimirescu no. 14 A
300041, Timişoara
Email: proiectetim@gmail.com

Dana Brehar-Cioflec, MD, PhD
Institute of Public Health *"Prof. Dr. Leonida Georgescu"* Timişoara
Bd. Victor Babeş no. 16
300226, Timişoara
Phone: 0256-492101
Email: danabreharcioflec@yahoo.com

Descoperiți elmex®.
Specialistul de încredere în îngrijire orală.

*Sondaj telefonic reprezentativ privind recomandările de pastă de dinți, organizat de Ipsos pe un eșantion de 300 de stomatologi, în ian-feb 2018.

elmex®
Healthy teeth for life.

Acest număr a apărut cu suportul COLGATE-PALMOLIVE